

SIGNAL DESIGNS FOR MIMO OFDM SYSTEMS

by

Yuansheng Jin

A dissertation submitted to the Faculty of the University of Delaware in partial fulfillment of the requirements for the degree of Doctor of Philosophy in Electrical and Computer Engineering

Winter 2017

© 2017 Yuansheng Jin
All Rights Reserved

ProQuest Number:10257226

All rights reserved

INFORMATION TO ALL USERS

The quality of this reproduction is dependent upon the quality of the copy submitted.

In the unlikely event that the author did not send a complete manuscript and there are missing pages, these will be noted. Also, if material had to be removed, a note will indicate the deletion.



ProQuest 10257226

Published by ProQuest LLC (2017). Copyright of the Dissertation is held by the Author.

All rights reserved.

This work is protected against unauthorized copying under Title 17, United States Code
Microform Edition © ProQuest LLC.

ProQuest LLC.
789 East Eisenhower Parkway
P.O. Box 1346
Ann Arbor, MI 48106 – 1346

SIGNAL DESIGNS FOR MIMO OFDM SYSTEMS

by

Yuansheng Jin

Approved: _____

Kenneth E. Barner, Ph.D.

Chair of the Department of Electrical and Computer Engineering

Approved: _____

Babatunde A. Ogunnaike, Ph.D.

Dean of the College of Engineering of the University of Delaware

Approved: _____

Ann L. Ardis, Ph.D.

Senior Vice Provost for Graduate and Professional Education

I certify that I have read this dissertation and that in my opinion it meets the academic and professional standard required by the University as a dissertation for the degree of Doctor of Philosophy.

Signed: _____

Xiang-Gen Xia, Ph.D.
Professor in charge of dissertation

I certify that I have read this dissertation and that in my opinion it meets the academic and professional standard required by the University as a dissertation for the degree of Doctor of Philosophy.

Signed: _____

Leonard J. Cimini, Jr., Ph.D.
Member of dissertation committee

I certify that I have read this dissertation and that in my opinion it meets the academic and professional standard required by the University as a dissertation for the degree of Doctor of Philosophy.

Signed: _____

Javier Garcia-Frias, Ph.D.
Member of dissertation committee

I certify that I have read this dissertation and that in my opinion it meets the academic and professional standard required by the University as a dissertation for the degree of Doctor of Philosophy.

Signed: _____

Qing Xiang, Ph.D.
Member of dissertation committee

ACKNOWLEDGEMENTS

I would like to express my sincere gratitude to all the people who helped me during my Ph.D. study at University of Delaware.

First, I would like to thank my advisor, Prof. Xiang-Gen Xia, who led my way to the realm of research and also supported me to propose several original results. I am always motivated by his hard-working spirit and research enthusiasm during my entire Ph.D. study. Without his help and guidance, I could not have had a productive graduate life.

I would like to thank Prof. Leonard J. Cimini, Prof. Javier Garcia-Frias and Prof. Qing Xiang, for serving on my defense committee. I have learned a lot from their classes and also received invaluable suggestions and encouragement during my research work.

I also would like to thank my groupmates: Tianyi Xu, Zheng Li, Xiaowei Li, Guoquan Li, Li Xiao, Cheng Wang, Long Shi, Shengbo Zhang and Zujun Liu for their help and all the fun we have had during the Ph.D. study. Lastly and most importantly, I would like to express my greatest appreciation to my parents Congguo Jin, Lan Li and my aunt Congyun Jin and my girlfriend Manman Lu. Without their love and support, it is impossible for me to finish my Ph.D. study. To them I dedicate this dissertation.

TABLE OF CONTENTS

LIST OF FIGURES	vi
ABSTRACT	vii
Chapter	
1 INTRODUCTION	1
1.1 Channel Independent Precoding Design For MIMO OFDM With Insufficient CP	1
1.2 Robust Precoding For MIMO OFDM With Insufficient CP	3
1.3 Amplify And Forward Full Duplex Relay OFDM Transmission Scheme	4
1.4 Contributions And Outline	4
2 INTERFERENCE NULLING BASED CHANNEL INDEPENDENT PRECODING DESIGNS FOR MIMO-OFDM SYSTEMS WITH INSUFFICIENT CYCLIC PREFIX	7
2.1 Introduction	7
2.2 System Model	9
2.2.1 SISO-OFDM Model	9
2.2.2 MIMO-OFDM Model	12
2.3 Channel Independent Precoding	14
2.3.1 SISO-OFDM Precoding Example	14
2.3.2 MIMO-OFDM Channel Independent Precoding	16
2.3.3 Precoding When $n_r \leq n_t$	17
2.3.4 IBI Cancellation When $n_r > n_t$	30
2.3.5 Relationships With The Existing Block Based Transmission Systems	31
2.4 Simulations	32
2.5 Conclusions	36

3	A ROBUST PRECODER DESIGN BASED ON CHANNEL STATISTICS FOR MIMO-OFDM SYSTEMS WITH INSUFFICIENT CYCLIC PREFIX	42
3.1	Introduction	42
3.2	MIMO-OFDM Model	45
3.3	Receiver Structure And Precoder Design	49
	3.3.1 Receiver Structure	49
	3.3.2 Precoder Design	54
3.4	Simulation Results	59
3.5	Conclusion	66
4	FULL DUPLEX DELAY DIVERSITY RELAY TRANSMISSION USING BIT-INTERLEAVED CODED OFDM	68
4.1	Introduction	68
4.2	Signal Model	71
4.3	Block Based Full-Duplex Delay Diversity Transmission	75
	4.3.1 Full-Duplex Delay Diversity Transmission	75
	4.3.2 Power Allocation Scheme	82
4.4	Simulation Results	83
4.5	Conclusion	87
5	CONCLUSIONS AND FUTURE WORKS	89
5.1	Conclusions	89
	5.1.1 Channel Independent Precoding Design For MIMO OFDM With Insufficient CP	90
	5.1.2 A Robust Precoder Design Based On Channel Statistics For MIMO-OFDM Systems With Insufficient Cyclic Prefix	90

5.1.3	Full Duplex Delay Diversity Relay Transmission Using Bit-Interleaved Coded OFDM	91
5.2	Future Works	91
5.2.1	The Incorporation Of Self-Interference Cancellation In Full-Duplex Relay OFDM Communications	91
5.2.2	More Complicated Full-Duplex Relay Networks	92
BIBLIOGRAPHY		94
Appendix		
A PROOF OF THE IDENTICAL MSE'S FOR FULL CP SISO-OFDM WITH CHANNEL INDEPENDENT PRECODING		101
B REPRINT PERMISSIONS		102

LIST OF FIGURES

2.1	BER performances of the IA based precoding, SC-FDE, CP-OFDM, ZP-only	37
2.2	SISO case: BER performances of IA based precoding of different CP lengths and different numbers of information symbols	38
2.3	MISO case: BER performances of IA based precoding of different CP lengths and different numbers of information symbols	39
2.4	MIMO case: BER performances of IA based precoding of different CP lengths and different numbers of information symbols	40
2.5	MIMO case: BER performances of IA based precoding of different CP lengths and different numbers of information symbols	41
3.1	MIMO case: BER performances of SC-FDE, CP-OFDM, ZP-only, our channel independent precoding and the proposed precoding based on statistical CSIT	60
3.2	MIMO case: BER performances of the proposed precoding without/with interblock interference	62
3.3	MIMO case: BER performances of statistical CSIT precoding and the channel independent precoding	64
3.4	MIMO case: BER performances of IA based precoding of different CP lengths and different numbers of information symbols	66
4.1	Dual-hop full-duplex relay network	71
4.2	Source node signal processing diagram	76
4.3	Relay node signal processing diagram	78

4.4	Coded BER comparison of full-duplex OFDM without the source-to-destination link, full-duplex DD OFDM, 2-path coded OFDM, and half-duplex OFDM	84
4.5	Coded BER versus SNR_D with $SNR_R = 25$ dB	86
4.6	BER comparison for different effective residual SI lengths	87
4.7	BER comparison for different power allocations, including the proposed power allocation and power allocations with γ ranging from 0.1 to 0.9	88

ABSTRACT

Multiple-input multiple-output (MIMO) is a promising wireless communication technique to boost the wireless link capacity without requiring additional power or bandwidth. Combined with orthogonal frequency division multiplexing (OFDM) the MIMO OFDM system is considered an attractive candidate for high data rate wideband wireless communications over frequency selective channels. 4G-LTE, WiFi (802.11) and WiMax (802.16e) all adopt MIMO OFDM in their standards.

In real world applications of MIMO OFDM system, diversified sources of interference often exist and significantly influence the system performance of MIMO OFDM. Firstly let's consider the single user point-to-point MIMO OFDM system. The interference may be often caused by a long time delay spread of the channel. Typically MIMO OFDM systems resort to cyclic prefix (CP) to protect the system from interference. The simple one-tap equalization in OFDM also relies on the assumption that the CP length is at least as large as the channel memory length. However, in a number of applications, the sufficient CP length requirement is not practically satisfied for various reasons. For example, in the next generation of WiFi standard, outdoor transmission is much more involved. The time delay spread of the outdoor channel may be much longer than that considered in the typical channel models in the current WiFi standards. If the current OFDM symbol structure is inherited, we may face the insufficient CP problem in the outdoor transmission scenario. Next consider the interference scenario in MIMO OFDM cooperative communication system. In the emerging 5G cooperative communication system, the relay node may adopt the amplify-and-forward (AF) relay protocol and the in-band full-duplex (FD) mode. The simultaneous transmission and reception at the relay node gives rise to severe self loopback interference. All the mentioned types of interference have detrimental influence on the error rate performance

of the MIMO OFDM system. Therefore signal designs for MIMO OFDM system must take interference cancellation or management into consideration.

In the first topic, a new interference nulling based channel independent precoding for MIMO OFDM systems of n_t transmit and n_r receive antennas with insufficient CP is proposed. When the CP length is insufficient, intercarrier interference (ICI) from the symbols in the current transmission block and interblock interference (IBI) from the previous transmission block occur in the OFDM system. To cope with ICI and IBI induced by the insufficient CP, we have proposed a design framework to completely nulling the IBI. In our first channel independent precoding scheme, no channel state information is needed. When MIMO OFDM system equips the same number of transmit and receive antennas or the transmit antennas are more than the receive antennas, we have shown that precoding at the transmitter combined with interference nulling at the receiver can assist to either cancel interblock interference (IBI) or separate the subspace occupied by IBI from the subspace used for information symbols. When the transmit antennas are less than the receive antennas, it is demonstrated that information symbols can be decoded without any precoding at the transmitter but just with interference nulling and block linear equalization at the receiver.

In the next topic, we consider a robust precoder design which combines statistical CSI at the transmitter and the interference nulling based precoding structure to gain a better performance compared to the channel independent precoding scheme. Statistical channel state information at the transmitter in the form of covariance matrix of the MIMO OFDM channel matrix is utilized to perform the robust precoding. Standard optimization problem is formulated with regard to the largest mean square error (MSE) of the minimum mean square error (MMSE) equalized symbol in the insufficient CP signal model. By employing convex optimization technique, a closed-form solution is derived for the optimization problem. Since the average MSEs are set equal using this precoder, the BER performance is better than our previously proposed channel independent precoder.

In the third topic, we consider the OFDM-based transmission in the AF full

duplex relay system with residual self-interference. A delay diversity OFDM (DD OFDM) transmission scheme in amplify-and-forward (AF) full-duplex relay systems is investigated. One direct source-to-destination link, one relay forwarding link and residual self-interference (RSI) are considered in the system. The necessary cyclic prefix (CP) length is investigated and a suitable AF relay protocol in the full-duplex relay OFDM system is proposed. This paper demonstrates that the AF relay link and the direct source-to-destination link can be combined to provide spatial diversity. The key is that the DD OFDM scheme is used to transform the spatial diversity into increased channel frequency diversity that is further exploited by using the bit-interleaved coding. The BER performance of the proposed system is verified by simulation results.

Chapter 1

INTRODUCTION

In this chapter, we first introduce the channel independent precoding for multiple input and multiple output (MIMO) orthogonal frequency division multiplexing (OFDM) communication systems with insufficient cyclic prefix (CP) and introduce the robust precoding for MIMO OFDM with insufficient CP respectively. In the next, we introduce the full-duplex amplify-and-forward (AF) relay communication system and the OFDM based relay transmission scheme. At last, we concisely highlight our contributions and render the outline of each chapters in the sequel.

1.1 Channel Independent Precoding Design For MIMO OFDM With Insufficient CP

In OFDM system, the frequency domain channel is divided into a set of parallel narrow subchannels, therefore eliminating or reducing the innate intersymbol interference (ISI) in the wideband channel. OFDM systems transform from the ISI channel to the ISI free subchannels by resorting to IDFT and CP insertion at the transmitter and DFT and CP removal at the receiver respectively. The DFT based OFDM system also enable the simple one-tap equalization by using sufficient CP as guard interval. The enormous capability of MIMO systems in terms of boosting data transmission rate has been witnessed in the past two decades. Exploiting the so-called spatial multiplexing, MIMO systems allow for an increase of bit rate in the wireless communication link without requiring extra power and bandwidth. Combining MIMO and OFDM is a natural choice for broadband wireless communication system in pursuit of higher data rate. Either spatial multiplexing or beamforming can be achieved on a per subcarrier basis in the MIMO OFDM system. The concise MIMO OFDM system model relies on

the employment of sufficient guard interval, for example, sufficient duration of CP as the guard interval. However, wireless communication standards, which utilize MIMO OFDM as the modulation technique, usually set a length constraint for the CP, since the CP portion is merely a repeated information symbols and thereby a considerably large portion of CP results in a lower bandwidth efficiency. One of the major consequences of constraint on CP is the insufficient CP transmission in the MIMO OFDM system. Moreover, the burgeoning trend of extension coverage in wireless communication system leads to the long delay spread propagation scenario, which alternatively increases the probability of insufficient CP transmission. Insufficient CP destroys the orthogonality of OFDM signal structure and it gives rise to the interblock interference (IBI) and intercarrier interference (ICI).

MIMO OFDM system, or the single input single output OFDM/DMT counterpart, with insufficient CP have been researched extensively in the past, in, for example, [6, 7, 14, 19, 20, 29, 35, 60, 61, 62, 65]. In [6] a transmitter based scheme based on the Tomlinson-Harashima precoder is proposed. The precoder for DMT eliminates interference by processing the signals at the transmitter so that the signal is ISI free at the receiver. In essence, this type of processing aims at channel shortening. However, the time varying nature of the wireless channel limits the application of this method in OFDM. [47] proposes structure preventing ICI that utilizes redundancy in the frequency domain at the transmitter and removes ISI with a simple cancellation method at the receiver. [62] proposed a training-based two stage solution to first shorten the channel and then perform the per-tone equalization. In [61], a novel and efficient ICI/ISI-aware beamforming solution is proposed based on the optimal steering vector design, whose advantage is this solution uses low complexity one-tap per subcarrier processing at both transmitter and receiver. Yet this solution requires precise channel state information (CSI) at the transmitter. My works in [27] have partially referred to [61].

1.2 Robust Precoding For MIMO OFDM With Insufficient CP

MIMO channels arising from the use of multiple antennas at both transmitter and receiver have received continuously attention because they provide an significant increase in capacity over the single input single output (SISO) counterpart. Alternatively, techniques can also be applied to MIMO for enhancement of the link robustness. However, MIMO channels are not only restricted to the multiple antenna scenario. The block transmission schemes over time dispersive or frequency selective channel, for example OFDM or single-carrier frequency domain equalization (SC-FDE), can be considered as signal models using MIMO channels. The equivalent channel in MIMO OFDM systems can be viewed as a generalized MIMO channel which consists of both spatial domain and frequency domain channel uses.

Each scalar data symbol in the vector input to the MIMO channel can be treated as a substream to a MIMO system. Assuming the signal constellations and coding schemes have been specified for each substream, it is viable to optimize the link quality of all the substreams by designing precoder at the transmitter and equalizer at the receiver. The joint optimization of precoder and equalizer is often intractable. One can find suboptimal solutions by fixing the receiver processing to be minimum mean square error (MSE) equalizer and design the precoder for specific requirement. [44] has shown that MIMO channel diagonalizing structure is optimal for a variety of minimization problems regarding the MSE of all the substreams, or the signal to noise plus interference ratio (SINR) or bit error rate (BER). The channel-diagonalizing techniques require CSI at the transmitter, which imposes stringent requirement on the channel estimation and CSI feedback. To ease this burden, statistically robust designs can be employed since the statistics of the channel is more likely to be long term static. When the mean and covariance CSI at the transmitter is available, robust designs are more involved. For example, [73] designs a robust transceiver based a general cost function of the average MSEs, which takes advantage of the mean and covariance information at the transmitter.

1.3 Amplify And Forward Full Duplex Relay OFDM Transmission Scheme

Recently, relay-assisted wireless communication system has been undergoing extensive development in both industry and academia [43]. By receiving, processing, and retransmitting radio signals, relay networks offer an energy efficient and low cost solution to expand coverage of wireless connections. The two most typical relaying protocols are AF and decode-and forward (DF). The AF protocol outperforms the DF counterpart in terms of less computational demand and shorter processing delay.

An in-band full-duplex relay performs concurrent reception and transmission in the same frequency band, hence improving the spectral efficiency significantly. However, practical realization and implementation of full-duplex networks still confront numerous challenges. One of the most noticeable problem is the so termed self-interference (SI), which directly results from the concurrent transmission and reception at the same frequency. The strong SI looped back from the transmitter at the relay node can easily diminish the throughput gain of the full-duplex relay system. A substantial amount of effort has been paid to the SI suppression techniques. For instance, directional antennas, or sufficient large separation distance between transmit and receive antennas, should be taken to partially remove the SI. A combination of RF interference cancellation, baseband digital interference cancellation as well as some other additional cancellation mechanisms, are also required to suppress the SI to a fairly low level. Although the SI can be minimized by interference suppression techniques, residual self-interference still poses a main issue in reality and residual self-interference management is an indispensable requirement in the designs of all practical full-duplex relay networks.

1.4 Contributions And Outline

MIMO OFDM is in prevalence across nearly all the major wireless standards, such as 802.11, WiMax, 4G-LTE. In terms of system design for certain purposes, MIMO OFDM enjoys design flexibility because of the orthogonality among all the frequency subcarriers. For example, on each subcarrier bit loading, power allocation, spatial

multiplexing and beamforming schemes can be selected independently. However, the performance of MIMO OFDM is very sensitive to all kinds of interference. The causes of interference are diversified, such as doppler frequency, frequency offset, timing offset, insufficient guard interval, and co-channel interference, etc. In my work, two real-world interference scenarios are considered: first the interference due to insufficient CP is considered; secondly the self-interference in the full duplex amplify-and-forward relay communication is considered.

For the insufficient CP problem, we investigate the insufficient CP problem from the block-based transmission perspective, where each OFDM symbol is treated as a vector block of modulated symbols. We utilize vector space as a tool to explore methods which makes the signal subspace disjoint from the IBI subspace occupied by the ISI from the previous block In [27]. The core issue in this work is the rank calculations which help to explain how we can maintain the desired signal separable from the IBI. We will discuss whether the precoder is needed at the transmitter, what is the design principle of the precoder, and also what receivers used at the receiver. In the next work in [28], the concept of robust transceiver design is combined with the interference nulling transceiver design for MIMO OFDM system with insufficient CP. The proposed precoder design manages to provide the optimized power allocation to minimize the maximum substream MSE at the receiver. For the full duplex relay with self-interference problem, I considered a novel OFDM transmission scheme to minimize the effect of self-interference.

The outline of this dissertation is organized as follows.

In chapter 2, a new interference nulling based channel independent precoding for MIMO-OFDM systems of n_t transmit and n_r receive antennas with insufficient CP is proposed. By employing the notion of interference nulling, we show that our proposed channel independent precoding scheme can eliminate the IBI caused by the insufficient CP with higher bandwidth efficiency than the conventional zero-padded or a sufficient CP added block transmission system when $n_r \leq n_t$. It is also shown that when $n_r > n_t$, the IBI can be eliminated without the need of any zero-padding or

adding CP or precoding when the OFDM block length is not too small.

In chapter 3, we study the precoder design problem for MIMO-OFDM systems with insufficient CP using statistical channel state information (CSI) at the transmitter. After our previously proposed channel independent precoding scheme, we consider the interference nulling based precoding structure for this robust precoder design. This structure can assist to either cancel IBI or separate the subspace occupied by IBI from the subspace used for information symbols. Statistical channel state information at the transmitter in the form of covariance matrix of the MIMO-OFDM channel matrix is utilized to perform the robust precoding. The design criterion for the precoder design is to minimize the maximum average mean squared error (MSE) of all the transmitted symbols during one OFDM block interval. To achieve this goal, the precoder design exhibits a similar procedure to the optimized design framework for MIMO transceivers for either perfect or statistical CSI with no interference effect, but with a distinct equivalent channel.

In chapter 4, a novel OFDM transmission scheme for full duplex amplify-and-forward relay communication system is proposed. We investigate a delay diversity OFDM (DD OFDM) transmission scheme in AF full-duplex relay systems. One direct source-to-destination link, one relay forwarding link and residual self-interference (RSI) are considered in the system. The necessary CP length is investigated and a suitable AF relay protocol in the full-duplex relay OFDM system is proposed. This paper demonstrates that the AF relay link and the direct source-to-destination link can be combined to provide spatial diversity. The key is that the DD OFDM scheme is used to transform the spatial diversity into increased channel frequency diversity that is further exploited by using the bit-interleaved coding. The BER performance of the proposed system is verified by simulation results.

Finally, chapter 5 summarizes our work and briefly discusses some future research topics.

Chapter 2

INTERFERENCE NULLING BASED CHANNEL INDEPENDENT PRECODING DESIGNS FOR MIMO-OFDM SYSTEMS WITH INSUFFICIENT CYCLIC PREFIX

2.1 Introduction

In the conventional MIMO-OFDM system, IDFT and CP insertion at the transmitter together with CP removal and DFT at the receiver help to convert an inter-symbol interference channel into several ISI free subchannels. The CP length is designed no less than the length of the channel impulse response (CIR) in order to eliminate the effects of the inter-block interference (IBI) and inter-carrier interference (ICI). A considerably long CP is needed if the multipath delay spread is large, resulting in a substantial loss in both bandwidth and power efficiencies. In order to improve the transmission efficiency, MIMO-OFDM systems with insufficient CP have been studied significantly in the past, see, for example, [35, 19, 20, 60, 61, 29, 7], and OFDM/DMT systems with insufficient CP, in, for example, [6, 66, 47]. In [61], an ICI and ISI aware beamforming algorithm is proposed based on the optimal steering vector design that requires the channel state information at the transmitter (CSIT). In [6], a precoding is proposed to eliminate the distortion by processing the information symbols at the transmitter and it also requires the perfect CSIT. Instead of adding sufficient redundancies in the time domain, the technique proposed in [47] adds redundancies in the frequency domain by adding unused subcarriers. Some other techniques have been also proposed in [66, 35, 19, 20, 29, 7].

In a MIMO-OFDM system with insufficient CP, if the IBI from the previous OFDM block can be separated and eliminated, it will be easier to detect the current OFDM block from the desired signal term and the ICI term both of which contain

the information of the current OFDM symbol. Interference alignment (IA) [25, 5, 18] provides a novel concept to deal with interferences. The basic idea of IA is to use well-designed “beamforming” vectors at the transmitter such that the interference vectors are aligned at the receiver in one subspace which is disjoint from the signal subspace. As a result, the interference vectors are separated from the desired signal subspace and are limited in the minimum dimensions and therefore can be eliminated by the zero-forcing operator at the receiver. This basically provides an interference nulling technique.

In this paper, we adopt the notion of interference nulling in a MIMO-OFDM system and treat the IBI part as an interference channel. We propose a channel independent precoding scheme for a MIMO-OFDM system with insufficient CP or even no CP. We show that our proposed precoding scheme can eliminate the IBI caused by the insufficient CP with a higher bandwidth efficiency than the conventional zero-padding or a sufficient CP adding when the number, n_r , of receive antennas is no more than the number, n_t , of transmit antennas, i.e., $n_r \leq n_t$. Interestingly, when $n_t = 1$ and $n_r = 1$, i.e., the single antenna case, in this paper, the IBI incurred from the insufficient CP can be aligned to a subspace of dimensions no more than a half of the difference of the ISI channel length and the insufficient CP length, thus the other half can be used for sending more information symbols. In this paper, it is also shown that when $n_r > n_t$, the IBI can be eliminated similarly without any zero-padding or adding CP or precoding when the OFDM block length is not too small.

The remainder of this paper is organized as follows. The SISO-OFDM and MIMO-OFDM system models are introduced in Section 2.2. Our IA based precoding scheme is proposed in Section 2.3. The relationships of the proposed IA based precoding with the existing block based transmissions are also discussed in Section 2.3. Simulations results with some concrete examples are presented in Section 2.4 to illustrate the theory developed in this paper. Conclusions are given in Section 2.5.

Some notations in this paper are defined as follows: Boldface upper-case letters denote matrices, boldface lower-case letters denote vectors. $\mathbf{0}_{m \times n}$ denotes a zero matrix

with m rows and n columns. The operators $(\cdot)^T$ and $(\cdot)^H$ denote the transpose and Hermitian operations, respectively. $Pr(\cdot)$ denotes probability. $\mathbf{x}(i)$ and $[\mathbf{H}]_{i,j}$ denote the i th entry of a vector \mathbf{x} and the entry at the i th row and the j th column of a matrix \mathbf{H} , respectively. $rank(\cdot)$ stands for the column rank of a matrix and $span\{\cdot\}$ stands for the linearly spanned space of the column vectors of a matrix. Lastly, for any $m \times n$ matrix \mathbf{A} , notation $\mathbf{A} \otimes \mathbf{I}_k$ denotes the $nk \times mk$ Kronecker product of matrix \mathbf{A} and the identity matrix \mathbf{I}_k of size k . $det(\cdot)$ stands for the determinant of a square matrix. v is the CP length, L is the CIR order, and N is the number of subcarriers (or IDFT size).

2.2 System Model

To describe the signal model with concise but necessary notations, let us start with single antenna (single input and single output (SISO)) OFDM systems.

2.2.1 SISO-OFDM Model

Consider a SISO-OFDM system with N subcarriers over a frequency-selective fading channel. The frequency-selective multipath channel is represented by a vector $\mathbf{h} = [h(0), h(1), \dots, h(L)]^T$, where $L + 1$ is the length of the CIR and L is called the order of the CIR. For convenience, these coefficients $h(l)$ are assumed i.i.d. complex Gaussian with 0 mean [15, 1]. In this paper, we assume that $N \geq L$. We use $\mathbf{r}_k = [r_k^0, r_k^1, \dots, r_k^{N-1}]^T$ to denote the input signal vector of the k th OFDM block. Let \mathbf{W}_N denote the normalized IDFT matrix of size N with entries $[\mathbf{W}_N]_{m,n} = (1/\sqrt{N}) \exp(j2\pi mn/N)$. The IDFT operation is performed at the transmitter and changes the input signal from frequency domain to time domain. A CP of length v is appended to each time domain vector. Since CP is generally insufficient in our study, we have $v \leq L$. The transmitted OFDM block is thus affected by both ICI and IBI components. After the insufficient CP is removed at the receiver, the time domain expression of the k th received OFDM block is given, see, for example [6]:

$$\mathbf{y}_k = (\mathbf{H} - \mathbf{A})\mathbf{W}_N \mathbf{r}_k + \mathbf{B}\mathbf{W}_N \mathbf{r}_{k-1} + \mathbf{n}_k, \quad (2.1)$$

where \mathbf{n}_k denotes the time domain received noise vector with the complex Gaussian distribution $\mathcal{CN}(\mathbf{0}, \sigma^2 \mathbf{I})$. The channel matrix \mathbf{H} is a circulant matrix of size $N \times N$, the entry of which at the m th row and the n th column is defined as $[\mathbf{H}]_{m,n} = h((m-n)_N)$, where $(l)_N$ means l modulo N . \mathbf{A} and \mathbf{B} denote the $N \times N$ ICI and IBI components of the channel, respectively, defined as, see, for example [61, 47],

$$\mathbf{A} = \begin{bmatrix} \mathbf{0}_{(L-v) \times (N-L)} & \mathbf{S} & \mathbf{0}_{(L-v) \times v} \\ \mathbf{0}_{(N-L+v) \times (N-L)} & \mathbf{0}_{(N-L+v) \times (L-v)} & \mathbf{0}_{(N-L+v) \times v} \end{bmatrix}, \quad (2.2)$$

$$\mathbf{B} = \begin{bmatrix} \mathbf{0}_{(L-v) \times (N-L+v)} & \mathbf{S} \\ \mathbf{0}_{(N-L+v) \times (N-L+v)} & \mathbf{0}_{(N-L+v) \times (L-v)} \end{bmatrix}, \quad (2.3)$$

where the $(L-v) \times (L-v)$ block matrix \mathbf{S} is defined as:

$$\mathbf{S} = \begin{bmatrix} h(L) & h(L-1) & \cdots & h(v+1) \\ 0 & h(L) & \cdots & h(v+2) \\ \vdots & \ddots & \ddots & \vdots \\ 0 & \cdots & 0 & h(L) \end{bmatrix}. \quad (2.4)$$

In the above equations (2.2) and (2.3), matrices \mathbf{A} and \mathbf{B} are the time domain expressions derived under the assumption of perfect synchronization and a rectangular pulse shape. If CP length v is larger than or equal to the CIR order L , \mathbf{A} and \mathbf{B} are both the all zero matrices. Therefore, no ICI or IBI exists in the received signal. For convenience, we denote the effective channel matrix $\mathbf{C} = \mathbf{H} - \mathbf{A}$ in (2.1), which is

expressed explicitly in the following matrix of size $N \times N$:

$$\mathbf{C} = \begin{bmatrix} h(0) & 0 & \cdots & 0 & \cdots & 0 & h(v) & \cdots & h(1) \\ \vdots & \ddots & \ddots & & \ddots & \vdots & \vdots & \ddots & \vdots \\ \vdots & & \ddots & \ddots & & 0 & h(L) & & h(v) \\ \vdots & & & \ddots & \ddots & & 0 & \ddots & \vdots \\ \vdots & & & & \ddots & \ddots & & \ddots & h(L) \\ h(L) & & & & & \ddots & \ddots & & 0 \\ 0 & \ddots & & & & & \ddots & \ddots & \vdots \\ \vdots & \ddots & \ddots & & & & & \ddots & 0 \\ 0 & \cdots & 0 & h(L) & \cdots & \cdots & h(v-1) & \cdots & h(0) \end{bmatrix}. \quad (2.5)$$

At the receiver, the time domain signal \mathbf{y}_k in (2.1) is transformed into the frequency domain signal \mathbf{z}_k by the DFT matrix \mathbf{W}_N^{-1} of size N . We then have

$$\mathbf{z}_k = \mathbf{W}_N^{-1} \mathbf{C} \mathbf{W}_N \mathbf{r}_k + \mathbf{W}_N^{-1} \mathbf{B} \mathbf{W}_N \mathbf{r}_{k-1} + \tilde{\mathbf{n}}_k, \quad (2.6)$$

where $\tilde{\mathbf{n}}_k = \mathbf{W}_N^{-1} \mathbf{n}_k$, and $\tilde{\mathbf{n}}_k$ is also distributed as $\mathcal{CN}(\mathbf{0}, \sigma^2 \mathbf{I})$.

Since we need to perform a precoding, signal \mathbf{r}_k is the precoded output of an $N \times 1$ vector \mathbf{x}_k of tentative information symbols (some of the components of \mathbf{x}_k may be intentionally set to zero) passing through a precoding matrix \mathbf{P} of size $N \times N$, i.e.,

$$\mathbf{r}_k = \mathbf{P} \mathbf{x}_k. \quad (2.7)$$

We want to emphasize here that unlike the conventional precoding studies, the above precoding matrix \mathbf{P} may not be full rank as we will see later. Since the IDFT matrix \mathbf{W}_N is taken after the precoding matrix \mathbf{P} and it is also a unitary matrix, the design of the precoding matrix \mathbf{P} will be simplified if we consider $\mathbf{W}_N \mathbf{P}$ together. The time domain precoding matrix is defined as $\mathbf{Q} \triangleq \mathbf{W}_N \mathbf{P}$. After the design of \mathbf{Q} , the precoding matrix \mathbf{P} can be obtained by multiplying with the inverse \mathbf{W}_N^{-1} . So, \mathbf{P} and \mathbf{Q} are equivalent and, in what follows, we call both \mathbf{P} and \mathbf{Q} precoders interchangeably.

From (2.6), the received frequency domain signal for the k th OFDM block can be equivalently expressed as:

$$\mathbf{z}_k = \mathbf{W}_N^{-1} \mathbf{C} \mathbf{Q} \mathbf{x}_k + \mathbf{W}_N^{-1} \mathbf{B} \mathbf{Q} \mathbf{x}_{k-1} + \tilde{\mathbf{n}}_k, \quad (2.8)$$

When insufficient CP is used, i.e., $v < L$, the IBI, $\mathbf{W}_N^{-1} \mathbf{B} \mathbf{Q} \mathbf{x}_{k-1}$, as shown in (2.8) causes that not all the information symbols in \mathbf{x}_k can be solved freely. In Section 2.3, we will first explore a SISO-OFDM example and then generalize our result to MIMO-OFDM to see how a precoder can be designed to help to solve for the variables in \mathbf{x}_k and find how many such independent information symbols/variables, that corresponds to the rank of the precoder \mathbf{Q} , can be solved freely.

2.2.2 MIMO-OFDM Model

By considering a MIMO system with n_t transmit, n_r receive antennas, and by using the signal model in the SISO-OFDM system, the model of OFDM with insufficient CP is further extended to MIMO-OFDM in spatial multiplexing mode.

The overall input to the MIMO-OFDM system is noted by $\bar{\mathbf{r}}_k = [(\mathbf{r}_k^0)^T, (\mathbf{r}_k^1)^T, \dots, (\mathbf{r}_k^{N-1})^T]^T$, where \mathbf{r}_k^i denotes the $n_t \times 1$ vector for the n_t transmit antennas at the i th subcarrier, $0 \leq i \leq N - 1$, in frequency domain. Next, the input vector $\bar{\mathbf{r}}_k$ is transformed into time domain signal by n_t IDFT matrices of size N at n_t transmit antennas. The overall IDFT operation over $\bar{\mathbf{r}}_k$ can be represented by $\bar{\mathbf{W}} \triangleq \mathbf{W}_N \otimes \mathbf{I}_{n_t}$. At each transmit antenna, a CP of length v is added to the input signal block and propagates via a multipath channel $\mathbf{h}_{ij} = [h_{ij}(0), h_{ij}(1), \dots, h_{ij}(L)]^T$ between the i th receive antenna and the j th transmit antenna, where we assume that all the entries of \mathbf{h}_{ij} are i.i.d. complex Gaussian random variables with 0 mean and the channel length, $L + 1$, is identical for all the channels. We now define $n_r \times n_t$ channel matrices $\mathbf{H}(l)$, $l = 0, 1, \dots, L$, as

$$\mathbf{H}(l) = \begin{bmatrix} h_{11}(l) & \cdots & h_{1n_t}(l) \\ \vdots & \ddots & \vdots \\ h_{n_r 1}(l) & \cdots & h_{n_r n_t}(l) \end{bmatrix}. \quad (2.9)$$

These matrices $\mathbf{H}(l)$, $l = 0, 1, \dots, L$, are the multipath channel matrices for the time domain vectors \mathbf{r}_k^i serially transmitted at n_t transmit antennas. Due to the randomness of the channel coefficients, all the matrices $\mathbf{H}(l)$ are of full rank almost surely.

At the receiver, the CP is removed and the overall time domain received block is given, for example [19]:

$$\bar{\mathbf{y}}_k = \mathbf{C}\bar{\mathbf{W}}\bar{\mathbf{r}}_k + \mathbf{B}\bar{\mathbf{W}}\bar{\mathbf{r}}_{k-1} + \mathbf{n}_k, \quad (2.10)$$

where \mathbf{n}_k is the $Nn_r \times 1$ noise vector with the complex Gaussian distribution $\mathcal{CN}(\mathbf{0}, \sigma^2\mathbf{I})$, \mathbf{C} and \mathbf{B} of size $Nn_r \times Nn_t$ are the overall channel matrix and IBI matrix, respectively, constructed by stacking submatrices $\mathbf{H}(l)$ in (3.1) in the following way:

$$\mathbf{C} = \begin{bmatrix} \mathbf{H}(0) & \mathbf{0} & \cdots & \mathbf{0} & \cdots & \mathbf{0} & \mathbf{H}(v) & \cdots & \mathbf{H}(1) \\ \vdots & \ddots & \ddots & & \ddots & \vdots & \vdots & \ddots & \vdots \\ \vdots & & \ddots & \ddots & & \mathbf{0} & \mathbf{H}(L) & & \mathbf{H}(v) \\ \vdots & & & \ddots & \ddots & & \mathbf{0} & \ddots & \vdots \\ \vdots & & & & \ddots & \ddots & & \ddots & \mathbf{H}(L) \\ \mathbf{H}(L) & & & & \ddots & \ddots & & & \mathbf{0} \\ 0 & \ddots & & & & & \ddots & \ddots & \vdots \\ \vdots & \ddots & \ddots & & & & & \ddots & \mathbf{0} \\ 0 & \cdots & \mathbf{0} & \mathbf{H}(L) & \cdots & \cdots & \mathbf{H}(v-1) & \cdots & \mathbf{H}(0) \end{bmatrix}, \quad (2.11)$$

$$\mathbf{B} = \begin{bmatrix} \mathbf{0} & \cdots & \mathbf{0} & \mathbf{H}(L) & \cdots & \mathbf{H}(v+1) \\ \vdots & & & \ddots & \ddots & \vdots \\ \vdots & & & & \ddots & \mathbf{H}(L) \\ \vdots & & & & & \mathbf{0} \\ \vdots & & & & & \vdots \\ \mathbf{0} & \cdots & \cdots & \cdots & \cdots & \mathbf{0} \end{bmatrix}. \quad (2.12)$$

Before the signal detection, the DFT operation $\mathbf{W}_N^{-1} \otimes \mathbf{I}_{n_r}$ is applied to $\bar{\mathbf{y}}_k$ yielding the received signal in frequency domain. For this MIMO-OFDM system, the input vector $\bar{\mathbf{r}}_k$ is also the precoded output of information symbol vector $\bar{\mathbf{x}}_k =$

$[(\mathbf{x}_k^0)^T, (\mathbf{x}_k^1)^T, \dots, (\mathbf{x}_k^{N-1})^T]^T$ by an $Nn_t \times Nn_t$ precoding matrix \mathbf{P} , where \mathbf{x}_k^i is the $n_t \times 1$ information symbol vector associated with \mathbf{r}_k^i :

$$\bar{\mathbf{r}}_k = \mathbf{P}\bar{\mathbf{x}}_k \quad (2.13)$$

$$= \mathbf{P}[(\mathbf{x}_k^0)^T, (\mathbf{x}_k^1)^T, \dots, (\mathbf{x}_k^{N-1})^T]^T. \quad (2.14)$$

Again, for the convenience of designing the precoding matrix, we consider the design of precoder $\mathbf{Q} \triangleq \bar{\mathbf{W}}\mathbf{P}$. The precoding matrix \mathbf{P} can then be obtained by multiplying \mathbf{Q} with $\bar{\mathbf{W}}^{-1} = \mathbf{W}_N^{-1} \otimes \mathbf{I}_{n_t}$. So, both \mathbf{P} and \mathbf{Q} are called precoders interchangeably.

Then, we can represent the received frequency domain signal as

$$\bar{\mathbf{z}}_k = (\mathbf{W}_N^{-1} \otimes \mathbf{I}_{n_r})\mathbf{C}\mathbf{Q}\bar{\mathbf{x}}_k + (\mathbf{W}_N^{-1} \otimes \mathbf{I}_{n_r})\mathbf{B}\mathbf{Q}\bar{\mathbf{x}}_{k-1} + \tilde{\mathbf{n}}_k, \quad (2.15)$$

in the k th OFDM block.

2.3 Channel Independent Precoding

The main idea in the following is to design \mathbf{Q} in (2.15) properly to align the received IBI in one subspace of as small dimension as possible which is also disjoint from the subspace occupied by the current information symbols. This coincides with the interference alignment concept[25, 5, 18], which means overlapping all the interference in one subspace and leaving the other subspace free from interference for the desired signal. We initialize the theory in this section by a simple SISO-OFDM example illustration and then provide our main results for MIMO-OFDM.

2.3.1 SISO-OFDM Precoding Example

Go back to the signal model (2.8) or equivalently,

$$\mathbf{y}_k = \mathbf{C}\mathbf{Q}\mathbf{x}_k + \mathbf{B}\mathbf{Q}\mathbf{x}_{k-1} + \mathbf{n}_k. \quad (2.16)$$

For the current k th OFDM block, the signal to solve is \mathbf{x}_k and $\mathbf{B}\mathbf{Q}\mathbf{x}_{k-1}$ is the IBI. For convenience, assume that the additive noise \mathbf{n}_k is negligible. In order to freely solve for \mathbf{x}_k from (2.16), the space \mathcal{V}_{signal} linearly spanned by the column vectors of $\mathbf{C}\mathbf{Q}$ and the space \mathcal{V}_{IBI} linearly spanned by the column vectors of $\mathbf{B}\mathbf{Q}$ need to be disjoint.

For channel matrix \mathbf{C} in (2.5), since its components $h(l)$ are i.i.d., the probability of its determinant, as a function of these random channel coefficients, to be zero is zero. This means that matrix \mathbf{C} is full rank almost surely, i.e., its rank is N almost surely. Its detailed proof is in Lemma 1.

For the IBI matrix \mathbf{B} in (2.3), due to its form in (2.3) and (2.4), its rank (or column rank) is $L - v$ almost surely similarly, where v is the CP length.

Assume that the rank of the precoder \mathbf{Q} is $N - d$ and it is aligned well enough such that the rank of the IBI matrix \mathbf{BQ} is $L - v - d$ almost surely. For example, this can be achieved by setting the last d row vectors of matrix \mathbf{Q} all zero vectors. With such a precoder \mathbf{Q} , the rank of \mathbf{CQ} is $N - d$ almost surely. In order for the spaces \mathcal{V}_{signal} and \mathcal{V}_{IBI} to be disjoint, the sum of their ranks has to be not more than the vector size N , i.e.,

$$N - d + L - v - d \leq N. \quad (2.17)$$

With this dimension requirement, due to the randomness of the coefficients $h(l)$ in matrix \mathbf{C} in (2.5) and matrix \mathbf{B} in (2.3) and (2.4), the spaces \mathcal{V}_{signal} and \mathcal{V}_{IBI} are disjoint almost surely and $N - d$ variables in $\mathbf{CQ}\mathbf{x}_k$ (or in \mathbf{x}_k) can be solved freely.

What the inequality (2.17) means is that the precoding \mathbf{Q} sacrifices d dimensions and uses these d dimensions to align the IBI into a space of dimension $L - v - d$. From (2.17), one can solve for d :

$$d \geq \frac{L - v}{2},$$

and the smallest d is

$$d = \frac{L - v}{2}, \quad (2.18)$$

and in this case, the dimension of the space spanned by the IBI is also $(L - v)/2$. Note that v is the CP length and L is CIR order. In the conventional OFDM system (or unprecoded OFDM system), additional $L - v$ zeros or redundant symbols are needed to make the IBI disappear. From the above analysis, only half of $L - v$ zeros or redundant symbols are needed to separate the spaces of the signal and the IBI for the signal to be solved freely.

To see a particular example for the above SISO-OFDM precoding idea, let us consider the case when $N = 64$ subcarriers, CIR length $L + 1 = 17$, i.e., $L = 16$, and the insufficient CP length $v = 12$. The time domain input to the OFDM system is precoded by a 64×64 precoding matrix \mathbf{Q} . From (2.18), $d = 2$. Consider the following precoder

$$\mathbf{Q} = [\mathbf{e}_{61} \ \mathbf{e}_{62} \ \mathbf{e}_1 \ \cdots \ \mathbf{e}_{60} \ \mathbf{0} \ \mathbf{0}], \quad (2.19)$$

where $\mathbf{e}_i \triangleq \underbrace{[0, \dots, 0, 1, 0, \dots, 0]^T}_{i-1}$, $1 \leq i \leq 64$, is a set of 64×1 orthonormal vectors.

It is easy to verify that $\text{rank}(\mathbf{CQ}) = 62$, $\text{rank}(\mathbf{BQ}) = 2$, and the column vectors of \mathbf{CQ} are linearly independent of the only two nonzero column vectors $[h(0), 0, \dots, 0]^T$ and $[h(0), h(1), 0, \dots, 0]^T$ of \mathbf{BQ} , almost surely. In this example, 62 independent information symbols can be solved freely. With CP length $v = 12$, in the conventional OFDM of block size $N = 64$, 4 more zeros or redundant symbols in the OFDM block are needed to completely eliminate the IBI, and thus only 60 independent information symbols can be included.

The detailed theory and the precoder construction will be given in the following subsection in a general form for MIMO-OFDM systems.

2.3.2 MIMO-OFDM Channel Independent Precoding

In this subsection, we present a general theory and precoder construction for MIMO-OFDM systems by generalizing the idea discussed in the previous subsection.

For MIMO-OFDM systems, we can see from (3.2), (3.3) and (3.4) that the IBI term from the previous OFDM block needs to be suppressed and in the meantime the current OFDM block should be preserved. To do so, the same as the SISO-OFDM case, the basic idea is to design the precoding matrix \mathbf{Q} such that the IBI can be aligned to an interference subspace which is disjoint from the signal subspace (spanned by signal vectors with the independent information symbols in $\bar{\mathbf{x}}_k$) that then can be solved freely as discussed in the preceding subsection. Furthermore, the dimensions of the interference subspace should be minimized, while the signal subspace occupies as

many dimensions as possible in the receive signal space so that as many independent information symbols can be solved freely (without interference) as possible. For this purpose, the design criteria can be summarized as

- $\text{span}\{\mathbf{CQ}\} \cap \text{span}\{\mathbf{BQ}\} = \{\mathbf{0}\}$;
- $\text{dim}(\mathbf{BQ})$ should be as small as possible;
- $\text{dim}([\mathbf{CQ} \ \mathbf{BQ}]) \leq n_r N$,

where dim means the dimension of the space linearly spanned by the column vectors of the matrix, which is the same as the column rank of the matrix. We next consider the problem in two different cases for the numbers n_t and n_r of transmit and receive antennas, respectively.

2.3.3 Precoding When $n_r \leq n_t$

In this case, we will design the precoding based on the fact that matrix \mathbf{C} is full row rank almost surely. For the completeness of the context, this fact is summarized in the following lemma.

Lemma 1 *For the effective channel matrix \mathbf{C} of the SISO case in (2.5) or for the effective channel matrix \mathbf{C} of the generalized MIMO case in (3.3), \mathbf{C} is full rank almost surely, i.e.,*

$$\Pr(\text{rank}(\mathbf{C}) \neq n_r N) = 0.$$

Proof: Let us first consider the SISO-OFDM case for channel matrix \mathbf{C} in (2.5). By observing the determinant expansion of the channel matrix \mathbf{C} in (2.5), we notice that there is one term, $(h(0))^N$, in the determinant, which is resulted from multiplying all the N entries on the main diagonal of matrix \mathbf{C} . Furthermore, we check all other non-zero terms in the determinant expansion and conclude that all these terms are products of N entries with $h(0)$ appearing strictly less than N times. As a result, the expansion of the determinant of channel matrix \mathbf{C} can be expressed as

$$\det(\mathbf{C}) = (h(0))^N + \tau_1 (h(0))^{N-1} + \cdots + \tau_{N-1} h(0) + \tau_N, \quad (2.20)$$

where $\tau_i, i = 1, \dots, N$, is a polynomial of degree i consisting of $h(1), \dots, h(L)$. Since $(h(0))^N$ is the non-zero term in the determinant expansion in (2.20), $\det(\mathbf{C})$ is $h(0)$'s polynomial of degree N . In our system model, channel coefficients $h(0), \dots, h(L)$ are assumed i.i.d. complex Gaussian distributed, therefore the resultant polynomial in (2.20) is a continuously distributed random variable and furthermore $\det(\mathbf{C}) = 0$ occurs with zero probability. This means that channel matrix \mathbf{C} is almost surely full rank.

For the general MIMO-OFDM case with channel matrix \mathbf{C} in (3.3), every channel coefficient $h(i)$ above is replaced by a channel coefficient matrix $\mathbf{H}(i)$ in (3.1) of size $n_r \times n_t$ with i.i.d. components $h_{mn}(i)$. In this case, we permute the block matrix \mathbf{C} row and column wisely such that the permuted matrix is another block matrix where the (m, n) th subblock is the SISO-OFDM matrix \mathbf{C}_{mn} in (2.5) with channel coefficients $h_{mn}(l)$. As what is just proved, every such a subblock \mathbf{C}_{mn} has full rank almost surely, i.e., its columns or rows are almost surely linearly independent. Since all these subblocks \mathbf{C}_{mn} are independent each other and all complex Gaussian distributed, the overall block matrix \mathbf{C} 's rows or columns are almost surely linearly independent, i.e., full rank. ■

The IBI matrix \mathbf{B} in (3.4) is a block upper-triangular matrix and the upper right corner submatrix of \mathbf{B} is \mathbf{B}_s :

$$\mathbf{B}_s = \begin{bmatrix} \mathbf{H}(L) & \cdots & \cdots & \mathbf{H}(v+1) \\ 0 & \ddots & & \vdots \\ \vdots & \ddots & \ddots & \vdots \\ 0 & \cdots & 0 & \mathbf{H}(L) \end{bmatrix}, \quad (2.21)$$

which is of full (row) rank almost surely. Our goal is to design the precoding to cope with this $n_r(L-v) \times n_t(L-v)$ submatrix \mathbf{B}_s . To do so, the $n_t N \times n_t N$ precoding matrix \mathbf{Q} is partitioned into submatrices:

$$\mathbf{Q} = [\mathbf{Q}_1 \quad \mathbf{Q}_2] = \begin{bmatrix} \mathbf{Q}_{11} & \mathbf{Q}_{12} \\ \mathbf{Q}_{21} & \mathbf{Q}_{22} \end{bmatrix}, \quad (2.22)$$

where \mathbf{Q}_{21} and \mathbf{Q}_{22} are of the sizes $n_t(L - v) \times n_1$ and $n_t(L - v) \times n_2$, respectively. These two submatrices have the same number of rows as that of the columns of \mathbf{B}_s and they are designed to suppress the IBI. The size of \mathbf{Q}_{11} is $n_t(N - L + v) \times n_1$ and the size of \mathbf{Q}_{12} is $n_t(N - L + v) \times n_2$. Submatrices \mathbf{Q}_{11} and \mathbf{Q}_{12} should be designed to achieve more transmission rate, i.e., to have signal space dimension as large as possible. \mathbf{Q}_1 and \mathbf{Q}_2 are defined as $\mathbf{Q}_1 = [\mathbf{Q}_{11}^T \quad \mathbf{Q}_{21}^T]^T$, $\mathbf{Q}_2 = [\mathbf{Q}_{12}^T \quad \mathbf{Q}_{22}^T]^T$ and $n_1 + n_2 = n_t N$.

Lemma 2 *If $\text{span}\{\mathbf{Q}_{22}\} \subset \text{span}\{\mathbf{Q}_{21}\}$, $n_1 \leq n_r(L - v)$, and \mathbf{Q}_{21} is full column rank, then, we have (almost surely)*

$$\text{rank}(\mathbf{BQ}) = \text{rank}(\mathbf{B}_s \mathbf{Q}_{21}) = n_1. \quad (2.23)$$

Proof:

$$\mathbf{BQ} = \begin{bmatrix} \mathbf{0} & \mathbf{B}_s \\ \mathbf{0} & \mathbf{0} \end{bmatrix} \begin{bmatrix} \mathbf{Q}_{11} & \mathbf{Q}_{12} \\ \mathbf{Q}_{21} & \mathbf{Q}_{22} \end{bmatrix} = \begin{bmatrix} \mathbf{B}_s \mathbf{Q}_{21} & \mathbf{B}_s \mathbf{Q}_{22} \\ \mathbf{0} & \mathbf{0} \end{bmatrix}.$$

Let $\mathbf{q}_{21}^1, \dots, \mathbf{q}_{21}^{n_1}$ and $\mathbf{q}_{22}^1, \dots, \mathbf{q}_{22}^{n_2}$ be the column vectors of \mathbf{Q}_{21} and \mathbf{Q}_{22} , respectively.

Then, $\mathbf{B}_s \mathbf{Q}_{21}$ and $\mathbf{B}_s \mathbf{Q}_{22}$ can be expressed as

$$\begin{aligned} \mathbf{B}_s \mathbf{Q}_{21} &= [\mathbf{B}_s \mathbf{q}_{21}^1 \quad \mathbf{B}_s \mathbf{q}_{21}^2 \quad \dots \quad \mathbf{B}_s \mathbf{q}_{21}^{n_1}], \\ \mathbf{B}_s \mathbf{Q}_{22} &= [\mathbf{B}_s \mathbf{q}_{22}^1 \quad \mathbf{B}_s \mathbf{q}_{22}^2 \quad \dots \quad \mathbf{B}_s \mathbf{q}_{22}^{n_2}]. \end{aligned}$$

From $\text{span}(\mathbf{Q}_{22}) \subset \text{span}(\mathbf{Q}_{21})$, we have

$$\text{span}\{\mathbf{B}_s \mathbf{q}_{22}^1, \mathbf{B}_s \mathbf{q}_{22}^2, \dots, \mathbf{B}_s \mathbf{q}_{22}^{n_2}\} \subset \text{span}\{\mathbf{B}_s \mathbf{q}_{21}^1, \mathbf{B}_s \mathbf{q}_{21}^2, \dots, \mathbf{B}_s \mathbf{q}_{21}^{n_1}\}.$$

Thus, we have proved the first equality in (2.23). The second equality in (2.23) is because matrix \mathbf{B}_s in (2.21) has full row rank, $n_r(L - v)$, almost surely and $n_1 \leq n_r(L - v)$. \blacksquare

In the MIMO-OFDM system with n_t transmit and n_r receive antennas and N subcarriers, for each OFDM block there are total $n_r N$ linear equations after the CP removal. In order to be able to linearly solve for all the information symbols, the number of independent information symbols transmitted through the n_t transmit

antennas should be no more than $n_r N$. In what follows, we always impose this condition to the system. We next consider the following precodings.

(i) When $n_t(N - L + v) < n_r N$, we design the precoding matrix \mathbf{Q} with the following properties: 1) $\text{span}\{\mathbf{Q}_{22}\} \subset \text{span}\{\mathbf{Q}_{21}\}$; 2) Take

$$n_1 \triangleq \lfloor \frac{n_r N - n_t(N - L + v)}{2} \rfloor. \quad (2.24)$$

Both \mathbf{Q}_1 and \mathbf{Q}_{21} are full column rank;

3) Submatrix \mathbf{Q}_{12} has $n_t(N - L + v)$ linearly independent column vectors, say the first $n_t(N - L + v)$ column vectors in \mathbf{Q}_{12} are linearly independent;

4) The first $n_t(N - L + v)$ column vectors of \mathbf{Q}_2 do not belong to $\text{span}\{\mathbf{Q}_1\}$.

To show the feasibility of the above precoder \mathbf{Q} design, we need to show the feasibility of the design of the submatrices \mathbf{Q}_{21} and \mathbf{Q}_1 that are full column rank required in 2) and the feasibility of the design of the submatrix \mathbf{Q}_{12} that can have $n_t(N - L + v)$ linearly independent columns required in 3). From (2.24) and $n_r \leq n_t$, we have the following inequality:

$$n_1 = \lfloor \frac{n_r N - n_t(N - L + v)}{2} \rfloor \leq \lfloor \frac{n_r(L - v)}{2} \rfloor \leq n_t(L - v). \quad (2.25)$$

This means that the number of columns of \mathbf{Q}_{21} (also \mathbf{Q}_1) is no more than the number of rows of \mathbf{Q}_{21} (also \mathbf{Q}_1), which implies that a full column rank \mathbf{Q}_{21} (also \mathbf{Q}_1) can be designed. In the meantime, we have

$$n_2 = n_t N - n_1 \geq n_t N - n_t(L - v) = n_t(N - L + v).$$

This shows that \mathbf{Q}_{12} is a fat matrix. Since its number of columns, n_2 , is greater than or equal to its number of rows, $n_t(N - L + v)$, \mathbf{Q}_{12} can always be designed to be full row rank, which means that the column rank, i.e., the number of linearly independent columns, can be $n_t(N - L + v)$.

(ii) When $n_t(N - L + v) \geq n_r N$, the precoding matrix \mathbf{Q} is designed as follows. We design $[\mathbf{Q}_{11} \quad \mathbf{Q}_{12}]$ to be full row rank that is $n_t(N - L + v)$, and set $\mathbf{Q}_{21} = \mathbf{Q}_{22} = \mathbf{0}$. Thus,

$$\mathbf{Q} = \mathbf{\Pi} \begin{bmatrix} \mathbf{Q}_{11} & \mathbf{Q}_{12} \\ \mathbf{0} & \mathbf{0} \end{bmatrix}, \quad (2.26)$$

where $\mathbf{\Pi}$ is a permutation matrix. When $n_r(L + 1) \geq n_t$, we can choose $\mathbf{\Pi} = \mathbf{I}$. When $n_r(L + 1) < n_t$, $\mathbf{\Pi}$ is chosen to make \mathbf{CQ} and \mathbf{BQ} satisfy the rank requirements.

With the above precoding, we have the following result.

Lemma 3 *The subspace $\text{span}\{\mathbf{CQ}\}$ and subspace $\text{span}\{\mathbf{BQ}\}$ are disjointed almost surely, i.e., we have*

$$\text{span}\{\mathbf{CQ}\} \cap \text{span}\{\mathbf{BQ}\} = \{\mathbf{0}\}, \quad (2.27)$$

with probability one.

Proof: We also first consider the SISO-OFDM case, the IBI matrix \mathbf{B} is specified in (2.3) and (2.4) and the channel matrix \mathbf{C} is defined in (2.5). We restate that $n_1 = \lfloor (L - v)/2 \rfloor$, $n_\alpha = N - L + v$ and $n_\beta = n_1 + n_\alpha$. Consider the design example with $\mathbf{Q}_z = \mathbf{0}$, i.e., $\mathbf{Q}' = [\mathbf{e}_{n_\alpha+1}, \dots, \mathbf{e}_{n_\beta}, \mathbf{e}_{n_1}, \dots, \mathbf{e}_{n_\alpha}, \mathbf{0}, \dots, \mathbf{0}]$, proposed in this paper previously.

We next first show that $\text{span}\{\mathbf{CQ}'\} \cap \text{span}\{\mathbf{BQ}'\} = \{\mathbf{0}\}$ holds almost surely for this particular precoder \mathbf{Q}' and then we show that it is also true for a general precoder \mathbf{Q} .

Let \mathbf{b}_i and \mathbf{c}_i denote the i th columns of matrices \mathbf{B} and \mathbf{C} , respectively. Without loss of generality, assume that $\{\mathbf{c}_1, \dots, \mathbf{c}_{n_\beta}\}$ is a maximal set of n_β independent columns in \mathbf{CQ}' , and $\{\mathbf{b}_{n_\alpha+1}, \dots, \mathbf{b}_{n_\beta}\}$ is a maximal set of n_1 independent columns in \mathbf{BQ}' . Then, let $\mathbf{B}' = [\mathbf{b}_{n_\alpha+1}, \dots, \mathbf{b}_{n_\beta}]$ that is an $N \times n_1$ matrix and $\mathbf{C}' = [\mathbf{c}_1, \dots, \mathbf{c}_{n_\beta}]$ that is an $N \times n_\beta$ matrix. We construct an $N \times (n_\beta + n_1)$ matrix $\mathbf{H}_Q = [\mathbf{B}' \quad \mathbf{C}']$. Notice that when $L - v$ is even, $n_\beta + n_1 = N$, \mathbf{H}_Q is a square matrix. When $L - v$ is odd, $n_\beta + n_1 = N - 1$. But for this proof we only need to show that \mathbf{H}_Q is full column rank, i.e., the column rank of \mathbf{H}_Q is $n_1 + n_\beta$, almost surely.

and

$$\mathbf{H}_Q^{(2)} = \begin{bmatrix} h(0) & & & h(v) & \dots & h(L-v-n_1+1) \\ \vdots & \ddots & & \vdots & & \vdots \\ h(n_1-1) & & \ddots & h(L) & & \vdots \\ h(n_1) & & h(0) & & \ddots & \vdots \\ \vdots & & \vdots & \ddots & & h(L) \\ \vdots & & \vdots & h(0) & & \\ h(L) & & \vdots & & \ddots & \\ & \ddots & \vdots & & & h(0) \\ & & \ddots & \vdots & & \vdots \\ & & & h(L) & \dots & h(v-1) & \dots & h(L-v-n_1) \end{bmatrix}. \quad (2.31)$$

We only prove that \mathbf{H}_Q has a full column rank when $n_1 \geq v$ here. Applying the same argument, the case when $n_1 < v$ can be proved too.

First, we denote the upper-left $n_1 \times n_1$ submatrix in (2.28) as

$$\mathbf{H}_1 = \begin{bmatrix} h(L) & \dots & h(L-n_1+1) \\ & \ddots & \vdots \\ & & h(L) \end{bmatrix}. \quad (2.32)$$

Since $\det(\mathbf{H}_1) = (h(L))^{n_1}$, this matrix is almost surely full rank.

Next, we perform column elementary operations on \mathbf{H}_Q in (2.28). Using the first n_1 columns, all the non-zero entries from the (n_1+1) th to the last column of the first n_1 rows can be eliminated without influencing the entries below the n_1 th row.

Thus, we transform \mathbf{H}_Q into \mathbf{H}'_Q which has the identical column rank:

$$\mathbf{H}'_Q = \begin{bmatrix} h(L) & \dots & h(L - n_1 + 1) & 0 & \dots & \dots & 0 \\ & \ddots & \vdots & \vdots & & & \\ & & h(L) & 0 & \dots & \dots & 0 \\ & & & h(n_1) & \dots & h(0) & \\ & & & \vdots & & \vdots & \ddots \\ & & & h(L) & & \vdots & h(0) \\ & & & & \ddots & \vdots & \vdots \\ & & & & & h(L) & \dots & h(L - v - n_1) \end{bmatrix}. \quad (2.33)$$

Take the entries in \mathbf{H}'_Q with both row and column indices belonging to $\{n_1 + 1, \dots, n_1 + n_\beta\}$ to form the Toeplitz submatrix \mathbf{H}_2 :

$$\mathbf{H}_2 = \begin{bmatrix} h(n_1) & \dots & h(0) & & \\ \vdots & \ddots & & \ddots & \\ h(L) & & \ddots & & h(0) \\ & \ddots & & \ddots & \vdots \\ & & h(L) & \dots & h(n_1) \end{bmatrix}. \quad (2.34)$$

Define

$$\mathbf{H}_a = \begin{bmatrix} \mathbf{H}_1 & \mathbf{0} \\ \mathbf{0} & \mathbf{H}_2 \end{bmatrix}. \quad (2.35)$$

\mathbf{H}_a is just \mathbf{H}'_Q when $L - v$ is even or \mathbf{H}_a is the $(n_1 + n_\beta) \times (n_1 + n_\beta)$ submatrix in \mathbf{H}'_Q by deleting the last row of \mathbf{H}'_Q when $L - v$ is odd.

Now compute the determinant of \mathbf{H}_2 . We similarly expand the determinant as a polynomial of $h(n_1)$,

$$\det(\mathbf{H}_2) = (h(n_1))^{n_\beta} + \gamma_1 (h(n_1))^{n_\beta - 1} + \dots + \gamma_{N-1} h(n_1) + \gamma_N \quad (2.36)$$

where γ_i , $i = 1, \dots, n_\beta$ is a polynomial of degree i consisting of $h(0), \dots, h(n_1 - 1), h(n_1 + 1), \dots, h(L)$. Thus, $\det(\mathbf{H}_2) = 0$ with zero probability, i.e., \mathbf{H}_2 is almost

surely full rank and hence \mathbf{H}_a is almost surely full rank or \mathbf{H}'_Q and \mathbf{H}_Q are almost surely full column rank. Therefore, we have $\text{span}\{\mathbf{CQ}'\} \cap \text{span}\{\mathbf{BQ}'\} = \{\mathbf{0}\}$ almost surely.

For a general precoder \mathbf{Q} that satisfies all the design requirements, we can give a structure of such a precoder:

$$\mathbf{Q} = \begin{bmatrix} \mathbf{Q}_u & \mathbf{0} \\ \mathbf{0} & \mathbf{0} \end{bmatrix}. \quad (2.37)$$

where \mathbf{Q}_u is an $n_\beta \times n_\beta$ nonzero submatrix. Due to the special structure of \mathbf{Q}' , it can be easily seen that each column of \mathbf{CQ} is a linear combination of the maximal independent column set $\{\mathbf{c}_1, \dots, \mathbf{c}_{n_\beta}\}$ of \mathbf{CQ}' and each column of \mathbf{BQ} is a linear combination of $\{\mathbf{b}_{n_\alpha+1}, \dots, \mathbf{b}_{n_\beta}\}$. This means $\text{span}\{\mathbf{CQ}\} \cap \text{span}\{\mathbf{BQ}\} = \{\mathbf{0}\}$ also holds almost surely.

The general MIMO-OFDM case can be proved similarly by using the same argument as in the SISO-OFDM case. \blacksquare

Theorem 1 *For the insufficient CP MIMO-OFDM system with $n_r \leq n_t$, the total number of independent information symbols can be solved by the zero-forcing operator during each OFDM block is*

$$\begin{cases} n_t(N - L + v) + \lfloor \frac{n_r N - n_t(N - L + v)}{2} \rfloor, & \text{if } n_t(N - L + v) < n_r N, \\ n_r N, & \text{if } n_t(N - L + v) \geq n_r N. \end{cases} \quad (2.38)$$

Proof: We first consider the case when $n_t(N - L + v) < n_r N$.

From the above precoder property 2) we have almost surely (since matrix \mathbf{C} is almost surely full row rank and from (2.24), one can see that the number of rows of \mathbf{C} , $n_r N > n_1$)

$$\text{rank}(\mathbf{CQ}_1) = n_1. \quad (2.39)$$

From the precoder property 3) and the number of rows of \mathbf{C} , $n_r N$ is greater than $n_t(N - L + v)$, we can derive (almost surely)

$$\text{rank}(\mathbf{CQ}_2) = n_t(N - L + v). \quad (2.40)$$

From the precoder property 4), we know that $\text{span}\{\mathbf{Q}_1\} \cap \text{span}\{\mathbf{Q}_2\} = \{\mathbf{0}\}$. As a result,

$$\begin{aligned} \text{rank}(\mathbf{CQ}) &= \text{rank}(\mathbf{CQ}_1) + \text{rank}(\mathbf{CQ}_2) \\ &= n_1 + n_t(N - L + v). \end{aligned} \quad (2.41)$$

With the properties 1) and 2) and (2.25), we have the result (2.23) in Lemma 2, i.e.,

$$\text{rank}(\mathbf{BQ}) = n_1.$$

Thus,

$$\begin{aligned} \text{rank}(\mathbf{BQ}) + \text{rank}(\mathbf{CQ}) &= 2n_1 + n_t(N - L + v) \\ &= 2 \lfloor \frac{n_r N - n_t(N - L + v)}{2} \rfloor + n_t(N - L + v) \leq n_r N. \end{aligned} \quad (2.42)$$

From lemma 3, the following equation holds almost surely:

$$\text{span}\{\mathbf{CQ}\} \cap \text{span}\{\mathbf{BQ}\} = \{\mathbf{0}\}. \quad (2.43)$$

With the zero-forcing operator, the number of independent information symbols that can be solved equals to the dimension of the desired signal subspace that is the column rank of \mathbf{CQ} , i.e.,

$$n_t(N - L + v) + \lfloor \frac{n_r N - n_t(N - L + v)}{2} \rfloor,$$

in one OFDM block for all n_t transmit antennas.

We next consider the case when $n_t(N - L + v) \geq n_r N$. In this case, from the precoder design, we have $\text{rank}([\mathbf{Q}_{11} \ \mathbf{Q}_{12}]) \geq n_t(N - L + v) \geq n_r N$. Thus, $\text{rank}(\mathbf{CQ}) = n_r N$, since \mathbf{C} is full row rank almost surely. Furthermore, $\mathbf{BQ} = \mathbf{0}$, i.e., the IBI is totally eliminated. Since there are total $n_r N$ linear equations, the number of independent information symbols transmitted through the n_t transmit antennas should be no more than $n_r N$ to linearly solve for all the information symbols. ■

From (2.42) in the above proof, one can see that the number of a part of independent information symbols, n_1 , can not be larger, since otherwise the sum of the

numbers of columns in matrices \mathbf{BQ} and \mathbf{CQ} will be more than the number of rows, i.e., will exceed the receive signal space dimension. This implies that $n_1 = \lfloor \frac{n_r N - n_t(N-L+v)}{2} \rfloor$ in (2.24) in 2) is optimal already. We next present a precoder example for \mathbf{Q} .

Example 1: ($n_t = n_r$ case) For the $n_t N$ dimensional vector space, $\{\mathbf{e}_1, \mathbf{e}_2, \dots, \mathbf{e}_{n_t N}\}$ is a set of $n_t N \times 1$ orthonormal basis elements where $\mathbf{e}_i = [0, \dots, 0, 1, 0, \dots, 0]^T$ is as before. Let

$$\mathbf{Q}_2 = [\mathbf{e}_1, \dots, \mathbf{e}_{n_t(N-L+v)}, \mathbf{e}_1, \dots, \mathbf{e}_1] = [\mathbf{e}_1, \dots, \mathbf{e}_{n_\alpha}, \overbrace{\mathbf{e}_1, \dots, \mathbf{e}_1}^{n_t N - n_1 - n_\alpha}], \quad (2.44)$$

$$\mathbf{Q}_1 = [\mathbf{e}_{n_t(N-L+v)+1}, \dots, \mathbf{e}_{n_t(N-L+v)+n_1}] = [\mathbf{e}_{n_\alpha+1}, \dots, \mathbf{e}_{n_\beta}], \quad (2.45)$$

where n_1 is defined in (2.24) and for simplicity, we denote

$$n_\alpha \triangleq n_t(N-L+v), \quad n_\beta \triangleq n_\alpha + n_1.$$

In this example, \mathbf{Q}_{12} contains an identity matrix of size n_α , i.e.,

$$\mathbf{Q}_{12} = [\mathbf{I}_{n_\alpha}, \tilde{\mathbf{e}}_1, \dots, \tilde{\mathbf{e}}_1], \quad (2.46)$$

where $\tilde{\mathbf{e}}_1 = [1, 0, \dots, 0]^T$ is an $n_\alpha \times 1$ vector. Thus, the precoder property 3) is satisfied. The orthogonality among \mathbf{e}_i , $i = 1, \dots, n_t N$, ensures the precoder properties 2) and 4). Lastly, \mathbf{Q}_{22} is a zero matrix now and therefore $\text{span}\{\mathbf{Q}_{22}\} \subset \text{span}\{\mathbf{Q}_{21}\}$, i.e., the precoder property 1) holds as well. Interestingly, the submatrix \mathbf{Q}_{21} here is not a zero matrix. Also note that, the last $(n_t N - n_1 - n_\alpha)$ columns in \mathbf{Q}_2 in (2.44) do not have to be all \mathbf{e}_1 and in fact, they can be any vectors, for example, all zero vectors, which does not affect the precoder design properties 1)-4). It is noticeable that the SISO-OFDM precoder example in (2.19) satisfies these 4 properties and exhibits a special case of the above precoder design.

Using the precoder defined in (2.44)-(2.45), we are able to specify the final signals to be transmitted at the n_t transmit antennas when $x_k(n)$ are independent information symbols as follows. In this example, n_β is the number of total independent information symbols to be transmitted through n_t transmit antennas in every *data block* of length N where there are total $n_t N - n_\beta$ zeros inserted in the block. Every

data block of length N is preceded by a CP of length v . The overall *transmission block* length is $N + v$.

Firstly, for each time index k , all n_β independent information symbols, $x_k(n)$, $0 \leq n \leq n_\beta - 1$, are padded with $n_t N - n_\beta$ zeros to yield

$$\bar{\mathbf{x}}_k = [x_k(0), x_k(1), \dots, x_k(n_\beta - 1), 0, \dots, 0]^T, \quad (2.47)$$

which is then fed to $\mathbf{Q}\bar{\mathbf{x}}_k$. This is that each of the n_t transmit antennas alternatively takes one symbol from $\bar{\mathbf{x}}_k$ consecutively for N times to fill its data block of length N . To see this, for convenience, let us define

$$\theta \triangleq \lfloor \frac{n_\beta}{n_t} \rfloor \quad \text{and} \quad n_{t1} \triangleq n_\beta - \theta n_t.$$

In this manner, for the first n_{t1} transmit antennas, the j th antenna, $j = 0, \dots, n_{t1} - 1$, transmits the following data block of length N :

$$\bar{\mathbf{x}}_k^j = [x_k(n_t \cdot 0 + j), x_k(n_t \cdot 1 + j), \dots, x_k(n_t \cdot \theta + j), 0, \dots, 0]^T, \quad (2.48)$$

where $N - (\theta + 1)$ zeros are inserted. For the remaining $n_t - n_{t1}$ transmit antennas, the j th antenna, $j = n_{t1}, \dots, n_t - 1$, transmits the following data block of length N :

$$\bar{\mathbf{x}}_k^j = [x_k(n_t \cdot 0 + j), x_k(n_t \cdot 1 + j), \dots, x_k(n_t \cdot (\theta - 1) + j), 0, \dots, 0]^T, \quad (2.49)$$

where $N - \theta$ zeros are inserted. Then, the last v symbols of $\bar{\mathbf{x}}_k^j$ for each antenna j are added in the front of the data block as a CP (usually insufficient in our IA based precoding) for every k th data block of length N . Finally, the k th transmission block of total length $N + v$ with CP is transmitted through all the n_t antennas. More detailed examples are given in the simulations in the next section.

For a general precoder \mathbf{Q} , according to Theorem 1, the number of independent information symbols that can be put in $\bar{\mathbf{x}}_k$ in (3.5) and can be solved with the IBI free is shown in (3.7), which can be encoded as follows. To illustrate it, let us first see the previous example where the precoder $\mathbf{Q} = [\mathbf{Q}_1 \quad \mathbf{Q}_2]$ is shown in (2.44)-(2.45). In this example, all the n_1 columns in \mathbf{Q}_1 plus the first n_α columns,

$\mathbf{e}_1, \dots, \mathbf{e}_{n_\alpha}$, in \mathbf{Q}_2 are linearly independent. We can consider them altogether denoted as $\mathbf{Q}_u = [\mathbf{e}_{n_\alpha+1}, \dots, \mathbf{e}_{n_\beta}, \mathbf{e}_1, \dots, \mathbf{e}_{n_\alpha}]$. This submatrix \mathbf{Q}_u corresponds to the first n_β independent information symbols in $\bar{\mathbf{x}}_k$. The last $n_t N - n_\beta$ columns of \mathbf{Q}_2 are denoted as $\mathbf{Q}_z = [\mathbf{e}_1, \dots, \mathbf{e}_1]$. The last $n_t N - n_\beta$ signals in $\bar{\mathbf{x}}_k$ in (3.5) corresponding to this submatrix \mathbf{Q}_z are aligned in the space spanned by the IBI and can not be solved freely and thus these signals are set to zeros in $\bar{\mathbf{x}}_k$. As a result, the precoder \mathbf{Q} is structured as

$$\mathbf{Q} = [\mathbf{Q}_u \quad \mathbf{Q}_z], \quad (2.50)$$

which can be obtained similarly if the design of \mathbf{Q} follows the general design properties 1) – 4) obtained previously. Note that, as mentioned before, the matrix \mathbf{Q}_z in (2.50) can be anything and does not affect the design properties 1)-4). If we only take the first $K = n_\beta$ columns of the precoder \mathbf{Q} , i.e., if we let $\mathbf{Q}_{n_t N \times K} = \mathbf{Q}_u$ and the signal $\bar{\mathbf{x}}_k$ in (3.5) be of size $K \times 1$ only consisting of n_β independent information symbols, then the precoder encoding is equivalent to

$$\mathbf{Q}_{n_t N \times K} \bar{\mathbf{x}}_k. \quad (2.51)$$

Notice that, for the transmissions in (2.48) and (2.49), the corresponding precoding matrix $\mathbf{Q}_{n_t N \times K} = \mathbf{Q}_u$ is in fact a tall unitary matrix.

Remark: Let us compare the above proposed precoding with the conventional zero-padded system. For convenience, we only consider CP free MIMO-OFDM systems, i.e., $v = 0$ in the above study. In the zero-padded system, among every block of N symbols, L of them are zeros, i.e., in one block of N symbols, only $\min\{n_r N, n_t(N - L)\}$ independent information symbols are transmitted for all n_t transmit antennas, where the reason to take the minimum is because there are only $n_r N$ received signals, i.e., only $n_r N$ linear equations and the number of independent information symbols can be solved linearly can not be above $n_r N$ as we explained before. In comparison, in our channel independent precoded MIMO-OFDM system,

$$\min \left\{ n_r N, n_t(N - L) + \left\lfloor \frac{n_r N - n_t(N - L)}{2} \right\rfloor \right\}$$

independent information symbols can be transmitted and linearly solved freely in one OFDM block across all n_t transmit antennas. Clearly, one can see that, when $n_t \geq n_r > n_t(N - L)/N$, more independent information symbols than the conventional zero-padding MIMO system can be transmitted and solved linearly with free of IBI interference in our channel independent precoded MIMO-OFDM system. A similar argument applies to an insufficient CP added MIMO-OFDM system.

2.3.4 IBI Cancellation When $n_r > n_t$

In this case, we show that no precoding, or CP or zero-padding is needed to eliminate the IBI in the following theorem.

Theorem 2 *For the insufficient CP MIMO-OFDM system with $n_r > n_t$, the total number of independent information symbols can be solved by the zero-forcing operator is $n_t N$, where no zero-padding or precoding is needed, when*

$$N \geq \frac{n_t}{n_r - n_t}(L - v). \quad (2.52)$$

Proof: Since all the channel coefficients are drawn from an i.i.d. continuous distribution, from lemma 1, the dimensions of channel matrix \mathbf{C} and IBI matrix \mathbf{B} are (almost surely)

$$\dim(\mathbf{C}) = n_t N \quad (2.53)$$

$$\dim(\mathbf{B}) = n_t(L - v), \quad (2.54)$$

respectively, while the dimension of the receive signal space is $n_r N$. When the dimension of the receive signal space is not smaller than the sum of the dimensions of the channel matrix \mathbf{C} and IBI matrix \mathbf{B} , i.e.,

$$n_t N + n_t(L - v) \leq n_r N,$$

which is (2.52), it is almost surely that the signal space $\text{span}\{\mathbf{C}\}$ is disjoint from the IBI space $\text{span}\{\mathbf{B}\}$. Thus, all the independent information symbols can be solved by the zero-forcing operator. ■

2.3.5 Relationships With The Existing Block Based Transmission Systems

We now discuss the relationships of our above IA based channel independent precoding scheme with the existing block based transmission systems, namely zero-padded (ZP) only, CP-OFDM and single carrier frequency domain equalizer (SC-FDE). Without loss of generality, for convenience we only consider the SISO configuration, i.e., $n_t = n_r = 1$, for the discussions below.

Let us first consider the ZP-only transmission system, see, for example [68, 64, 42], with information symbol block length M and ZP length L (in order to eliminate the IBI completely). Note that the ZP idea appears in [69, 70] where a precoder in the time domain is

$$\begin{bmatrix} \mathbf{I}_K \\ \mathbf{0}_{(N-K) \times K} \end{bmatrix}, \quad (2.55)$$

which becomes the ZP-only scheme when $K = M$ and $N - K = L$. Comparing to the IA based precoding scheme proposed in the preceding sections to completely eliminate the IBI, we choose $N = M + L$, $K = M$ in (2.51) with $n_t = 1$, and $v = 0$, i.e., no CP is used in this case. The precoding matrix \mathbf{P} is designed as the $N \times K$ submatrix of the $N \times N$ DFT matrix, i.e., the (m, n) th entry of this precoding is expressed as $[\mathbf{P}]_{m,n} = (1/\sqrt{N})\exp(-j2\pi mn/N)$. As a result, we have $\mathbf{Q}_{zp} = \mathbf{W}_N \mathbf{P} = [\mathbf{I}_K, \mathbf{0}_{K \times L}]^T$ that is the same as the precoder (3.10) proposed in [69, 70].

We next consider the CP-OFDM system, i.e., the conventional OFDM system, with information symbol block length M , i.e., the IDFT size M , and CP length L (in order to eliminate the IBI completely). Comparing to the IA based precoding scheme proposed in the preceding sections to completely eliminate the IBI, we choose $N = K = M$ and $v = L$, i.e., full CP length is used in this case. Then, the precoding matrix is the identity matrix, i.e., $\mathbf{P} = \mathbf{I}_N$. In other words, CP-OFDM can be considered as a special case of the IA based precoding in this paper.

We finally consider the SC-FDE system, see for example [56, 9, 13, 46], with information symbol block length M and CP length L (in order to eliminate the IBI completely). Comparing to the IA based precoding scheme proposed in the preceding

sections to completely eliminate the IBI, we choose $N = K = M$ and $v = L$, i.e., full CP length is used in this case. The precoding matrix \mathbf{P} in this case is, however, chosen as the $N \times N$ DFT matrix, i.e., $\mathbf{P} = \mathbf{W}_N^H$. Clearly, in this case, the precoding cancels the IDFT operation, i.e., the transmission matrix \mathbf{Q} is the identity matrix, and thus leads to transmit the information symbols directly. Note that when the CP length $v = L$, i.e., full (or sufficient) CP is used, our proposed precoded system with the precoder example (2.44)-(2.45) always becomes the SC-FDE.

From the above discussions, one can see that the three existing block based transmission systems, ZP-only, CP-OFDM, and SC-FDE systems, can be all considered as special cases of our proposed IA based channel independent precoding scheme in this paper. Interestingly, as we have shown in the preceding sections, with the IA concept we may choose better channel independent precoding matrices \mathbf{P} (or \mathbf{Q}) such that less number of CP or ZP are needed to completely eliminate the IBI caused from the ISI of the channel, when the number of information symbols is fixed. Some concrete examples are given in the simulations in the next section.

2.4 Simulations

In this section, we present some simulation results to validate our proposed IA based channel independent precoding where the precoder in (2.44)-(2.45) is used. In the meantime, some particular and concrete examples of the proposed precoded transmissions are illustrated as well. In the following figures, the SNR at the receiver is accounted.

In Fig. 2.1, we consider the SISO case and depict the BER performances of our proposed IA based precodings with different CP lengths and the numbers of independent information symbols that satisfy Theorem 3, i.e., the IBI can be completely eliminated. In Fig. 2.1, IA stands for the IA based precoding. The simulations in Fig. 2.1 also include the cases of CP-OFDM, ZP-only, and SC-FDE systems. The order of the CIR is $L = 16$ in this simulation. The block length for CP-OFDM, ZP-only, SC-FDE is $N = 64$, i.e., 64 independent information symbols are sent, where full

CP or ZP length, 16, is used. The block length for the proposed IA based precoding is $N = 64$ and the CP lengths are $v = 16, 12, 8, 0$, and the corresponding numbers of independent information symbols $x_k(n)$ are 64, 62, 60, 56, respectively, according to Theorem 3. To illustrate the structure of transmission block in our IA based precoding, the transmission block for the $v = 12$ case in Fig. 2.1 is:

$$\underbrace{[x_k(52), \dots, x_k(61), 0, 0]}_{\text{CP of length } v=12} \underbrace{, x_k(0), x_k(1), \dots, x_k(61), 0, 0]}_{\text{data block of length } N=64}, \quad (2.56)$$

and the transmission block for the $v = 0$ case in Fig. 2.1 is:

$$\underbrace{[x_k(0), x_k(1), \dots, x_k(55), \overbrace{0, \dots, 0}^{8 \text{ zeros}}]}_{\text{data block of length } N=64}. \quad (2.57)$$

As mentioned previously in Section 2.3.5, our IA based precoded system, when the full CP, i.e., $v = 16$, is added, coincides with SC-FDE as also shown in Fig. 2.1 with solid curves marked by \diamond and \times , respectively.

For CP-OFDM, ZP-only, SC-FDE, in order to completely eliminate the IBI, the CP/ZP lengths should be at least all 16, 14, 12, 8, when 64, 62, 60, 56 independent information symbols are sent in a data block of length $N = 64$, respectively, which are clearly higher than the CP lengths 16, 12, 8, 0, in our proposed IA based precoding, respectively, for the last three cases. After saying so, although in all these cases, the IBI can be completely eliminated, their performances are different. One can see that the ZP-only scheme performs the best, since it achieves the full multipath diversity with the MMSE or ZF receiver [64]. In fact, this case is equivalent to the MISO case with quasi-static flat fading channels when the delay diversity code (or Toeplitz code) is used. It is theoretically shown in [72, 37] that this code achieves the full spatial diversity (corresponding to the full multipath diversity in the ISI channel case) with the ZF/MMSE receiver.

In Fig. 2.2, we consider the same SISO case as in Fig. 2.1 with two cases that do not satisfy the condition obtained in Theorem 3. These two cases are when $v = 8$ and $v = 12$ and the numbers of transmitted independent information symbols

in one block are 62 and 64, respectively. The BER performances for these two cases are dashed curves in Fig. 2.2, where one can see that error floors occur when SNR becomes high because the IBI can not be completely eliminated. Notice that when insufficient CP/ZP is added for CP-OFDM, ZP-only or SC-FDE, error floor will also occur because there is residual IBI.

In Fig. 2.3, we simulate the IA based precoding scheme proposed in this paper for the MISO configuration of $n_t = 2$ and $n_r = 1$. We consider both cases of satisfying (solid curves in Fig. 2.3) and not-satisfying (dashed curves in Fig. 2.3) Theorem 3. For the convenience of having the same number of transmitted independent information symbols $x_k(n)$ in both cases, we choose the block size $N = 32$ and the CIR order $L = 19$. In each case, two different CP lengths are considered. We take the $v = 2$ case as an example to specify the transmission block:

$$\begin{bmatrix} 0 & 0 & x_k(0) & x_k(2) & \cdots & x_k(28) & x_k(30) & 0 & \cdots & 0 \\ 0 & 0 & x_k(1) & x_k(3) & \cdots & x_k(29) & 0 & 0 & \cdots & 0 \end{bmatrix}, \quad (2.58)$$

where there are 16 consecutive zeros at the end of each row, each row represents the transmission block at one transmit antenna, and the first two zeros are the CP of length $v = 2$ in each row.

In Fig. 2.4, we simulate the IA based precoding scheme proposed in this paper for a MIMO configuration of four transmit and two receive antennas, i.e., $n_t = 4$ and $n_r = 2$. We also consider both cases of satisfying (solid curves in Fig. 2.4) and not-satisfying (dashed curves in Fig. 2.4) Theorem 3. For the convenience of having the same number of transmitted independent information symbols $x_k(n)$ in both cases, we also choose the block size $N = 32$ and the CIR order $L = 19$. In each case, two different CP lengths are considered. Again, the $v = 2$ case is used as an example to specify the transmission block:

$$\begin{bmatrix} 0 & 0 & x_k(0) & x_k(4) & \cdots & x_k(56) & x_k(60) & 0 & \cdots & 0 \\ 0 & 0 & x_k(1) & x_k(5) & \cdots & x_k(57) & x_k(61) & 0 & \cdots & 0 \\ 0 & 0 & x_k(2) & x_k(6) & \cdots & x_k(58) & 0 & 0 & \cdots & 0 \\ 0 & 0 & x_k(3) & x_k(7) & \cdots & x_k(59) & 0 & 0 & \cdots & 0 \end{bmatrix}, \quad (2.59)$$

where there are 16 consecutive zeros at the end of each row for the first two rows and 17 consecutive zeros at the end of each row for the last two rows, and the first two columns of zeros are the CP of length $v = 2$. Each row of (2.59) is for one transmit antenna. Comparing the results in Fig. 2.3 and Fig. 2.4 for the cases of two transmit and one receive antennas and four transmit and two receive antennas, respectively, we can see that the channels are the same (i.e., the CIR orders L , the CP lengths v , the data block sizes N , and the ratios between the numbers of transmit and receive antennas are the same) but the number of independent information symbols can be solved for the later case almost doubles that of the former case. Although the bandwidth efficiency gets better for more antennas for our precodings, as one can see from these two figures the BER performance degrades, which may be improved by, for example, employing forward error correction coding. Another remark is that the total ZP length for each of the last two transmit antennas in (2.59) is already 19 that is the same as the CIR order L here. In other words, for the last two transmit antennas, the IBIs do not appear. However, since there are four transmit antennas but only two receive antennas, the signals may not be solved freely as in the SISO case.

In Fig. 2.5, we simulate the IA based precoding scheme proposed in this paper for another MIMO configuration of $n_t = 4$, $n_r = 4$. Both cases of satisfying (solid curves in Fig. 2.5) and not-satisfying (dashed curves in Fig. 2.5) are studied. Two different CP lengths are considered for each case. We choose the block size $N = 32$ and CIR order $L = 12$. In the $v = 6$ case, transmission block is specified as

$$\begin{bmatrix} x_k(104) & x_k(108) & x_k(112) & 0 & 0 & 0 & x_k(0) & \cdots & x_k(112) & 0 & 0 & 0 \\ x_k(105) & x_k(109) & x_k(113) & 0 & 0 & 0 & x_k(1) & \cdots & x_k(113) & 0 & 0 & 0 \\ x_k(106) & x_k(110) & x_k(114) & 0 & 0 & 0 & x_k(2) & \cdots & x_k(114) & 0 & 0 & 0 \\ x_k(107) & x_k(111) & x_k(115) & 0 & 0 & 0 & x_k(3) & \cdots & x_k(115) & 0 & 0 & 0 \end{bmatrix}, \quad (2.60)$$

where the first 6 columns are the CP of length $v = 6$. One can see that even more independent information symbols $x_k(n)$ can be sent in this configuration.

2.5 Conclusions

In this paper, we proposed a channel independent precoding for MIMO-OFDM systems with insufficient CP by using the notion of interference nulling that has been also actively used in interference alignment lately. We showed that our proposed precoding is more bandwidth efficient than the conventional zero-padded or CP added MIMO systems, such as, ZP-only, CP-OFDM and SC-FDE systems, when the number of receive antennas is not more than the number of transmit antennas. When the number of receive antennas is more than the number of transmit antennas, it was shown that the IBI in an MIMO-OFDM system can be completely eliminated without any CP or zero-padding or precoding, when the OFDM block size is not too small. The key reason behind these is that instead of making the IBI disappears completely in the conventional sufficient CP or ZP based block transmission systems, the IA based channel independent precoding proposed in this paper aligns the IBI interference subspace disjoint from the signal subspace and then the zero-forcing operator is applied to eliminate the IBI while maintain the signal. Although we only considered CP based block transmission systems in this paper, the theory developed in this paper can be easily generalized to ZP based block transmission systems.

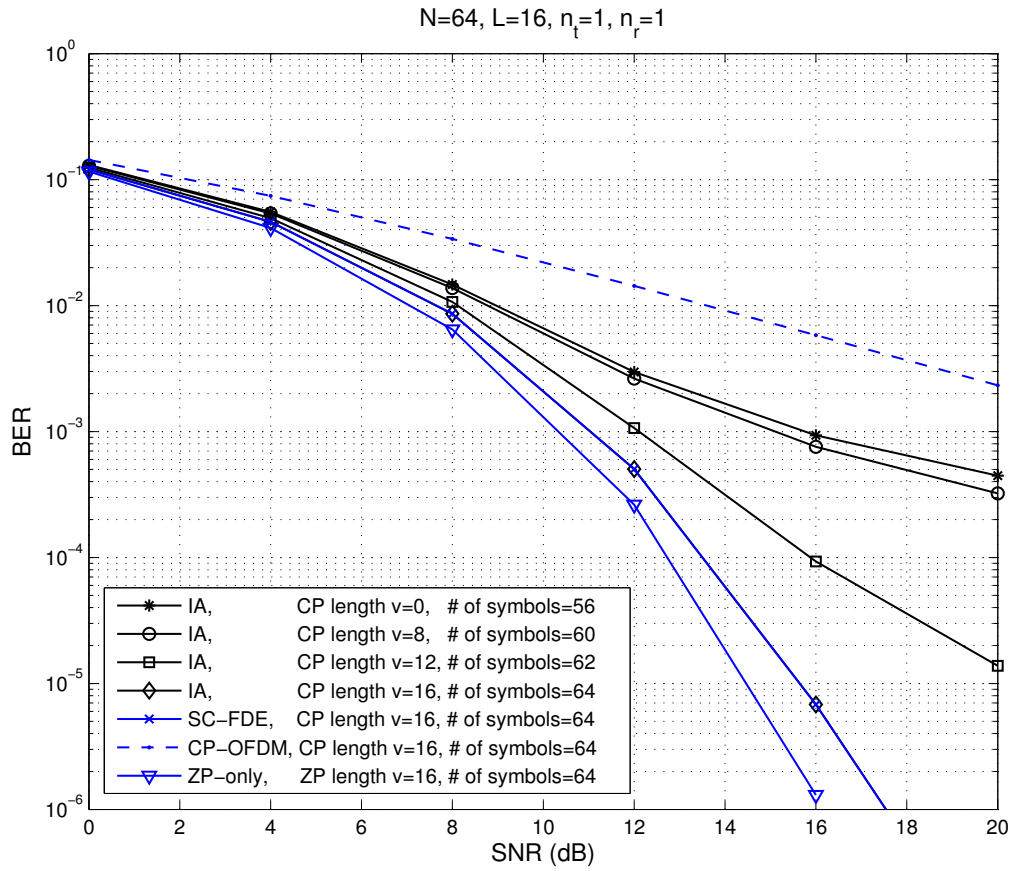


Figure 2.1: BER performances of the IA based precoding, SC-FDE, CP-OFDM, ZP-only

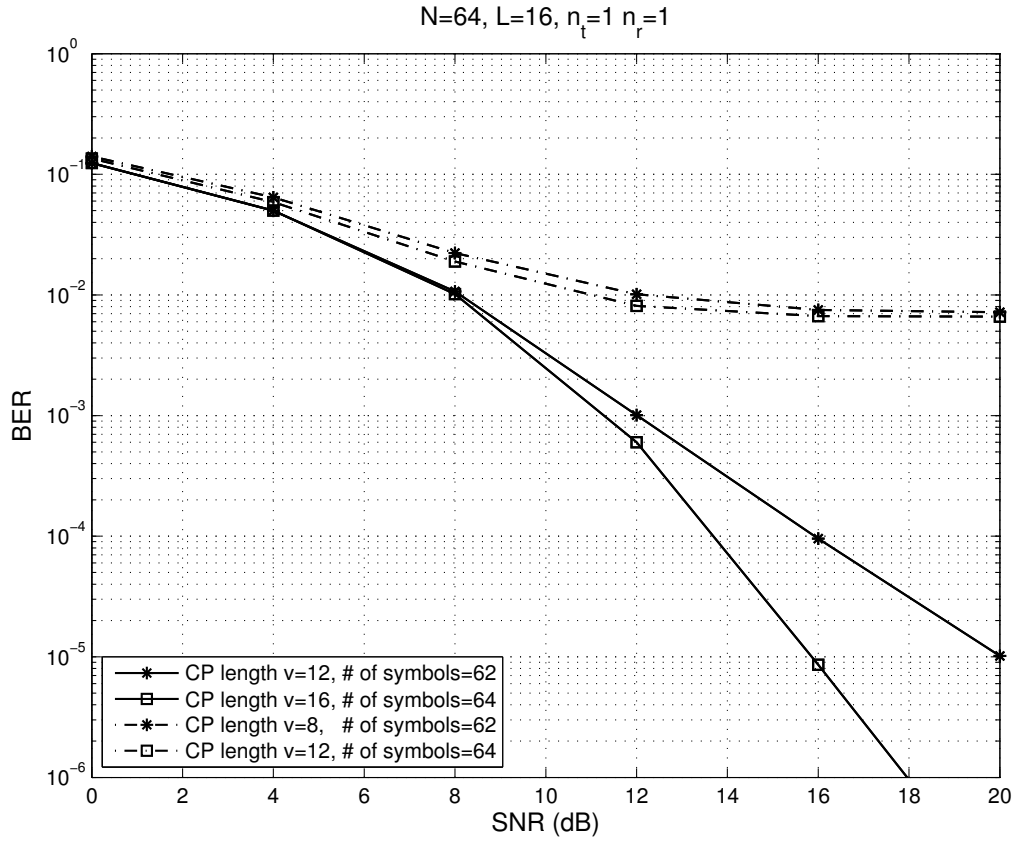


Figure 2.2: SISO case: BER performances of IA based precoding of different CP lengths and different numbers of information symbols

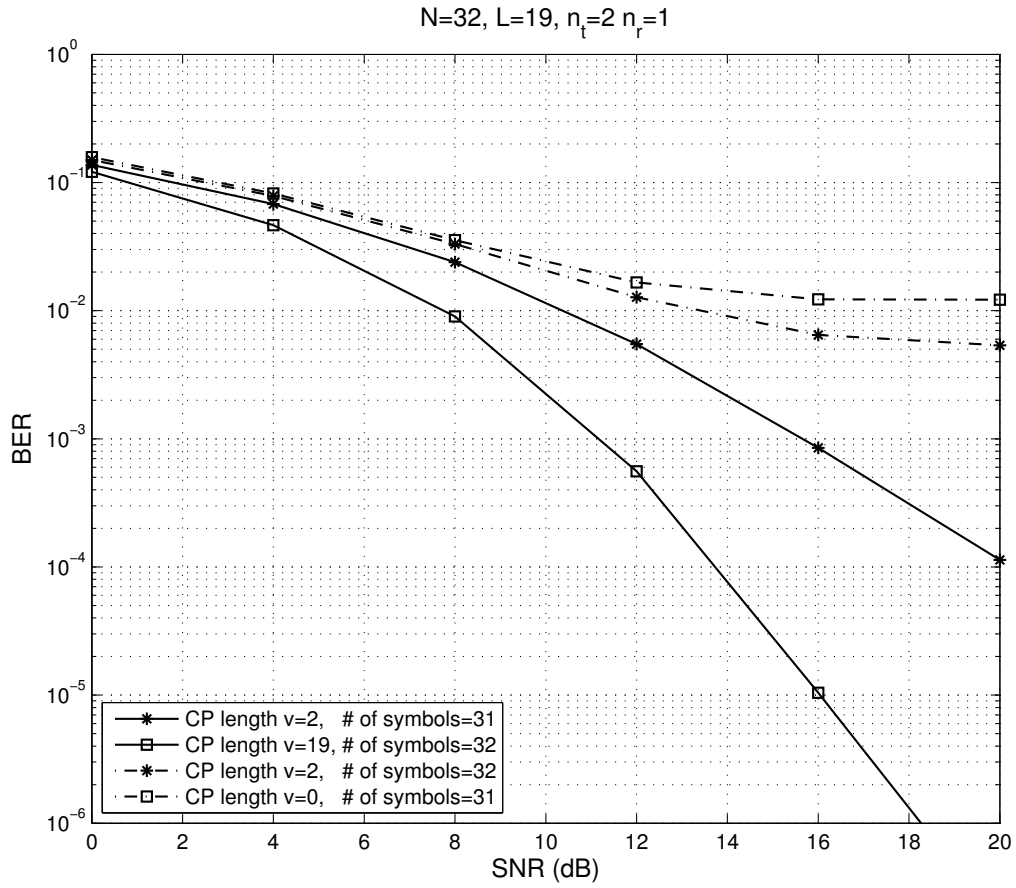


Figure 2.3: MISO case: BER performances of IA based precoding of different CP lengths and different numbers of information symbols

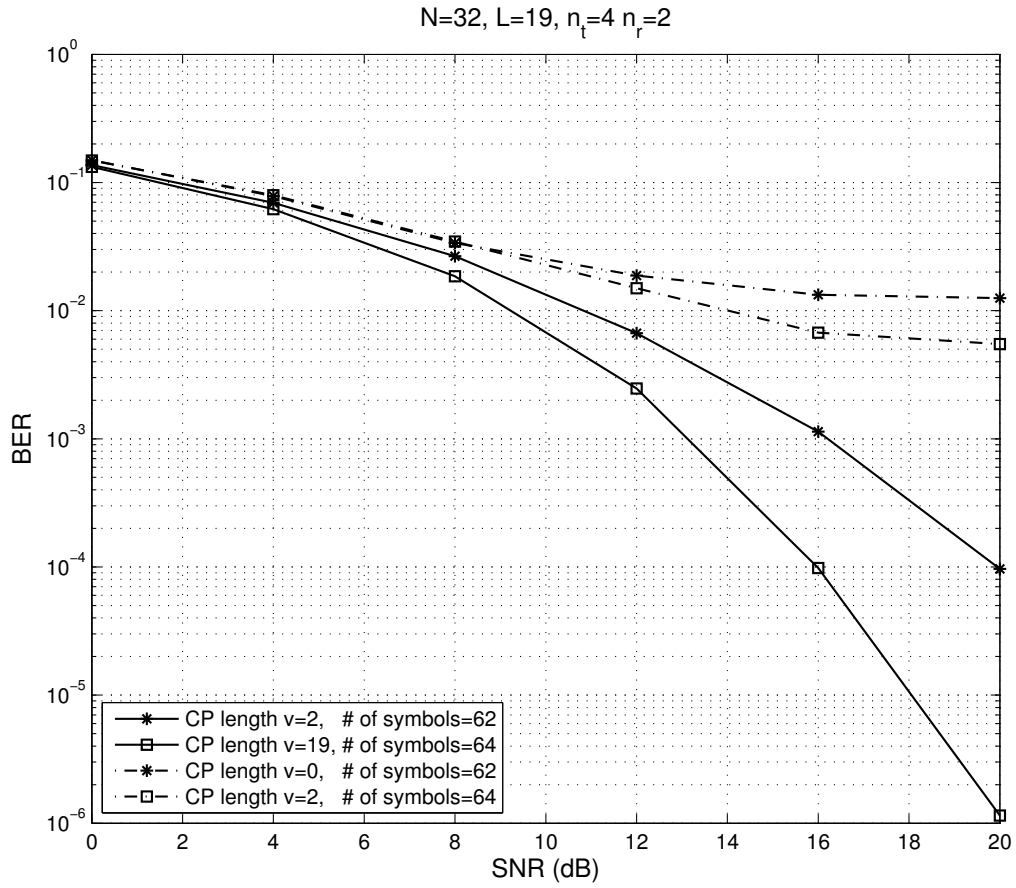


Figure 2.4: MIMO case: BER performances of IA based precoding of different CP lengths and different numbers of information symbols

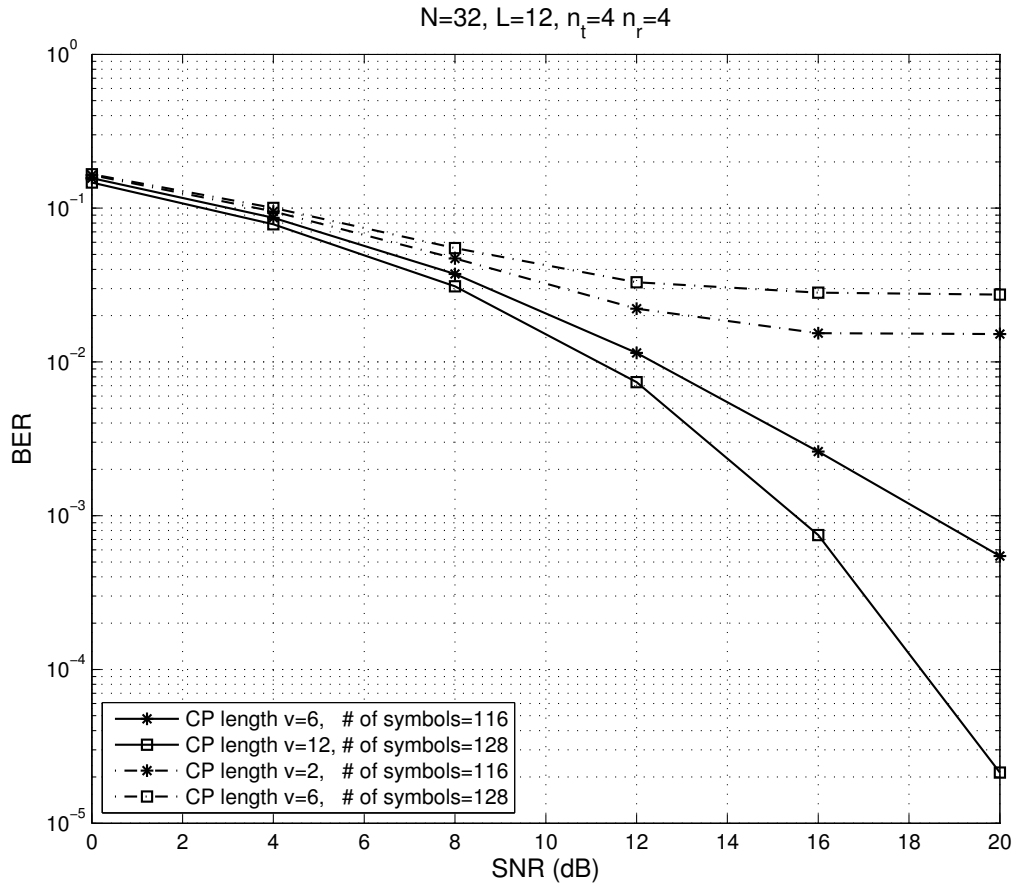


Figure 2.5: MIMO case: BER performances of IA based precoding of different CP lengths and different numbers of information symbols

Chapter 3

A ROBUST PRECODER DESIGN BASED ON CHANNEL STATISTICS FOR MIMO-OFDM SYSTEMS WITH INSUFFICIENT CYCLIC PREFIX

3.1 Introduction

Multiple-input multiple-output (MIMO) is a promising wireless communication technique to boost the wireless link capacity without requiring additional power or bandwidth [63] [16]. Further, combined with orthogonal frequency division multiplexing (OFDM) [50, 8], the MIMO-OFDM system is considered an attractive candidate for high data rate wideband wireless communications over frequency selective channels. 4G-LTE and WiMax (802.16e) both adopt MIMO-OFDM in their standards.

The equalization of OFDM modulated signal can be carried out by an one-tap equalizer. This simple receiver structure relies on the assumption that the CP length is at least as large as the channel memory length. However, in a number of applications, the sufficient CP length requirement is not practically satisfied for various reasons. For instance, when a low peak-to-average power ratio (PAPR) requirement is imposed, the inverse discrete Fourier transform (IDFT) size can not be too large and therefore the CP length is constrained too. Another scenario is that OFDM system might intentionally limit its CP length to a fixed proportion to the entire data block to meet the spectral efficiency demand. In this type of applications, there is a tradeoff between the goals to suppress ISI and to keep the spectral efficiency. When the CP length is insufficient, intercarrier interference (ICI) from the symbols in the current transmission block and interblock interference (IBI) from the previous transmission block occur in the OFDM system. To cope with ICI and IBI induced by the insufficient CP, several techniques have been proposed [6, 47, 62, 66, 19] for OFDM/DMT (discrete multitone). Under

the assumption of perfect channel state information (CSI) at the transmitter, [6] and [47] added sufficient redundancies in time domain and frequency domain respectively to eliminate the distortion. [62] proposed a training-based two stage scheme to first shorten the channel and then perform the per-tone equalization. Some other techniques should also be noticed in [66, 19].

In our recent work [27], a new IBI nulling based technique is proposed. The notion is to utilize a precoding to contain IBI into a distinct subspace with the minimum dimension from the signal subspace and then null IBI at the receiver, which will facilitate the subsequent signal detection using both the desired signal term and the ICI term. Our precoder design in [27] expands the minimum redundancy ISI free transceiver design for DMT system proposed in [36] for MIMO-OFDM and our result shows the feasibility of such a channel independent precoder design and a higher bandwidth efficiency than what is achieved by the conventional MIMO-OFDM system with sufficient CP. But no optimal design is studied for this type of precoder in [27], where the precoder design is channel independent. A natural question is whether we can design the precoder optimally and improve the performance, if some channel statistics is known at the transmitter.

With the statistical CSI at the transmitter, the optimal precoder designs have been studied for various MIMO applications[73, 49, 67]. Particularly, in [73] a robust design of linear transceivers is proposed for a MIMO system with imperfect CSI at the transmitter. It follows the basic ideas and techniques in [44], but exploits the channel mean and covariance as the imperfect CSI and develops a set of optimization criteria based on the tight lower bound of the average mean squared error (MSE) matrix. But the scheme in [73] can not be directly apply to our precoder design problem where the CP is insufficient and thus the residual IBI still exists at the receiver. The elimination of residual IBI requires changes in both the precoder and equalizer. More details will be seen later.

In the recent work [71], another approach is investigated to handle the robust

transceiver design problem for MIMO-OFDM with sufficient CP, which has taken channel estimation errors into account at both transmitter and receiver in their transceiver design. A closed form optimal solution of the precoder and equalizer is proposed. The solution is a per subcarrier water-filling and hence named cluster water-filling. Since frequency domain estimated CSI is required for every transmission block at the transmitter, this strategy is more suitable for sufficient CP scenarios. However, due to insufficient CP in our signal model, IBI and ICI occur and as a consequence, it is hard to design an optimization scheme on a per subcarrier basis. We, thus, need to consider an optimized precoder across all the available frequency and spatial dimensions.

In this paper, a robust linear precoder design is proposed based on the statistical CSI at the transmitter for a MIMO-OFDM system with insufficient CP. To clearly compare this work and our previous work [27], the following major distinctions should be noticed:

- The work in [27] is mainly to prove the feasibility of a precoder that is able to separate IBI into a disjoint subspace with the minimum dimension from the signal subspace, but the simple precoder example does not guarantee a good performance. In the present work, one of the main goals is to enhance the performance of our precoder.
- The channel independent precoding scheme in [27] indicates that no CSI is literally needed for the precoding. However, in this current precoding scheme, channel statistics serves as a necessity to improve the performance.

Specifically, we incorporate the statistical optimization technique in our linear precoding scheme in [27], which can realize the IBI separation and elimination goal combined with a projection operation at the receiver. The precoder fulfills the role of the minimum maximal MSE precoder when MMSE equalization is adopted for signal detection. For the explicitness of this paper, the main distinctive contributions are highlighted in the following:

- The optimization over all the spatial and frequency dimensions easily takes the intercarrier interference into account, which greatly simplifies our problem formulation and solution. The optimized precoding scheme for MIMO-OFDM is designed in a carrier cooperative way. This scheme can potentially gain a better performance than the carrier noncooperative scheme.

- At the transmitter only the covariance matrix of the equivalent channel matrix is required as the statistical CSI. The cost to feedback this statistical CSI is fairly acceptable, since the covariance matrix evolves rather slowly compared to the instant values of the equivalent channel matrix. Once computed and feedback, this covariance information can be valid through many transmission blocks.

The rest of the paper is structured as follows: In Section 3.2, the MIMO-OFDM model with insufficient CP is introduced. In Section 3.3, the receiver structure and its processing as well as the precoder design are described. Then, in Section 3.4 simulation results are presented.

Notations: Boldface upper-case letters denote matrices, boldface lower-case letters denote vectors. $\mathbf{0}_{m \times n}$ stands for a $m \times n$ matrix with all zero entries. \mathbf{I}_k stands for an identity matrix of size k . The operators $(\cdot)^T$ and $(\cdot)^H$ serve as the transpose and the Hermitian transpose, respectively. $[\mathbf{H}]_{i,j}$ stands for the the entry at the i th row and the j th column of the matrix and $[\mathbf{H}]_{i:j,:}$ stands for the submatrix consisting of the i th row to the j th row of \mathbf{H} . Likewise, $[\mathbf{x}]_{i:j}$ stands for the vector consisting of the i th to the j th elements of \mathbf{x} , and for convenience, $\mathbf{x}(i)$ stands for the i th element of vector \mathbf{x} . $\mathbf{A} \otimes \mathbf{B}$ denotes the Kronecker product of matrices \mathbf{A} and \mathbf{B} . $\text{span}\{\cdot\}$ denotes the space spanned by the column vectors of a matrix. $\text{dim}(\cdot)$ means the number of the column space dimension of a matrix. $\text{tr}(\cdot)$ takes the trace of a matrix. $(x)^+ = \max(0, x)$. $\text{diag}(x_1, \dots, x_n)$ stands for a diagonal matrix with the elements x_1, \dots, x_n on its main diagonal.

3.2 MIMO-OFDM Model

We consider a MIMO system with n_t transmit, n_r receive antennas, and OFDM modulated signal blocks (of block length N) transmitted at each antenna. The overall input to the MIMO-OFDM system is noted by $\bar{\mathbf{r}}_k = [(\mathbf{r}_k^0)^T, (\mathbf{r}_k^1)^T, \dots, (\mathbf{r}_k^{N-1})^T]^T$, where \mathbf{r}_k^i denotes the $n_t \times 1$ vector for the n_t transmit antennas at the i th subcarrier, $0 \leq i \leq N-1$, in frequency domain. Let \mathbf{W}_N represent the normalized IDFT matrix of size N with the entries $[\mathbf{W}_N]_{m,n} = (1/\sqrt{N}) \exp(j2\pi(m-1)(n-1)/N)$, for $1 \leq m \leq N$, $1 \leq n \leq N$. The input vector $\bar{\mathbf{r}}_k$ is polyphase decomposed into n_t N -dimensional vectors

and transformed into time domain signals individually by n_t IDFT matrices \mathbf{W}_N . Equivalently, the overall IDFT operation over $\bar{\mathbf{r}}_k$ can be represented by $\bar{\mathbf{W}} \triangleq \mathbf{W}_N \otimes \mathbf{I}_{n_t}$. At each transmit antenna, an insufficient CP of length v ($v < L$) is added to the input signal block and propagates via a multipath channel $\mathbf{h}_{ij} = [h_{ij}(0), h_{ij}(1), \dots, h_{ij}(L)]^T$ between the i th receive antenna and the j th transmit antenna, where we assume that all the entries of \mathbf{h}_{ij} are complex Gaussian random variables with 0 mean and the channel length, $L + 1$, is identical for all the channels. We now define $n_r \times n_t$ channel matrices $\mathbf{H}(l)$, $l = 0, 1, \dots, L$, as

$$\mathbf{H}(l) = \begin{bmatrix} h_{11}(l) & \cdots & h_{1n_t}(l) \\ \vdots & \ddots & \vdots \\ h_{n_r1}(l) & \cdots & h_{n_r n_t}(l) \end{bmatrix}. \quad (3.1)$$

$\mathbf{H}(l)$, $l = 0, 1, \dots, L$, are the $n_r \times n_t$ MIMO channel matrices for the l th multipath. Due to the randomness of the channel coefficients, all the matrices $\mathbf{H}(l)$ are of full rank almost surely.

At the receiver, the CP is removed and the overall time domain received block is given,

$$\bar{\mathbf{y}}_k = \mathbf{C}\bar{\mathbf{W}}\bar{\mathbf{r}}_k + \mathbf{B}\bar{\mathbf{W}}\bar{\mathbf{r}}_{k-1} + \mathbf{n}_k, \quad (3.2)$$

where \mathbf{n}_k is the $n_r N \times 1$ noise vector with the complex Gaussian distribution $\mathcal{CN}(\mathbf{0}, \mathbf{I})$, \mathbf{C} and \mathbf{B} of size $n_r N \times n_t N$ are the overall channel matrix and IBI matrix, respectively,

constructed by stacking submatrices $\mathbf{H}(l)$ in (3.1) and shown in (3.3) and (3.4).

$$\mathbf{C} = \begin{bmatrix} \mathbf{H}(0) & \mathbf{0} & \cdots & \mathbf{0} & \cdots & \mathbf{0} & \mathbf{H}(v) & \cdots & \mathbf{H}(1) \\ \vdots & \ddots & \ddots & & \ddots & \vdots & \vdots & \ddots & \vdots \\ \vdots & & \ddots & \ddots & & \mathbf{0} & \mathbf{H}(L) & & \mathbf{H}(v) \\ \vdots & & & \ddots & \ddots & & \mathbf{0} & \ddots & \vdots \\ \vdots & & & & \ddots & \ddots & & \ddots & \mathbf{H}(L) \\ \mathbf{H}(L) & & & & \ddots & \ddots & & & \mathbf{0} \\ \mathbf{0} & \ddots & & & & & \ddots & \ddots & \vdots \\ \vdots & \ddots & \ddots & & & & & \ddots & \mathbf{0} \\ \mathbf{0} & \cdots & \mathbf{0} & \mathbf{H}(L) & \cdots & \cdots & \mathbf{H}(v-1) & \cdots & \mathbf{H}(0) \end{bmatrix}, \quad (3.3)$$

$$\mathbf{B} = \begin{bmatrix} \mathbf{0} & \cdots & \mathbf{0} & \mathbf{H}(L) & \cdots & \mathbf{H}(v+1) \\ \vdots & & & \ddots & \ddots & \vdots \\ \vdots & & & & \ddots & \mathbf{H}(L) \\ \vdots & & & & & \mathbf{0} \\ \vdots & & & & & \vdots \\ \mathbf{0} & \cdots & \cdots & \cdots & \cdots & \mathbf{0} \end{bmatrix}. \quad (3.4)$$

For this MIMO-OFDM system, the input vector $\bar{\mathbf{r}}_k$ is also the precoded output of information symbol vector $\bar{\mathbf{x}}_k = [(\mathbf{x}_k^0)^T, (\mathbf{x}_k^1)^T, \dots, (\mathbf{x}_k^{N-1})^T]^T$ by an $n_t N \times n_t N$ precoding matrix \mathbf{P} ,

$$\bar{\mathbf{r}}_k = \mathbf{P}\bar{\mathbf{x}}_k \quad (3.5)$$

$$= \mathbf{P}[(\mathbf{x}_k^0)^T, (\mathbf{x}_k^1)^T, \dots, (\mathbf{x}_k^{N-1})^T]^T. \quad (3.6)$$

For the convenience of designing the precoding matrix, we consider the design of precoder $\mathbf{Q} \triangleq \bar{\mathbf{W}}\mathbf{P}$. The precoding matrix \mathbf{P} can then be obtained by multiplying \mathbf{Q} with $\bar{\mathbf{W}}^{-1} = \mathbf{W}_N^{-1} \otimes \mathbf{I}_{n_t}$, where \mathbf{W}_N^{-1} is the discrete Fourier transform (DFT) matrix of size N . In our context, both \mathbf{P} and \mathbf{Q} are called precoders interchangeably. According to the discussion in [27] we have the main results of [27] presented in Theorem 1 and Theorem 2,

Theorem 3 For the insufficient CP MIMO-OFDM system with $n_r \leq n_t$, the total number of independent information symbols can be solved by the zero-forcing operator during each OFDM block is n_β

$$n_\beta = \begin{cases} n_t(N - L + v) + \lfloor \frac{n_r N - n_t(N - L + v)}{2} \rfloor, & \text{if } n_t(N - L + v) < n_r N, \\ n_r N, & \text{if } n_t(N - L + v) \geq n_r N. \end{cases} \quad (3.7)$$

Theorem 4 For the insufficient CP MIMO-OFDM system with $n_r > n_t$, when the following condition for block size N is satisfied,

$$N \geq \frac{n_t}{n_r - n_t}(L - v), \quad (3.8)$$

no zero-padding or precoding is needed and the total number of independent information symbols can be solved by the zero-forcing operator is $n_t N$.

Since we are now taking the advantage of CSI at the transmitter, the precoder design for cases described in both Theorem 1 and Theorem 2 are considered.

We have concluded that, in Theorem 1, this $n_t N \times n_t N$ precoder \mathbf{Q} possesses a unifying structure

$$\mathbf{Q} = [\mathbf{Q}_u \quad \mathbf{Q}_z], \quad (3.9)$$

where the submatrix \mathbf{Q}_u is an $n_t N \times n_\beta$ tall matrix. \mathbf{Q}_u corresponds to the first n_β independent information symbols in $\bar{\mathbf{x}}_k$, which are denoted by the $n_\beta \times 1$ vector $\tilde{\mathbf{x}}_k$, with zero mean and equal average power, i.e., $\mathbb{E}\{\tilde{\mathbf{x}}_k \tilde{\mathbf{x}}_k^H\} = \sigma_s^2 \mathbf{I}_{n_\beta}$. The input signal vector $\bar{\mathbf{x}}_k$ can be represented by $\bar{\mathbf{x}}_k = [\tilde{\mathbf{x}}_k^T \quad \mathbf{0}_{(n_t N - n_\beta) \times 1}^T]^T$. $\tilde{\mathbf{x}}_k$ is our only concern in detecting the k -th data block $\bar{\mathbf{x}}_k$. The submatrix \mathbf{Q}_z is $n_t N \times (n_t N - n_\beta)$ and the columns of the submatrix \mathbf{Q}_z can be anything that is linearly dependent on the columns of \mathbf{Q}_u and does not affect the conditions that is imposed on the design of the precoder in Theorem 1. Thus, we henceforth set $\mathbf{Q}_z = \mathbf{0}$ for clarity. This submatrix \mathbf{Q}_z corresponds to the last $n_t N - n_\beta$ padding zeros in $\bar{\mathbf{x}}_k$.

When $n_t(N - L + v) < n_r N$ holds, the precoding submatrix \mathbf{Q}_u has the structure in (3.10) so as to separate the IBI and the current signal subspaces,

$$\mathbf{Q}_u = \left[\bar{\mathbf{Q}}^T \quad \mathbf{0}_{n_\beta \times (n_t N - n_\beta)} \right]^T, \quad (3.10)$$

where \mathbf{Q}_u consists of a full rank square submatrix $\bar{\mathbf{Q}}$ of size n_β that performs precoding and an $(n_t N - n_\beta) \times n_\beta$ zero padding submatrix. The rationale behind this structure is that by introducing redundancy using the zero-padding submatrix in (3.10), the ranks of both \mathbf{CQ} and \mathbf{BQ} shrink. The signal subspace and the IBI subspace are separated in the received signal space under the condition that $\text{span}\{\mathbf{CQ}\} \cap \text{span}\{\mathbf{BQ}\} = \{\mathbf{0}\}$. We have proved in [27] that this condition holds and the minimum redundancy is proved to be $n_t N - n_\beta$ zero rows in the trail of the precoding matrix.

On the other hand, when $n_t(N - L + v) \geq n_r N$, \mathbf{Q}_u is expressed below,

$$\mathbf{Q}_u = \begin{bmatrix} \bar{\mathbf{Q}}^T & \mathbf{0}_{n_\beta \times n_t(L-v)} \end{bmatrix}^T, \quad (3.11)$$

where $\bar{\mathbf{Q}}$ is of size $n_t(N - L + v) \times n_\beta$ and the $n_t(L - v) \times n_\beta$ zero padding submatrix is sufficient to remove all IBI, For this case, at the receiver there will be no residual IBI and therefore no zero-forcing operation is applied. Standard procedures as described in [73] can be carried out to design a robust precoder.

For Theorem 2, we have $\mathbf{Q} = \mathbf{Q}_u$ is a full rank square matrix of size $n_t N$. It can be analogously designed in the way we will handle \mathbf{Q}_u in (3.10) with some differences specified later.

3.3 Receiver Structure And Precoder Design

In this section, we first discuss the processing at the receiver and then a design criterion depends on what the receiver is used.

3.3.1 Receiver Structure

The zero-forcing is first performed over the received signal to suppress all the residual IBI. A linear MMSE equalizer is concatenated to extract the desired signal symbols from the zero-forcing output. We will initially and mainly discuss the first case in Theorem 1 and then discuss the precoding for Theorem 2.

According to the result in our previous work [27], in our Theorem 1, when the transmit antenna number is less than or equal to the receive antenna number

($n_r \leq n_t$), and the OFDM block length N and the CP length v are chosen properly so that $n_t(N - L + v) < n_r N$ holds, we can put $n_1 = \lfloor \frac{n_r N - n_t(N - L + v)}{2} \rfloor$ more data symbol in the MIMO-OFDM system. To do so, a properly designed precoder at the transmitter combined with an IBI zero-forcing matrix at the receiver is used.

By taking a maximal set of m_1 linearly independent column vectors $\{\tilde{\mathbf{b}}_1, \dots, \tilde{\mathbf{b}}_{m_1}\}$ in $\mathbf{B}\mathbf{Q}_u$, a full column rank matrix is formed: $\tilde{\mathbf{B}} = [\tilde{\mathbf{b}}_1, \dots, \tilde{\mathbf{b}}_{m_1}]$. Since the column vectors of $\tilde{\mathbf{B}}$ spans the range space of the interference vectors, a zero-forcing matrix that eliminates the IBI term $\mathbf{B}\mathbf{Q}_u\bar{\mathbf{x}}_{k-1}$ can be constructed as

$$\mathbf{F}_z = \mathbf{I} - \tilde{\mathbf{B}}(\tilde{\mathbf{B}}^H\tilde{\mathbf{B}})^{-1}\tilde{\mathbf{B}}^H. \quad (3.12)$$

Note that \mathbf{F}_z is determined by the IBI subspace after the precoding. Moreover, the IBI subspace is determined by the lower zero padding submatrix in \mathbf{Q}_u . The upper submatrix $\bar{\mathbf{Q}}$ only decides the basis of $\tilde{\mathbf{B}}$, but does not alter \mathbf{F}_z . This is easily tested using $\tilde{\mathbf{B}}\mathbf{T}$ to replace $\tilde{\mathbf{B}}$ and \mathbf{F}_z remains the same, where \mathbf{T} is an $m_1 \times m_1$ invertible matrix, This implies that for the explicit calculation of \mathbf{F}_z , the optimized solution of \mathbf{Q}_u is not a prerequisite. Consequently, to calculate \mathbf{F}_z , a simple and unoptimized choice of \mathbf{Q}_u in (3.13) also works.

$$\mathbf{Q}_u = [\mathbf{I}_{n_\beta} \quad \mathbf{0}_{n_\beta \times (n_t N - n_\beta)}]^T. \quad (3.13)$$

After \mathbf{Q}_u in (3.13) is used, we only need to have $\tilde{\mathbf{B}}$ to construct \mathbf{F}_z . Thus, the following procedures are provided to obtain $\tilde{\mathbf{B}}$. We use a brief expression $\mathbf{B} = [\mathbf{0}, \dots, \mathbf{0}, \mathbf{b}_1, \dots, \mathbf{b}_{n_t(L-v)}]$ for \mathbf{B} in (3.4), where \mathbf{b}_i is the i th non-zero column vector in \mathbf{B} . For this chosen \mathbf{Q}_u in (3.13), $\mathbf{B}\mathbf{Q}_u$ is given by

$$\mathbf{B}\mathbf{Q}_u = [\mathbf{0}, \dots, \mathbf{0}, \mathbf{b}_1, \dots, \mathbf{b}_{n_1}] = [\mathbf{0} \quad \mathbf{B}_c] \quad (3.14)$$

where $\mathbf{B}_c = [\mathbf{b}_1, \dots, \mathbf{b}_{n_1}]$.

Due to different MIMO configurations, two cases are separately discussed. If the number of transmitter and receiver antennas are the same ($n_r = n_t$), it is guaranteed that $\mathbf{b}_1, \dots, \mathbf{b}_{n_1}$ are linearly independent almost surely. In this case, $m_1 = n_1$. In the

sequel, without specific explanation, the linear independence is in the sense of almost surely. Using these m_1 column vectors $\mathbf{b}_1, \dots, \mathbf{b}_{m_1}$ as columns of $\tilde{\mathbf{B}}$, the zero forcing matrix in (3.12) is constructed.

On the other hand, if $n_r < n_t$, linear dependency exists among the column vectors \mathbf{H}_l in (3.1), and therefore linear dependency might exist among these n_1 columns $\mathbf{b}_1, \dots, \mathbf{b}_{n_1}$ in \mathbf{B}_c . We simply select m_1 ($m_1 < n_1$) linear independent column vectors $\mathbf{b}_1, \dots, \mathbf{b}_{m_1}$ from \mathbf{B}_c .

Observe \mathbf{B}_c 's expression closely in the following and suppose $n_1 = n_t K + D$, $0 \leq D < n_t$,

$$\begin{aligned} \mathbf{B}_c &= [\mathbf{b}_1, \dots, \mathbf{b}_{n_1}] \\ &= \begin{bmatrix} \mathbf{H}(L) & \cdots & \mathbf{H}(L-K+1) & \mathbf{H}_T(L-K) \\ \mathbf{0} & \ddots & \vdots & \vdots \\ \vdots & \ddots & \mathbf{H}(L) & \mathbf{H}_T(L-1) \\ \vdots & & \mathbf{0} & \mathbf{H}_T(L) \\ \vdots & & \vdots & \vdots \\ \mathbf{0} & \cdots & \mathbf{0} & \mathbf{0} \end{bmatrix} \end{aligned} \quad (3.15)$$

where $\mathbf{H}_T(l)$ is defined as

$$\mathbf{H}_T(l) = \begin{bmatrix} \mathbf{h}_{11}(l) & \cdots & \mathbf{h}_{1D}(l) \\ \vdots & & \vdots \\ \mathbf{h}_{n_r 1}(l) & \cdots & \mathbf{h}_{n_r D}(l) \end{bmatrix} \quad (3.16)$$

From (3.15), the first $n_t K$ columns have a block Toeplitz structure and therefore from the (kn_t+1) th to the $((k+1)n_t)$ th columns, n_r independent column vectors are included, $0 \leq k \leq K-1$. Take n_r independent columns in every n_t column vectors starting from the leftmost column and then take the rest D' independent columns from the last D column vectors in \mathbf{B}_c . $\tilde{\mathbf{B}} = [\tilde{\mathbf{b}}_1, \dots, \tilde{\mathbf{b}}_{m_1}]$ in (3.12) is constructed and $m_1 = n_r K + D'$.

Note that if we directly apply the zero forcing matrix to the received signal, the output noise $\mathbf{F}_z \mathbf{n}_k$ is no longer an i.i.d. Gaussian noise vector, which can complicate

both our precoder design and the MMSE equalizer. One method to cope with this defect is to perform eigen-decompose of the zero-forcing matrix \mathbf{F}_z , i.e.,

$$\mathbf{F}_z = \mathbf{U}_F^H \mathbf{D}_F \mathbf{U}_F,$$

where \mathbf{U}_F is an $n_r N \times n_r N$ unitary matrix and

$$\mathbf{D}_F = \begin{bmatrix} \mathbf{I}_{r \times r} & \mathbf{0}_{r \times (n_r N - r)} \\ \mathbf{0}_{(n_r N - r) \times r} & \mathbf{0}_{(n_r N - r) \times (n_r N - r)} \end{bmatrix},$$

where $r = \text{rank}(\mathbf{F}_z) = n_r N - m_1$. The reason to have this diagonal matrix form is because matrix \mathbf{F}_z is a projection matrix. Since $\mathbf{F}_z \mathbf{B} \mathbf{Q}_u = \mathbf{0}$, $\mathbf{F}_d = \mathbf{D}_F \mathbf{U}_F$ can actually also eliminate the interference ($\mathbf{F}_d \mathbf{B} \mathbf{Q}_u = \mathbf{0}$). Therefore, apply the zero-forcing matrix $\mathbf{F}_d = \mathbf{D}_F \mathbf{U}_F$ to the received signal represented in (3.2) and (3.5), we have the expression,

$$\mathbf{F}_d \tilde{\mathbf{y}}_k = \mathbf{F}_d \mathbf{C} \mathbf{Q}_u \tilde{\mathbf{x}}_k + \mathbf{F}_d \mathbf{n}_k. \quad (3.17)$$

Note that the effect of multiplying \mathbf{D}_F to the left of a matrix is to pick the first $n_r N - m_1$ rows and set the rest m_1 rows to be zero. Consequently, the last m_1 rows at both side of equation (3.17) are truncated. Therefore, define $(n_r N - m_1) \times 1$ receive signal $\tilde{\mathbf{y}}_k = [\mathbf{F}_d \tilde{\mathbf{y}}_k]_{1:r}$, $(n_r N - m_1) \times n_t N$ equivalent channel matrix $\mathbf{H}_{eq} = [\mathbf{F}_d \mathbf{C}]_{1:r}$, and the associated $(n_r N - m_1) \times 1$ noise vector $\tilde{\mathbf{n}}_k = [\mathbf{F}_d \mathbf{n}_k]_{1:r}$. The signal at the output of the zero-forcing can be equivalently expressed as,

$$\tilde{\mathbf{y}}_k = \mathbf{H}_{eq} \mathbf{Q}_u \tilde{\mathbf{x}}_k + \tilde{\mathbf{n}}_k, \quad (3.18)$$

where $\tilde{\mathbf{n}}_k$ is also with the complex Gaussian distribution $\mathcal{CN}(0, \mathbf{I})$.

For the case in Theorem 2, the zero-forcing operation also holds with some necessary changes in parameters. To be specific, we have $m_1 = n_t(L - v)$ and choose $\tilde{\mathbf{B}} = [\mathbf{b}_1, \dots, \mathbf{b}_{m_1}]$, where $\mathbf{b}_1, \dots, \mathbf{b}_{m_1}$ are the $n_t(L - v)$ nonzero columns in \mathbf{B} . The zero-forcing matrix \mathbf{F}_z can also be determined using (3.12). The equivalent signal model is also given in (3.18).

The MMSE equalizer for the signal detection in (3.18) is

$$\mathbf{G} = \left(\frac{1}{\sigma_s^2} \mathbf{I} + \mathbf{Q}_u^H \mathbf{H}_{eq}^H \mathbf{H}_{eq} \mathbf{Q}_u \right)^{-1} \mathbf{Q}_u^H \mathbf{H}_{eq}^H. \quad (3.19)$$

Applying the MMSE equalizer, the equalized signal associated with $\tilde{\mathbf{x}}_k$ can be expressed as

$$\hat{\mathbf{x}}_k = \mathbf{G} \mathbf{H}_{eq} \mathbf{Q}_u \tilde{\mathbf{x}}_k + \mathbf{G} \tilde{\mathbf{n}}_k. \quad (3.20)$$

The MSE matrix for the MMSE equalized signal vector $\hat{\mathbf{x}}_k$ is defined as

$$\begin{aligned} \mathbf{E} &= \mathbb{E}\{(\hat{\mathbf{x}}_k - \tilde{\mathbf{x}}_k)(\hat{\mathbf{x}}_k - \tilde{\mathbf{x}}_k)^H\} \\ &= \left[\frac{1}{\sigma_s^2} \mathbf{I} + \mathbf{Q}_u^H \mathbf{H}_{eq}^H \mathbf{H}_{eq} \mathbf{Q}_u \right]^{-1}, \end{aligned} \quad (3.21)$$

where the expectation is taken over the noise vector $\tilde{\mathbf{n}}_k$. In (3.21) each element of $\tilde{\mathbf{x}}_k$ has its MSE located on the corresponding diagonal entry in \mathbf{E} .

Since in our precoding scheme the instantaneous CSI at the transmitter is unavailable, the term $\mathbf{H}_{eq}^H \mathbf{H}_{eq}$ can not be computed using the instantaneous value. As a consequence, we employ the covariance matrix $\mathbf{R}_c = \mathbb{E}\{\mathbf{H}_{eq}^H \mathbf{H}_{eq}\}$ as the substitutional statistical CSI at the transmitter. The MSE matrix is then rewritten by

$$\bar{\mathbf{E}} = \left[\frac{1}{\sigma_s^2} \mathbf{I} + \mathbf{Q}_u^H \mathbb{E}\{\mathbf{H}_{eq}^H \mathbf{H}_{eq}\} \mathbf{Q}_u \right]^{-1} \quad (3.22)$$

$$= \left[\frac{1}{\sigma_s^2} \mathbf{I} + \mathbf{Q}_u^H \mathbf{R}_c \mathbf{Q}_u \right]^{-1}. \quad (3.23)$$

Note that from the results in [41] and [73], on the set of $n \times n$ positive definite Hermitian matrices, the function $\phi(\mathbf{A}) = \mathbf{A}^{-1}$ is strictly matrix-convex, namely, $\mathbb{E}\{\mathbf{A}^{-1}\} \geq \mathbb{E}\{\mathbf{A}\}^{-1}$. As a result, we have,

$$\bar{\mathbf{E}} = \left[\frac{1}{\sigma_s^2} \mathbf{I} + \mathbf{Q}_u^H \mathbb{E}\{\mathbf{H}_{eq}^H \mathbf{H}_{eq}\} \mathbf{Q}_u \right]^{-1} \leq \mathbb{E} \left[\frac{1}{\sigma_s^2} \mathbf{I} + \mathbf{Q}_u^H \mathbf{H}_{eq}^H \mathbf{H}_{eq} \mathbf{Q}_u \right]^{-1} \quad (3.24)$$

This means that the optimization criterion chosen in (3.23) is a lower bound of the averaged MSE on all the possible channel realizations. The work [73] additionally proved that this lower bound is asymptotically tight. Thus all of our design and simulation will be based on this lower bound $\bar{\mathbf{E}}$.

3.3.2 Precoder Design

Given the tight lower bound of the average MSE in (3.23) and the MMSE equalizer in (3.19), the precoder design problem can be generally formulated by choosing a certain cost function \mathcal{F}_0 of $\bar{\mathbf{E}}$ and minimizing this cost function subject to the transmit power constraint \mathcal{P}_T :

$$\begin{aligned} \min_{\mathbf{Q}_u} \quad & \mathcal{F}_0 \left(\left[\frac{1}{\sigma_s^2} \mathbf{I} + \mathbf{Q}_u^H \mathbf{R}_c \mathbf{Q}_u \right]^{-1} \right), \\ \text{s.t.} \quad & \text{tr}\{\mathbf{Q}_u \mathbf{Q}_u^H\} \leq \mathcal{P}_T. \end{aligned} \quad (3.25)$$

If we consider the data symbol transmitted at one transmit antenna in one symbol interval as a data stream, there are n_β data streams in total during one block transmission in our MIMO-OFDM system. The overall performance is mainly dominated by the data stream with the largest average MSE. Therefore the maximum stream MSE of all data streams is the function of interest to be minimized in this work. Choose $\mathcal{P}_T = n_\beta$, our optimization problem can be expressed as,

$$\begin{aligned} \min_{\mathbf{Q}_u} \quad & \max_{1 \leq i \leq n_\beta} \left[\left[\frac{1}{\sigma_s^2} \mathbf{I} + \mathbf{Q}_u^H \mathbf{R}_c \mathbf{Q}_u \right]^{-1} \right]_{i,i}, \\ \text{s.t.} \quad & \text{tr}\{\mathbf{Q}_u \mathbf{Q}_u^H\} \leq n_\beta. \end{aligned} \quad (3.26)$$

In the work [44] [45], a unified convex programming framework for optimized precoder design is proposed in the perfect CSI case. The conclusion is further extended to the statistical CSI case in [73], where it is shown that the optimized precoder structure remains the same when statistical CSI is acquired at the transmitter and perfect CSI is at the receiver. Their results for the statistical CSI case is then summarized as follows:

Assume the eigen-decomposition for the channel covariance matrix as,

$$\mathbf{R}_c = \mathbf{U}_c \mathbf{\Lambda}_c \mathbf{U}_c^H \quad (3.27)$$

where \mathbf{U}_c is unitary, and $\mathbf{\Lambda}_c = \text{diag}\{\lambda_{c,1}, \dots, \lambda_{n_{c,(n_t \times N)}}\}$ and all the eigenvalues are in increasing order, i.e., $\lambda_i \leq \lambda_j$, for $1 \leq i < j \leq n_t N$.

If the function \mathcal{F}_0 is Schur-concave over its domain, the solution to the problem in (3.25) is given by,

$$\mathbf{Q}_u = \mathbf{U}_{c,1} \mathbf{\Sigma}_{d,1}, \quad (3.28)$$

where $\mathbf{U}_{c,1} \in \mathbb{C}^{n_t N \times n_\beta}$ has the first n_β columns of \mathbf{U}_c as its columns, which are the eigenvectors of \mathbf{R}_c corresponding to the n_β largest eigenvalues in decreasing order. Let $\mathbf{\Sigma}$ be the $n_t N \times n_\beta$ power loading matrix. Except the power allocation elements $d_1^{1/2}, \dots, d_{n_\beta}^{1/2}$ arranged decreasingly on the upmost main diagonal of $\mathbf{\Sigma}$, other elements are all zeros. $\mathbf{\Sigma}_{d,1} = \mathbf{\Lambda}_c^{-1/2} \mathbf{\Sigma}$. For the concave case, the optimal precoder \mathbf{Q}_u will result in a diagonal structure of the averaged MSE matrix in (3.23).

On the other hand, if the function \mathcal{F}_0 is Schur-convex, the solution is expressed by,

$$\mathbf{Q}_u = \mathbf{U}_{c,1} \mathbf{\Sigma}_{d,1} \mathbf{V}, \quad (3.29)$$

where $\mathbf{U}_{c,1}$ and $\mathbf{\Sigma}_{d,1}$ are defined the same way as in (3.28). For the convex case, for example, the $\max\{\cdot\}$ cost function in our problem, there is an extra unitary matrix \mathbf{V} which produces a non-diagonal $\bar{\mathbf{E}}$ with identical diagonal elements. i.e., identical component MSEs for all data streams. Such unitary matrix \mathbf{V} can be chosen as the Hadamard matrix or the normalized DFT/IDFT matrix. Additionally, the optimized power loading d_i 's are solved by minimizing $tr\{\bar{\mathbf{E}}\}$ using waterfilling method.

However, for our optimization problem aiming at minimizing the maximum statistical MSE, we need the precoder \mathbf{Q}_u to achieve two goals: not only transmit n_β independent information symbols through n_β statistical eigenmodes but also satisfy our IBI separation condition so as to completely suppress the residual IBI before we decode the information symbols. Therefore, the optimal solution shown in [73] can not be directly adopted, since this $n_t N \times n_\beta$ matrix $\mathbf{U}_{c,1}$ on the left hand side of the precoder \mathbf{Q}_u violates the condition in (3.10) to separate IBI. So some necessary modifications to $\mathbf{U}_{c,1}$ and $\mathbf{\Sigma}_{d,1}$ are carried out.

For the first case in Theorem 1, i.e., $n_t(N - L + v) < n_r N$, our condition in (3.10) requires that the last $n_t N - n_\beta$ rows to be zero rows, which can be sufficed

by choosing another $n_t N \times n_\beta$ matrix \mathbf{U}_q to substitute $\mathbf{U}_{c,1}$, which should have both orthogonal columns and all last $n_t N - n_\beta$ rows to be zero rows. The resulting precoder can be expressed by,

$$\mathbf{Q}_u = \mathbf{U}_q \boldsymbol{\Sigma}_{q,1} \mathbf{W}_{n_\beta}, \quad (3.30)$$

where $\mathbf{U}_q = [\bar{\mathbf{U}}^T, \mathbf{0}_{n_\beta \times (n_t N - n_\beta)}]^T$, $\boldsymbol{\Sigma}_{q,1}$ is an $n_t N \times n_\beta$ diagonal matrix with the power allocation elements on the upmost main diagonal entries, and \mathbf{W}_{n_β} is the n_β dimensional DFT matrix.

To specify \mathbf{U}_q and $\boldsymbol{\Sigma}_{q,1}$, initially let

$$\mathbf{U}_c = [\mathbf{U}_{c,1} \quad \mathbf{U}_{c,2}] = \begin{bmatrix} \mathbf{U}_{11} & \mathbf{U}_{12} \\ \mathbf{U}_{21} & \mathbf{U}_{22} \end{bmatrix}, \quad (3.31)$$

where $\mathbf{U}_{11} \in \mathbb{C}^{n_\beta \times n_\beta}$, $\mathbf{U}_{21} \in \mathbb{C}^{(n_t N - n_\beta) \times n_\beta}$, $\mathbf{U}_{12} \in \mathbb{C}^{n_\beta \times (n_t N - n_\beta)}$ and $\mathbf{U}_{22} \in \mathbb{C}^{(n_t N - n_\beta) \times (n_t N - n_\beta)}$ are the submatrices that consisting of the unitary matrix \mathbf{U}_c .

Let

$$\mathbf{U}'_{c,1} = \begin{bmatrix} \mathbf{I}_{n_\beta} \\ \mathbf{0}_{(n_t N - n_\beta) \times n_\beta} \end{bmatrix}. \quad (3.32)$$

Then we have

$$\begin{aligned} \boldsymbol{\Xi} &= \mathbf{U}'_{c,1}{}^H \mathbf{R}_c \mathbf{U}'_{c,1} \\ &= \mathbf{U}'_{c,1}{}^H \mathbf{U}_c \boldsymbol{\Lambda}_c \mathbf{U}_c^H \mathbf{U}'_{c,1} \\ &= \mathbf{U}_{11} \boldsymbol{\Lambda}_1 \mathbf{U}_{11}^H + \mathbf{U}_{12} \boldsymbol{\Lambda}_2 \mathbf{U}_{12}^H, \end{aligned} \quad (3.33)$$

where $n_\beta \times n_\beta$ diagonal matrix $\boldsymbol{\Lambda}_1 = \text{diag}\{\lambda_1, \dots, \lambda_{n_\beta}\}$ and $(n_t N - n_\beta) \times (n_t N - n_\beta)$ diagonal matrix $\boldsymbol{\Lambda}_2 = \text{diag}\{\lambda_{n_\beta+1}, \dots, \lambda_{n_t N}\}$ are the first n_β and last $n_t N - n_\beta$ eigenvalues of \mathbf{R}_c respectively. This $n_\beta \times n_\beta$ matrix $\boldsymbol{\Xi}$ can be diagonalized by another unitary matrix \mathbf{U}_0 , i.e.,

$$\mathbf{U}_0^H \boldsymbol{\Xi} \mathbf{U}_0 = \tilde{\boldsymbol{\Lambda}} = \text{diag}\{\tilde{\lambda}_1, \dots, \tilde{\lambda}_{n_\beta}\}, \quad (3.34)$$

where $\tilde{\lambda}_i$'s are in increasing order. From (3.32) and (3.34), $\bar{\mathbf{U}} = \mathbf{U}_0$, \mathbf{U}_q is given by,

$$\mathbf{U}_q = \begin{bmatrix} \mathbf{U}_0 \\ \mathbf{0}_{(n_t N - n_\beta) \times n_\beta} \end{bmatrix}. \quad (3.35)$$

And

$$\Sigma_{q,1} = \tilde{\Lambda}^{-1/2} \Sigma \quad (3.36)$$

where Σ is an $n_t N \times n_\beta$ diagonal matrix with upmost main diagonal entries $d_1^{1/2}, \dots, d_{n_\beta}^{1/2}$ in decreasing order.

For the case described in Theorem 2, i.e., $n_r > n_t$ and $N \geq \frac{n_t}{n_r - n_t}(L - v)$, since no zero padding submatrix is included in \mathbf{Q}_u , the precoder matrix can be given by,

$$\mathbf{Q}_u = \mathbf{U}_q \Sigma_{q,1} \mathbf{W}_{n_\beta}, \quad (3.37)$$

where $n_\beta = n_t N$, $\mathbf{U}_q = \mathbf{U}_c$, $\Sigma_{q,1} = \Lambda_c \Sigma$ and $\Sigma = \text{diag}\{d_1^{1/2}, \dots, d_{n_\beta}^{1/2}\}$.

For these two cases of precoders, a unified procedure is carried out as follows to calculate the optimized power allocation $d_1^{1/2}, \dots, d_{n_\beta}^{1/2}$, which is equivalent to minimize $\text{tr}\{\bar{\mathbf{E}}\}$. Since $\text{tr}\{\cdot\}$ is Schur-concave, take $\mathbf{Q}_u = \mathbf{U}_q \Sigma_{q,1}$ into (3.25) and take $\mathcal{F}_0 = \text{tr}\{\bar{\mathbf{E}}\}$, after derivation the problem is simplified to be:

$$\begin{aligned} \min_{d_i} \quad & \sum_{i=1}^{n_\beta} \frac{\sigma_s^2}{1 + \sigma_s^2 d_i}, \\ \text{s.t.} \quad & \sum_{i=1}^{n_\beta} d_i \tilde{\lambda}_i^{-1} \leq n_\beta. \end{aligned} \quad (3.38)$$

Then write $p_i = d_i \tilde{\lambda}_i^{-1}$ and the problem is expressed as

$$\begin{aligned} \min_{p_i} \quad & \sum_{i=1}^{n_\beta} \frac{\sigma_s^2}{1 + \sigma_s^2 \tilde{\lambda}_i p_i}, \\ \text{s.t.} \quad & \sum_{i=1}^{n_\beta} p_i \leq n_\beta. \end{aligned} \quad (3.39)$$

This problem in (3.39) is a convex optimization problem. The solution of p_i 's or equivalently d_i 's can be obtained through the waterfilling approach. With the definition

$$\mathbf{p} = [p_1, \dots, p_{n_\beta}]^T \quad (3.40)$$

$$f(\mathbf{p}) = \sum_{i=1}^{n_\beta} f_i(p_i) \quad (3.41)$$

$$f_i(p_i) = \frac{\sigma_s^2}{1 + \sigma_s^2 \tilde{\lambda}_i p_i}, \quad (3.42)$$

Let

$$L(\mathbf{p}, \mu, \mu_i) = f(\mathbf{p}) + \mu \left[\sum_{i=1}^{n_\beta} p_i - n_\beta \right] - \sum_{i=1}^{n_\beta} \mu_i p_i \quad (3.43)$$

Then we solve for the following equation

$$\partial \frac{L(\mathbf{p}, \mu, \mu_i)}{\partial p_i} = 0 \quad (3.44)$$

The final result of (3.44) is that

$$p_i = \left[\frac{\mu^{-1/2}}{\tilde{\lambda}_i^{1/2}} - \frac{1}{\sigma_s^2 \tilde{\lambda}_i} \right]^+ \quad (3.45)$$

$$d_i = \left[\mu^{-1/2} \tilde{\lambda}_i^{1/2} - \frac{1}{\sigma_s^2} \right]^+ \quad (3.46)$$

The precoder design for our discussed problem is now concluded in (3.30), (3.35), (3.36), (3.37) and (3.46).

Generally, our proposed statistical CSIT based precoding has better performance compared to the channel independent precoding. But when the CP is sufficient, the SISO-OFDM is a special case in which there is no performance gap between the channel independent precoding and the statistical CSIT based precoding. Because in this case, our channel independent precoding in [27] is $\mathbf{Q}_u = \mathbf{I}_N$. With this idle precoding, the MSE's, i.e., the diagonal elements of $\bar{\mathbf{E}}$ are already equalized (The proof is given in Appendix A). $tr\{\bar{\mathbf{E}}\}$ also cannot be reduced using the statistical CSIT based precoding. This, however, does not hold for a general MIMO-OFDM with sufficient CP as we shall see later in simulations.

3.4 Simulation Results

In this section, we provide some simulations to show the performance of our precoder design based on statistical CSI. The performance of our new precoder in this paper is compared to the performance of our previous channel independent precoder in [27] and the performance of systems with residual IBI in both SISO and MIMO cases. For all the simulation results in the sequel, the SNR at the receiver is accounted. The modulation constellation is BPSK for all the simulations. The proposed precoder based on statistical CSI at transmitter and the channel independent precoder in [27] are referred to as “Stat CSIT” and “Indep. Precoder” respectively in the listed figures. The performance of the newly proposed precoder is also compared to that of the standard SC-FDE, OFDM with sufficient CP and zero padding systems in the SISO case and those standard systems are referred to as “SC-FDE”, “CP-OFDM” and “ZP-only”, respectively.

In Fig. 3.1, we demonstrate the BER performances of these block transmission scheme mentioned above. The channel memory length $L = 16$ in this simulation. The independent information symbols sent in one block, is $N = 64$ for SC-FDE, CP-OFDM and ZP-only which also equals the block size. In addition, sufficient guard intervals, i.e., $v = 16$ CP or ZP symbols are adopted here. Whereas for our channel independent precoding and the precoding based on statistical CSIT, the numbers of independent information symbols are 62, 60 and 56, respectively, with 2, 4 and 8 padding zeros at the end of the block. Accordingly, the CP symbol length are $v = 12, 8, 0$ for each case.

This figure shows that our statistical CSIT based precoding can improve BER performance compared with the previous channel independent precoding, especially when the CP is very short or totally absent. Note that the our channel independent precoding coincides with the SC-FDE when full CP $v = 16$ is adopted, and thus they have the same performance. As mentioned earlier, for the SISO-OFDM case, when the CP is sufficient, the channel independent precoding and the statistical precoding achieve the same performance, so the channel independent curve for full CP also represents the performance of the statistical CSIT based precoder here. One should also

observe that the ZP-only scheme's performance is superior among all these block transmission schemes, since it collects the full multipath diversity with the MMSE receiver [64][37].

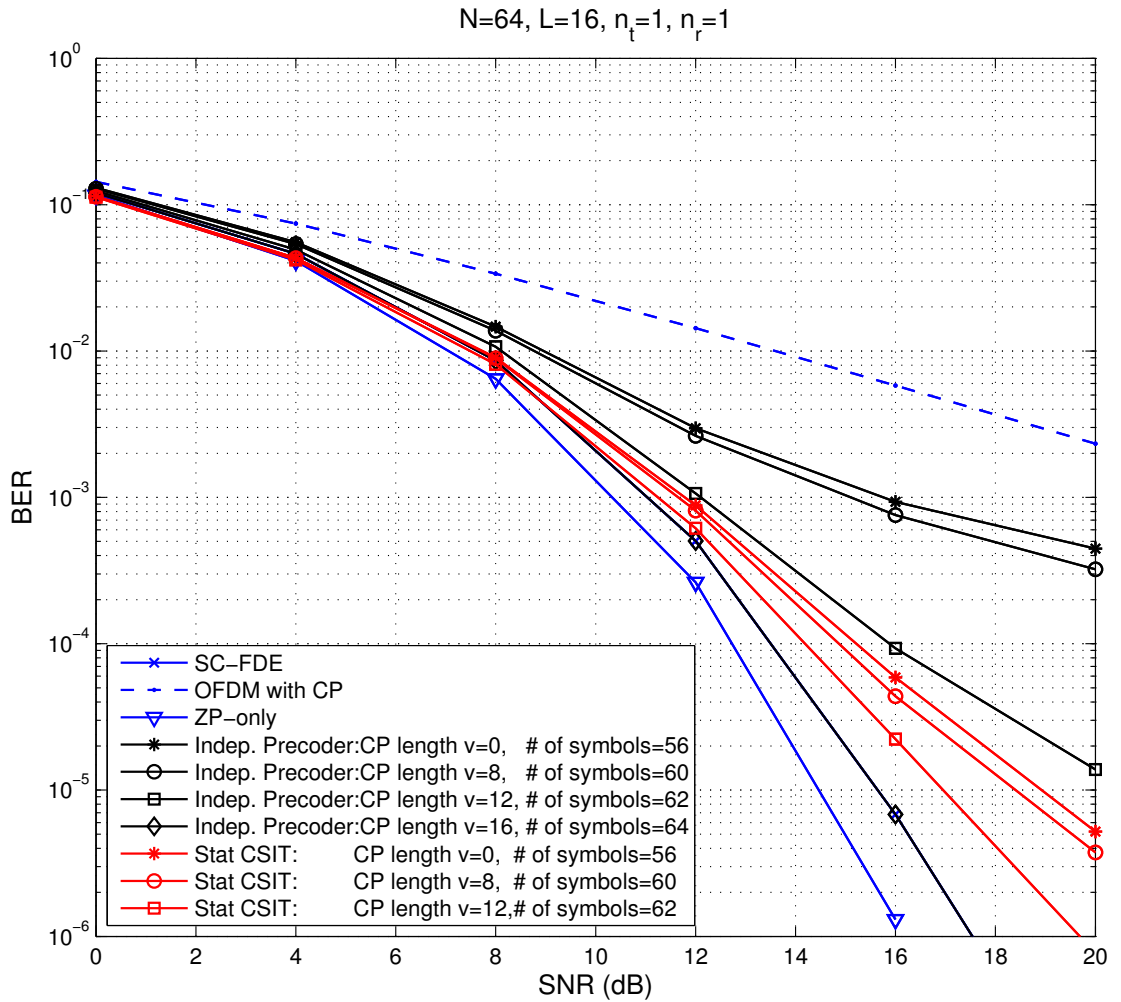


Figure 3.1: MIMO case: BER performances of SC-FDE, CP-OFDM, ZP-only, our channel independent precoding and the proposed precoding based on statistical CSIT

In Fig. 3.2, we demonstrate the system performance degradation when more independent information symbols than total number limit required by the Theorem 1 are transmitted using the channel independent precoding and the statistical CSIT based precoding. The channel memory length $L = 16$. We plot the performance for $v = 8$ and the independent symbol number 60 in one block for both the channel independent precoding and the statistical CSIT precoding. This result are compared to the performance for $v = 8$ and sending 62 independent symbols in one block for both schemes, which are the transmissions with residual IBI. Finally, sufficient CP performance, i.e., $v = 16$, is provided as a benchmark. From Fig. 2, we can observe that the statistical CSIT precoding can perform better than the channel independent precoding even with some remainder of IBI.

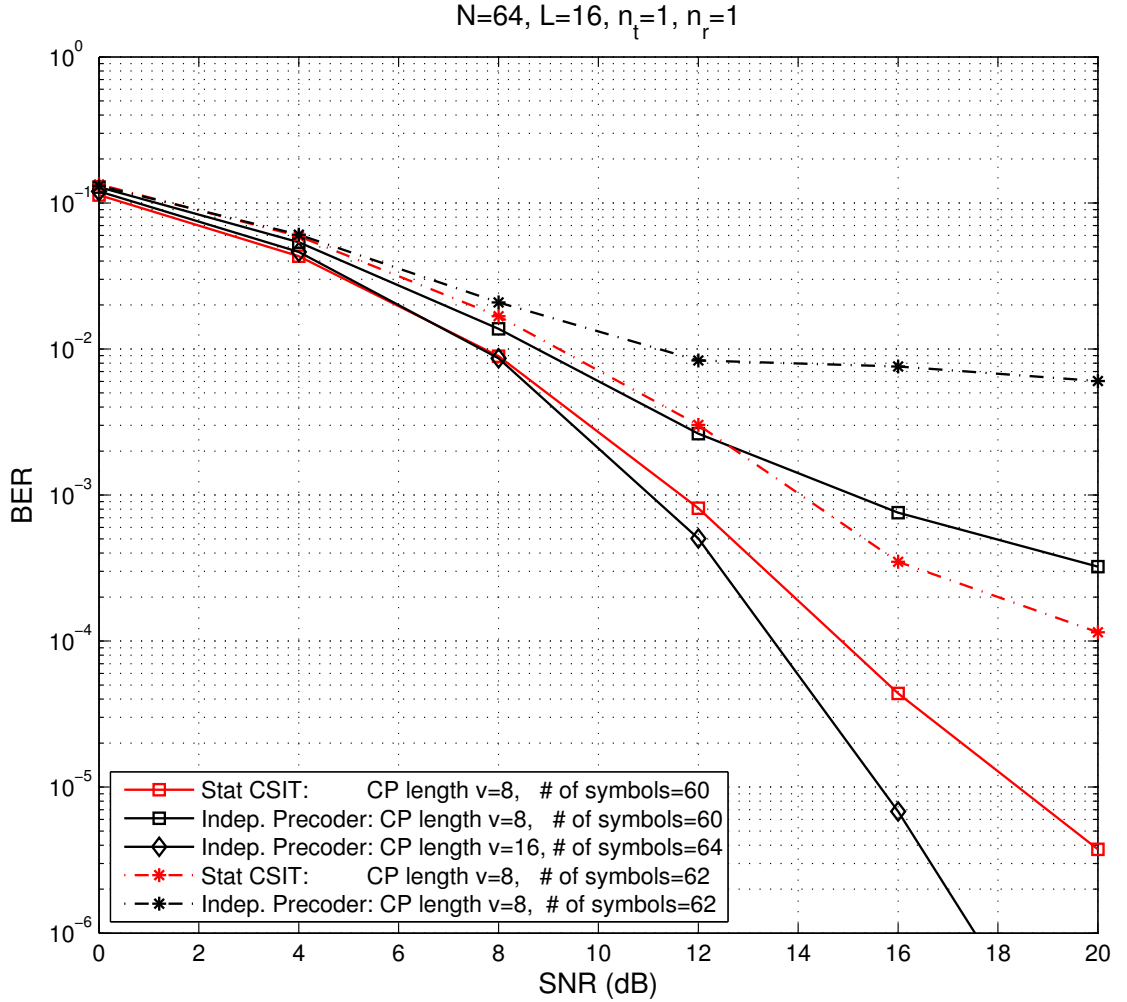


Figure 3.2: MIMO case: BER performances of the proposed precoding without/with interblock interference

In the next simulation in Fig. 3.3, we consider the statistical CSIT based precoder in this paper for a MIMO configuration of three transmit antennas and two receive antennas, i.e., $n_t = 3$ and $n_r = 2$. We choose the block size $N = 32$, channel memory length $L = 20$. For both channel independent and statistical CSIT based

precoders, the results of insufficient CP length $v = 8$ and sending 62 independent information symbols are provided, compared to the performance of full CP, i.e. $v = 20$, and sending 64 independent symbols. And another comparison for these two precoding schemes is between the transmissions with IBI. The results for sending 62 independent information symbols with CP length $v = 6$ are shown in dashed curves, which are the transmission with IBI. In Fig. 3, we notice that for the case of transmission with IBI, the statistical CSIT based precoder has better performance than the channel independent precoder, though the error floor occurs for both precoding schemes. For the cases of transmission without IBI, when $v = 8$, i.e., the CP is insufficient, the statistical CSIT precoder outperforms the channel independent precoder obviously. When $v = 20$, i.e., the CP is sufficient, the statistical CSIT precoder has slightly better performance when the SNR is high.

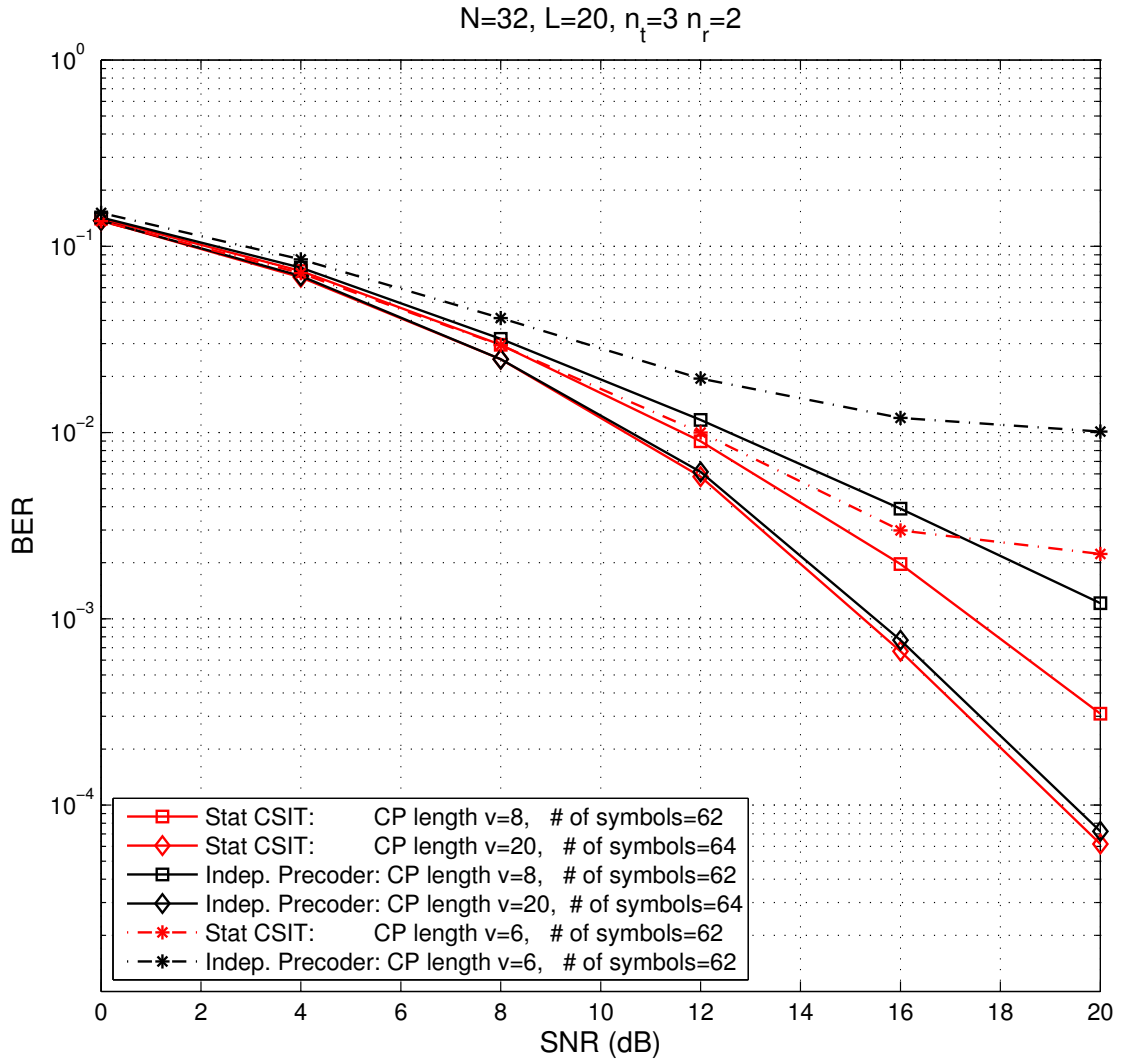


Figure 3.3: MIMO case: BER performances of statistical CSIT precoding and the channel independent precoding

Then in Fig. 3.4, we switch to a 4×4 MIMO configuration. Channel memory length is $L = 12$. Set the block size $N = 32$. When 128 information symbols are transmitted with insufficient CP length $v = 6$, IBI exists. In this case, the statistical

CSIT based precoder is better than the channel independent precoder shown in dashed curves. Both dashed curves have error floor when the SNR is high. When we go to the IBI free cases, if an insufficient CP is used, i.e., $v = 6$ and sending 116 information symbols, we can see that the performance of the statistical CSIT based precoder is superior to that of the independent precoder. If a sufficient CP is used, the statistical CSIT based precoder outperforms as well.

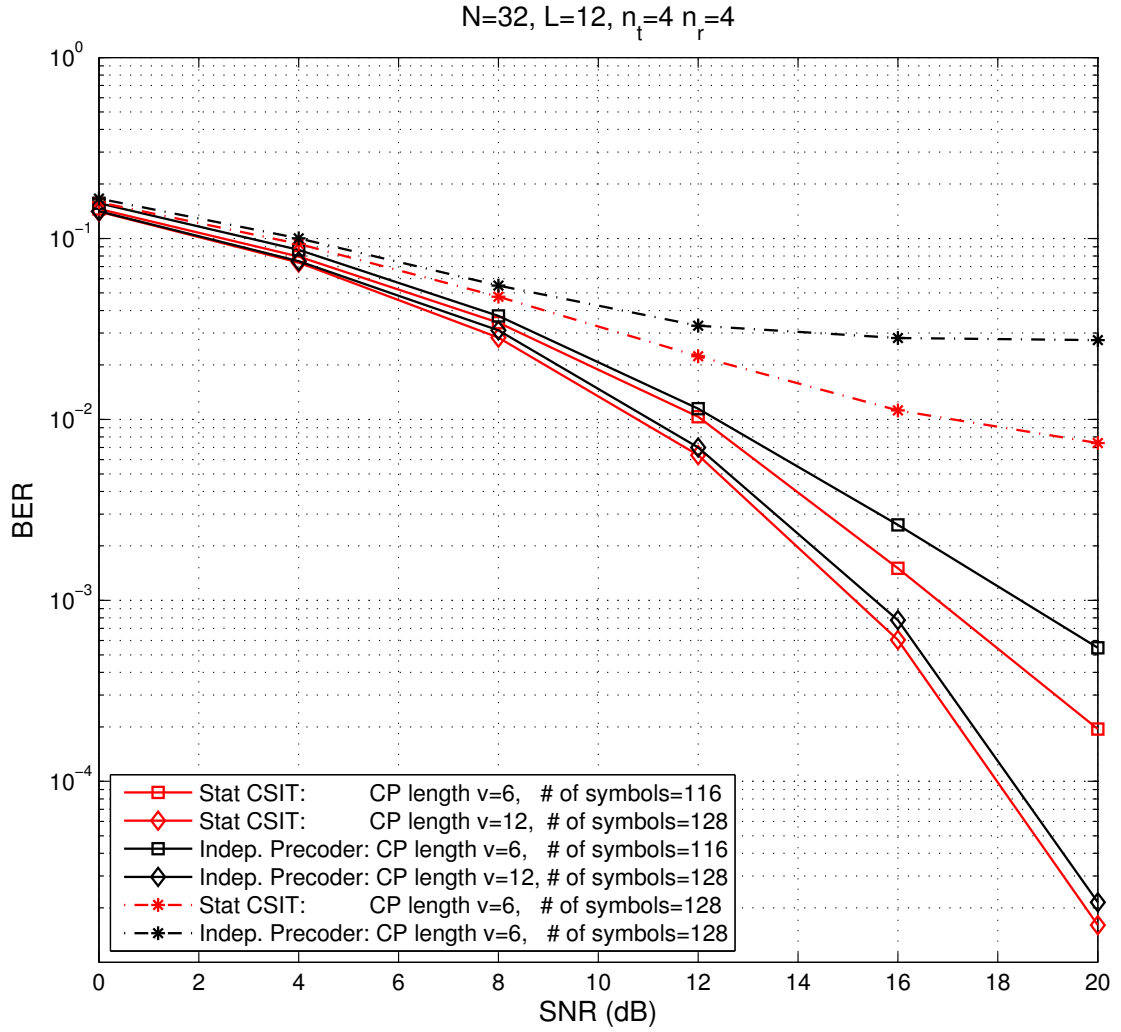


Figure 3.4: MIMO case: BER performances of IA based precoding of different CP lengths and different numbers of information symbols

3.5 Conclusion

In this paper, we continue our discussion in [27] on the precoding for MIMO-OFDM systems with insufficient CP. Instead of the channel independent precoding in

our previous work [27], new precoder based on the channel statistics at the transmitter is proposed. This design retains the property of IBI separation as what we have discussed in the channel independent precoding. Combined with the IBI zero forcing operation at the receiver, more data symbols are transmitted in the MIMO-OFDM system, and thus higher spectral efficiency is achieved. An interference free equivalent channel can be constructed from the compound of the zero-forcing and channel matrices. Toward this equivalent channel, an optimized precoder design has been carried out aiming at minimizing the maximal MSE of all the data streams. Substantial gains compared to the unoptimized channel independent precoding can be seen from the simulation results.

Chapter 4

FULL DUPLEX DELAY DIVERSITY RELAY TRANSMISSION USING BIT-INTERLEAVED CODED OFDM

4.1 Introduction

In recent years, relay-assisted wireless communication system has been undergoing extensive development in both industry and academia [43]. One of the most attractive benefits of relaying is the exploitation of the innate cooperative diversity to combat channel fading and boost the communication reliability, by combining multiple duplicates of signal from independent paths at the destination, see for example, [58, 57, 30, 34, 23, 11, 3]. By receiving, processing, and retransmitting radio signals, relay networks offer an energy efficient and low cost solution to expand coverage of wireless connections. The two most typical relaying protocols are amplify-and-forward (AF) [30, 34, 23, 11, 3, 31] and decode-and-forward (DF) [30, 21, 31, 24]. The AF protocol outperforms the DF counterpart in terms of less computational demand and shorter processing delay.

An in-band full-duplex relay performs concurrent reception and transmission in the same frequency band, hence improving the spectral efficiency significantly [55, 53, 52, 51, 38, 39] over that of the half-duplex relaying. However, practical realization and implementation of full-duplex networks still confront numerous challenges. One of the most noticeable problems is the self-interference (SI) [55, 53, 52], which directly results from the concurrent transmission and reception at the same frequency. The strong SI looped back from the transmitter at the relay node can easily diminish the throughput gain of the full-duplex relay system. A substantial amount of effort has been paid to the SI suppression techniques. First of all, physical isolation of the relay's transmit and receive antennas, for instance, directional antennas, or sufficient large separation

distance between transmit and receive antennas, should be taken to partially remove the SI. A combination of RF interference cancellation, baseband digital interference cancellation as well as some other additional cancellation mechanisms, are also required to suppress the SI to a fairly low level, see for example [55, 53, 52, 51, 38, 39, 12, 48]. Experiment reports, such as [12, 22], show that at least 110 dB of SI suppression can be achieved by employing both isolation and interference cancellation techniques. Although the SI can be minimized by interference suppression techniques, residual self-interference still poses a main issue in reality and residual SI management is an indispensable requirement in the designs of all practical full-duplex relay networks.

Based on different treatments over the residual SI, current literatures in the full-duplex relaying with SI are mainly in two categories:

1. The first category of papers focus on how to mitigate the SI efficiently. One of the representative works is reported in [53, 52], where the SI is suppressed to such an infinitesimal level that it can be simply regarded as additional relay noise. In the aforementioned works, SI is modeled as recursive loopback interference from the relay transmit signal to its receive signal. Time domain cancellation and spatial domain suppression and their combination are proposed to cancel the SI as much as possible.
2. The second category of papers only require partial cancellation of SI and treat the residual SI as a useful signal component rather than additional noise. Representative works can be found in [38, 39], where the SI is also modeled as recursive loopback interference and the SI is intended not to be cancelled entirely. The residual SI is treated as a self-coding and used to form a space-time code structure in the destination received signal. The advantage of this technique is that the SI is deemed as signal and adequately utilized to provide benefits in terms of full cooperative diversity.

Our proposed scheme is inspired by the idea from the second category of works, since the residual SI is bearing desired information and thus residual SI management should be able to take advantage of the interference to enhance the robustness of the full-duplex relay networks. A relay assisted cooperative system can be regarded as a virtual MISO system. For MISO systems, delay diversity techniques can be used to increase the system robustness[59, 17]. For MISO systems employing OFDM modulation, several variants of delay diversity (DD) and cyclic delay diversity (CDD) techniques

can be adopted to exploit the frequency diversity [32, 4, 40]. In the scope of full duplex relay systems, the spatial diversity offered by the distributedly located source antenna and the relay transmit antenna can be exploited by using OFDM and DD. Interestingly, in the relay network the necessary processing delay at the AF relay node provides a natural resource of delay spread. This delay spread can be fully exploited to provide more robustness to the relay system. Moreover, power allocation always plays an important role for the robustness of OFDM systems. Power allocation can be implemented either individually among subcarriers [?, 33] or all subcarriers can have equal power and different portions of power can be allocated respectively to source node subcarriers and relay node subcarriers[24]. We also consider the power allocation problem in order to further guarantee the robustness of the system performance of our full-duplex relaying system, where different amounts of power are allocated to source node and relay node, respectively.

Our paper contributes to the study of full-duplex OFDM relaying in the following aspects:

- Firstly, we carry forward the idea of utilizing residual SI as useful signal rather than noise. The direct link coefficient, relay link coefficient and the residual SI are altogether modeled as a virtual multipath channel at the destination, which is a novel idea for the full-duplex OFDM relay system and facilitates fully utilizing the residual SI as a beneficial signal component.
- Based on our proposed system model, the necessary CP length at the source node is discussed. Generally, if more residual SI is modeled as the virtual multipaths at the destination, a more extended CP is required and thus less interference is introduced to the proposed system.
- Next, we also propose a block-based AF relay protocol to realize the DD OFDM at the destination node. With the help of this protocol, the full-duplex relay link can act as an extra diversity branch to provide enhanced robustness to our proposed full-duplex relay system.
- In addition, we utilize bit-interleaved coded modulation (BICM) OFDM to collect the diversity order of two in the AF relay system. Simulation results show the effectiveness of our proposed scheme.
- Finally, we also discuss the power allocation problem for our proposed full-duplex relay communication system with a total sum power constraint on the source and

relay transmission powers. Simulation results demonstrate that the proposed power allocation performs better than equal power allocation.

The remainder of the paper is organized as follows. The full-duplex signal model is described in Section II. The DD OFDM full-duplex relay scheme is proposed in Section III. Some simulation results to verify the error probability performance of the proposed system are demonstrated in Section IV. Finally, this paper is concluded in Section V.

Notations: Lowercase letters are used to denote scalars. Lowercase bold letters and uppercase bold letters stand for vectors and matrices, respectively. $(\cdot)^T$, $|\cdot|$, and $\mathbb{E}\{\cdot\}$ denote transpose, modulus, and expectation.

4.2 Signal Model

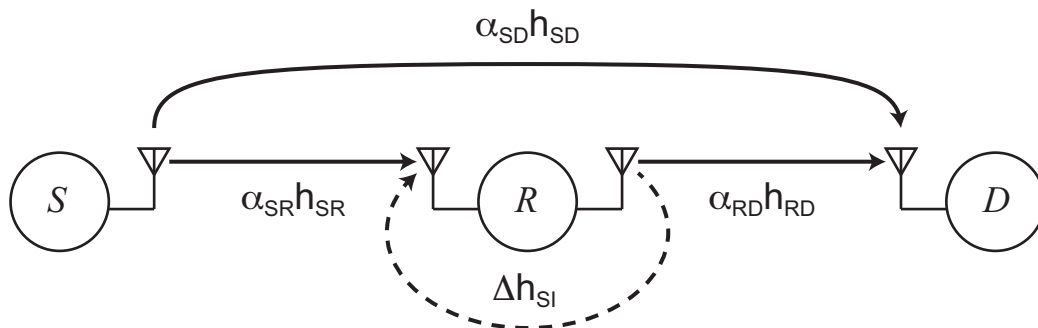


Figure 4.1: Dual-hop full-duplex relay network

In this section, we consider a dual-hop relay assisted communication system. As illustrated in Fig. 4.1, the relay system consists of a single antenna source node (S), a single antenna destination node (D), and a relay node (R) with one transmit antenna and one receive antenna. In-band full-duplex mode is employed, which allows for simultaneous transmission and reception at the relay node. The source node transmits a stream of data symbols to the destination node via two links, i.e the direct source-to-destination link, and the dual-hop relay link. At the receive antenna, the relay

node receives the signal from the source node, and in the meantime it amplifies and transmits the previous received signal to the destination via its transmit antenna. The concurrent transmitted signal at the relay loops back and interferes with the received signal. Although interference cancellation techniques, for example, successive interference cancellation or adaptive filtering can be utilized to suppress the loopback interference, a non-negligible residue of the loopback interference inevitably exists and may decrease the error probability performance of the relay system.

Both path loss and small-scale fading are considered in modeling the relay system. All the path loss coefficients, including from the source node to the destination node α_{SD} , from the source node to the relay node α_{SR} and from the relay node to the destination node α_{RD} , are positive constants. In addition, assume that there is no path loss for the loopback interference channel due to the comparatively small propagation distance. The relay system has three quasi-static, frequency flat communication channels, namely, the source-to-relay channel h_{SR} , the relay-to-destination channel h_{RD} and the direct source-to-destination channel h_{SD} . In this paper, we mainly focus on single tap channels, i.e., h_{SR} , h_{RD} and h_{SD} are all assumed zero mean complex Gaussian scalar random variables with unit variance. The loopback residual self-interference channel is modeled as a frequency flat channel and denoted by Δh_{SI} , which is assumed to be zero mean complex Gaussian with variance σ_{SI}^2 , i.e., $\Delta h_{SI} \sim \mathcal{CN}(0, \sigma_{SI}^2)$. The relay node is assumed to have no channel state information of all associated channels. But the relay node is able to estimate the average power of the residual self-loopback channel. The information of average power of the residual self-loopback channel will be fed back to the source node as a reference to add cyclic prefix (CP) with an appropriate length. Furthermore, perfect symbol and carrier synchronization are assumed in all the nodes.

The source node transmits signal $x(i)$ in the i -th time slot with average symbol energy $\mathbb{E}\{|x(i)|^2\} = 1$ and average transmit power

$$P_s = \gamma P, \quad (4.1)$$

where $\gamma \in (0, 1)$ is the power allocation factor and P is the total relay system power consumption. The relay receives signal $r(i)$ while transmits signal $t(i)$ concurrently with an amplification factor β . The received signal at the relay consists of the signal transmitted from the source and the loopback interference and the received noise. Thus, the received signal at the relay is represented by

$$r(i) = \sqrt{P_s} \alpha_{SR} h_{SR} x(i) + \Delta h_{SI} t(i) + n(i), \quad (4.2)$$

where $n(i)$ is the AWGN at the receive antenna of the relay, which has zero mean and average variance $\mathbb{E}\{|n(i)|^2\} = \sigma_R^2$. Upon reception, the relay can amplify and forward the signal with a power of

$$P_r = (1 - \gamma)P. \quad (4.3)$$

The received signal is re-transmitted by multiplying an amplification factor β , which is often chosen to normalize the received signal power [26]. In our signal model, we choose an amplification factor β , which is given by

$$\begin{aligned} \beta &= \frac{\sqrt{P_r}}{\sqrt{P_s \alpha_{SR}^2 + P \sigma_{SI}^2 + \sigma_R^2}}, \\ &= \frac{\sqrt{(1 - \gamma)P}}{\sqrt{\gamma P \alpha_{SR}^2 + P \sigma_{SI}^2 + \sigma_R^2}}. \end{aligned} \quad (4.4)$$

In (4.4), the denominator of β serves for normalizing the received signal in (4.2) so that the normalized signal has an average power of one and the numerator of β serves for relay power allocation so that the transmitted signal at the relay has power P_r .

The transmitted signal at the relay is a delayed version of $\tau \geq 1$ symbols due to the relay processing delay[54]. The transmitted signal at the relay is given by

$$t(i) = \begin{cases} 0, & \text{for } 0 \leq i \leq \tau - 1 \\ \beta r(i - \tau), & \text{for } i \geq \tau. \end{cases} \quad (4.5)$$

We assume without loss of generality that the interference cancellation in full-duplex relay takes a processing delay of one symbol period, i.e., $\tau = 1$. For $i \geq 1$, by recursively

implementing (4.2) and (4.5), the transmit signal at the relay can be represented by the summation of infinite echo of the received signal at the relay, i.e.,

$$t(i) = \beta \sum_{j=1}^{\infty} (\Delta h_{SI} \beta)^{j-1} \left[\sqrt{P_s} \alpha_{SR} h_{SR} x(i-j) + n(i-j) \right]. \quad (4.6)$$

However, it is not practical to think of infinite terms of feedback in the transmit signal $t(i)$, because the magnitude of residual interference, namely $|\Delta h_{SI}|$, is fairly small and $|(\Delta h_{SI})^j \beta^{j+1}|$ is insignificant for a large j . As a consequence, we only need to retain the first J terms of loopback interference in (4.6) as the effective loopback multipath channel, where J is chosen such that most of the energy, for example, 99.9%, is contained in the first J terms. Regard the rest of infinite trivial interference terms as noise. Then (4.6) can be alternatively expressed as,

$$t(i) = \beta \sum_{j=1}^J (\Delta h_{SI} \beta)^{j-1} \sqrt{P_s} \alpha_{SR} h_{SR} x(i-j) + \bar{n}(i), \quad (4.7)$$

where $\bar{n}(i)$ is given by

$$\bar{n}(i) = \beta \sum_{j=J+1}^{\infty} (\Delta h_{SI} \beta)^{j-1} \sqrt{P_s} \alpha_{SR} h_{SR} x(i-j) + \beta \sum_{j=1}^{\infty} (\Delta h_{SI} \beta)^{j-1} n(i-j). \quad (4.8)$$

It can be viewed that in (4.7) that $t(i)$ is the output of $x(i)$ passing through an effective residual self-interference channel \mathbf{h}_{RSI} , which has J non-zero paths. \mathbf{h}_{RSI} can be given by

$$\begin{aligned} \mathbf{h}_{RSI} &= \sqrt{P_s} \alpha_{SR} h_{SR} [\beta, \beta^2 \Delta h_{SI}, \dots, \beta^J (\Delta h_{SI})^{J-1}]^T \\ &\triangleq [h_{RSI}(0), h_{RSI}(1), \dots, h_{RSI}(J-1)]^T. \end{aligned} \quad (4.9)$$

At the destination node, the received signal can be represented by

$$y(i) = \sqrt{P_s} \alpha_{SD} h_{SD} x(i) + \alpha_{RD} h_{RD} t(i) + \eta(i), \quad (4.10)$$

where $\eta(i)$ denotes the AWGN with zero mean and average variance $\mathbb{E}\{|\eta(i)|^2\} = \sigma_D^2$.

We can rewrite the received signal expression (4.10) by substituting $t(i)$ with its expression in (4.7),

$$\begin{aligned}
y(i) &= \sqrt{P_s}\alpha_{SD}h_{SD}x(i) \\
&+ \sqrt{P_s}\alpha_{SR}h_{SR}\alpha_{RD}h_{RD}\sum_{j=1}^J(\Delta h_{SI})^{j-1}\beta^j x(i-j) \\
&+ \bar{\eta}(i),
\end{aligned} \tag{4.11}$$

where $\bar{\eta}(i)$ is the equivalent noise and is given by $\bar{\eta}(i) = \alpha_{RD}h_{RD}\bar{n}(i) + \eta(i)$. It is observed from (4.11) that the destination received signal $y(i)$ is essentially the convolution of the transmit signal $x(i)$ and a virtual multipath channel $\mathbf{h} \in \mathbb{C}^{(J+1) \times 1}$ of $J+1$ paths, which is represented by (4.12).

$$\mathbf{h} = [\sqrt{P_s}\alpha_{SD}h_{SD}, \alpha_{RD}h_{RD}h_{RSI}(0), \alpha_{RD}h_{RD}h_{RSI}(1), \dots, \alpha_{RD}h_{RD}h_{RSI}(J-1)]^T \tag{4.12}$$

4.3 Block Based Full-Duplex Delay Diversity Transmission

In this section, we propose a block based full-duplex DD transmission scheme by partitioning the continuous transmitting streams of data symbols into blocks of N symbols and by implementing CP insertion and removal at the source node and destination node, respectively. In our scheme, there are three factors which are crucial to the DD transmission, namely, CP length, relay processing delay and the relay processing. By employing CP with an appropriate length, positively utilizing the delay introduced at the relay and also the proposed relaying scheme at the relay node, we manage to transform the AF relay assisted communication system into a DD block based transmission system.

4.3.1 Full-Duplex Delay Diversity Transmission

Let us start with the source node transmission. The source node signal processing is illustrated in Fig. 4.2.

A.1 Source Node Implementation

As shown in Fig. 4.2, a stream of uncoded information bits $\{u_m\}$ is sent into a binary convolutional code (BCC) encoder and the output of the encoder is

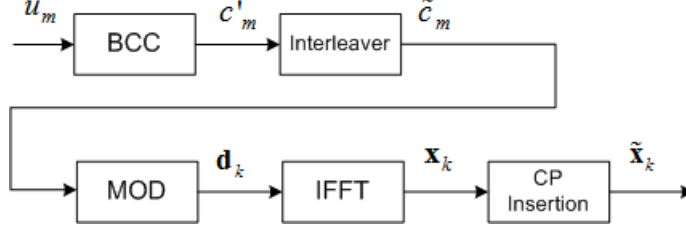


Figure 4.2: Source node signal processing diagram

a stream of coded bits $\{c'_m\}$. $\{c'_m\}$ is then separated into K segments $\{c_m^{(k)}\}$ of bN bits, $k = 1, 2, \dots, K$. Each segment is interleaved by a block interleaver Π . The interleaver should be designed in accordance with the rules in [2]. Concatenate all these K bit interleaved sequences to form a single bit stream $\{\tilde{c}_m\}$. The bits in $\{\tilde{c}_m\}$ are grouped into b -bit segments and mapped onto 2^b -ary modulation symbols using the Gray labelling, i.e., $d(1), d(2), d(3), \dots$, which are selected from a finite signal constellation \mathcal{A} .

The modulated data symbols are subsequently divided into blocks with block length N . The k -th data block \mathbf{d}_k is given by

$$\mathbf{d}_k = [d_k(0), d_k(1), \dots, d_k(N-1)]^T, \quad (4.13)$$

where $d_k(n)$ is the n -th symbol in the k -th block. Frequency domain data block \mathbf{d}_k is transformed into time domain data block \mathbf{x}_k by implementing N -point IDFT, which is represented by

$$\begin{aligned} \mathbf{x}_k &= \mathbf{F}_N \mathbf{d}_k, \\ &= [x_k(0), x_k(1), \dots, x_k(N-1)]^T, \end{aligned} \quad (4.14)$$

where \mathbf{F}_N denotes the normalized IDFT matrix of order N , i.e., $[\mathbf{F}_N]_{i,j} = (1/\sqrt{N}) \exp(-j2\pi(i-1)(j-1)/N)$, for $i = 1, 2, \dots, N$, and $j = 1, 2, \dots, N$.

For the DD processing, the relay node needs to transmit the cyclic delayed version of the blocks transmitted at the source node. But the relay in essence is a

repeater and only repeats the signal it receives from the source node. To realize the transmission of a cyclic delayed data block requires the selection of both a proper CP length at the source node and a time delay at the relay node.

Let's now take a close look at (4.11), where the received signal $y(i)$ at the destination node is the linear convolution of the transmitted signal $x(i)$ at the source and the virtual multipath channel \mathbf{h} with delay spread of J symbols. It is obvious that a CP with minimum length of J symbols is required at the source node, if we are attempting to convert the linear convolution of the transmit signal $x(i)$ and the multipath channel \mathbf{h} into a circular convolution of the transmit data block \mathbf{x}_k and the multipath channel \mathbf{h} . Thus, the CP length L_{CP} in the full-duplex AF relay system is required to be greater than or equal to the number of loopback multipath, which is given by

$$L_{CP} \geq J. \quad (4.15)$$

The k -th CP prepended block $\tilde{\mathbf{x}}_k \in \mathbb{C}^{(N+L_{CP}) \times 1}$ is formulated by prepending L_{CP} CP symbols to each of the data block \mathbf{x}_k , which is given by,

$$\begin{aligned} \tilde{\mathbf{x}}_k &= [x_k(N - L_{CP}), \dots, x_k(N - 1), x_k(0), x_k(1), \dots, x_k(N - 1)]^T \\ &\triangleq [\tilde{x}_k(0), \tilde{x}_k(1), \dots, \tilde{x}_k(N + L_{CP} - 1)]^T, \end{aligned} \quad (4.16)$$

where the data symbols and the cyclic prefix are re-denoted by $\tilde{x}_k(i)$ indexed from 0 to $N + L_{CP} - 1$. $\tilde{\mathbf{x}}$ is transmitted sequentially via the transmit antenna at the source node.

A.2 Relay Node Implementation

In the next, we discuss the relay processing, which is illustrated in Fig 4.3. During the transmission of the k -th CP prepended block at the source node, the relay stores each received symbol except the last one and re-transmits at its transmit antenna in the next time slot with an amplification factor β . The relay does not forward the last received symbol because the next time slot is allocated to transmit the symbol for

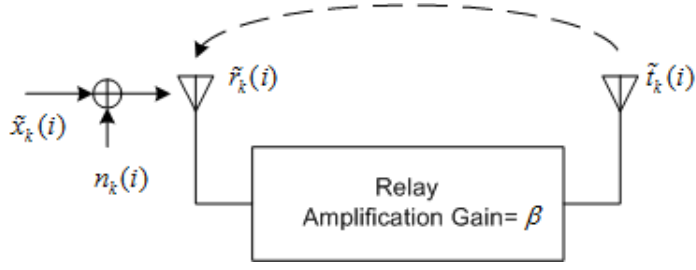


Figure 4.3: Relay node signal processing diagram

next transmission block. The special attention has been paid to the transmission of the first symbol and the reception of the last symbol in each block. In the first time slot of each block, because the relay is required to delay its transmission to increase the number of multipath in the equivalent circulant channel matrix at the destination and the channel h_{SD} has only one tap, we need to set the first transmitted symbol in each block to be zero, which is also the processing delay of $\tau = 1$. Therefore, the transmitted symbols during the k -th block can be represented by

$$\tilde{t}_k(i) = \begin{cases} 0, & \text{for } i = 0 \\ \beta \tilde{r}_k(i-1), & \text{for } i = 1, 2, \dots, N + L_{CP} - 1, \end{cases} \quad (4.17)$$

where r_k is the received signal at the i -th time slot, $0 \leq i \leq N + L_{CP} - 2$, during the transmission of the k -th block.

Note that the necessary delay at the relay node actually provides the delay diversity. With CP insertion and removal and also the above relaying protocol at the first and the last time slots, delay diversity is finally transformed into the multipath diversity at the destination as we shall see later.

Since the received signal at the relay is the combination of the transmitted signal from the source node, the loopback interference from the transmitter of the relay and the additive noise, $\tilde{r}_k(i)$ can be given by (4.18).

$$\tilde{r}_k(i) = \begin{cases} \alpha_{SR}h_{SR}\tilde{x}_k(i) + n_k(i), \\ \text{for } i = 0, \\ \alpha_{SR}h_{SR}\tilde{x}_k(i) + \sum_{j=\max\{1, i-J+1\}}^i h_{RSI}(i-j)\tilde{x}_k(j-1) + \bar{n}_k(i), \\ \text{for } i = 1, 2, \dots, N + L_{CP} - 1, \end{cases} \quad (4.18)$$

In (4.18) by defining $n_k(i)$, $i = 0, 1, \dots, N + L_{CP} - 1$, to be i.i.d. complex Gaussian with zero mean and variance σ_R^2 , we can use $\bar{n}_k(i)$ to represent the overall additive noise,

$$\bar{n}_k(i) = \begin{cases} \sum_{j=0}^i (\Delta h_{SI}\beta)^{i-j} n_k(j), \\ \text{for } i = 0, 1, \dots, J \\ \sum_{j=0}^i (\Delta h_{SI}\beta)^{i-j} n_k(j) + \sum_{j=0}^{i-J-1} (\Delta h_{SI}\beta)^{i-j} \alpha_{SR}h_{SR}x_k(j), \\ \text{for } i = J + 1, \dots, N + L_{CP} - 1. \end{cases} \quad (4.19)$$

Since the last information symbol $x_k(N - 1)$ has already been contained in the CP portion and has been forwarded by the relay node, the relay node receives the last symbol in the k -th transmission block but does not transmit, which will not destroy the circulant structure in the time domain equivalent channel matrix after the CP removal later. After forwarding the signal in the last symbol interval, the relay node clears all the stored signal. This processing can help to prevent interfering the next transmission block. The relay processing is summarized in the following Algorithm 1.

Algorithm 1 AF Relay Processing

OFDM symbol $k = 0, 1, 2, \dots$ **if** $i = 0$ **then**

$$\tilde{t}_k(0) = 0$$

$$\tilde{r}_k(0) = \alpha_{SR}h_{SR}\tilde{x}_k(0) + n_k(0)$$

end if**for** $i = 1, 2, \dots, N + L_{CP} - 1$ **do**

$$\tilde{t}_k(i) = \beta\tilde{r}_k(i - 1)$$

$$\tilde{r}_k(i) = \alpha_{SR}h_{SR}\tilde{x}_k(i) + \sum_{j=\max(1, i-J+1)}^i h_{RSI}(i-j)\tilde{x}_k(j-1) + \bar{n}_k(i)$$

if $i = N + L_{CP} - 1$ **then**

Clear the stored signal

end if**end for**

A.3 Destination Node Implementation

Since the relay transmission (4.17) follows the general principle (4.6), the received signal model (4.11)-(4.12) applies here. Without loss of generality, let us only consider the first block and the received signal at time slot i , $0 \leq i \leq N + L_{CP} - 1$, is given by

$$\tilde{y}_k(i) = \sqrt{P_s}\alpha_{SD}h_{SD}\tilde{x}_k(i) + \sqrt{P_s}\alpha_{SR}h_{SR}\alpha_{RD}h_{RD}\sum_{j=1}^J(\Delta h_{SI})^{j-1}\beta^j\tilde{x}_k(i-j) + \tilde{\eta}_k(i), \quad (4.20)$$

where we define $\tilde{x}_k(i) = 0$ for $i < 0$, $\eta_k(i)$ is AWGN distributed as $\mathcal{CN}(0, \sigma_D^2)$, $\tilde{\eta}_k(0) = \eta_k(0)$, and $\tilde{\eta}_k(i) = \eta_k(i) + \alpha_{RD}h_{RD}\beta\bar{n}_k(i-1)$ for $i = 1, \dots, N + L_{CP} - 1$.

The k -th received block $\tilde{\mathbf{y}}_k$ includes $N + L_{CP}$ symbols, we have

$$\tilde{\mathbf{y}}_k = [\tilde{y}_k(0), \tilde{y}_k(1), \dots, \tilde{y}_k(N + L_{CP} - 1)]^T. \quad (4.21)$$

The first L_{CP} symbols of $\tilde{\mathbf{y}}_k$ are the CP symbols and they are removed at the destination node according to (4.20). After the CP removal, the information symbols remained from the direct path, i.e., the first term in the right hand side of (4.20) are

$\tilde{x}(L_{CP}), \tilde{x}(L_{CP+1}), \dots, \tilde{x}(N + L_{CP} - 1)$, i.e., $x(0), x(1), \dots, x(N - 1)$; the information symbols remained from the second term of the right hand side of (4.20), corresponding to the path $\sqrt{P_s}\alpha_{SR}h_{SR}\alpha_{RD}h_{RD}\beta$, are $\tilde{x}(L_{CP} - 1), \tilde{x}(L_{CP}), \dots, \tilde{x}(N + L_{CP} - 2)$, i.e., $x(N - 1), x(0), \dots, x(N - 2)$; and so forth, the information symbols remained from the $(J + 1)$ -th term of the right hand side of (4.20), corresponding to the path $\sqrt{P_s}\alpha_{SR}h_{SR}\alpha_{RD}h_{RD}(\Delta h_{SI})^{J-1}\beta^J$, are $\tilde{x}(L_{CP} - J), \tilde{x}(L_{CP} - J + 1), \dots, \tilde{x}(N + L_{CP} - J - 1)$, i.e., $x(N - J), x(N - J + 1), \dots, x(N - J - 1)$. One can see from the above analysis, all the original information symbols $x(0), x(1), \dots, x(N - 1)$ are included in every path in the received signal (4.20).

Thus, if we denote the received signal after the CP removal by $\mathbf{y}_k \in \mathbb{C}^{N \times 1}$, we have

$$\mathbf{y}_k = \tilde{\mathbf{H}}_k \mathbf{x}_k + \check{\boldsymbol{\eta}}_k, \quad (4.22)$$

where $\tilde{\mathbf{H}}_k \in \mathbb{C}^{N \times N}$ is a circulant matrix and its first column is the virtual multipath channel \mathbf{h} in (4.12) padded by $N - J - 1$ zeros, i.e., $[\mathbf{h}^T, 0, \dots, 0]^T$ and $\check{\boldsymbol{\eta}}_k = [\check{\eta}_k(L_{CP}), \dots, \check{\eta}_k(N + L_{CP} - 1)]^T$ is the additive noise.

Transforming the received signal to the frequency domain by implementing the N -point DFT on \mathbf{y}_k , we have

$$\begin{aligned} \mathbf{z}_k &= \mathbf{F}_N^H \mathbf{y}_k \\ &= \mathbf{H}_k \mathbf{d}_k + \boldsymbol{\nu}_k \end{aligned} \quad (4.23)$$

where

$$\begin{aligned} \mathbf{H}_k &= \mathbf{F}_N^H \tilde{\mathbf{H}}_k \mathbf{F}_N \\ &= \text{diag}(H_k(0), H_k(1), \dots, H_k(N - 1)) \end{aligned} \quad (4.24)$$

is the diagonal frequency domain channel matrix with the subcarrier coefficients on the main diagonal and $\boldsymbol{\nu}_k = \mathbf{F}_N^H \check{\boldsymbol{\eta}}_k$ is the $N \times 1$ noise vector in the frequency domain.

An estimate of the transmitted block, i.e., $\hat{\mathbf{d}}_k$, can be obtained by per-subcarrier zero-forcing or MMSE equalization. After de-mapping, the interleaved coded bit sequence $\{\hat{c}_m\}$ is acquired. Then we get the coded bit sequence $\{\hat{c}'_m\}$ by passing $\{\hat{c}_m\}$

through the de-interleaver Π^{-1} . The estimate of the uncoded bit sequence $\{\hat{u}_m\}$ by decoding the coded sequence $\{\hat{c}'_m\}$. Following the design criteria of BICM [2], the full diversity order of two can be achieved on the error performance of $\{\hat{u}_m\}$.

4.3.2 Power Allocation Scheme

For the same relay topology, if it is half duplex, the equal power allocation is commonly used, i.e., selecting the power allocation factor $\gamma = 0.5$ so that $P_s = \gamma P = P/2$, $P_r = (1 - \gamma)P = P/2$. However, for the full-duplex system, there is an additional self-interference path and equal power allocation may not be optimal anymore.

One alternative approach is to adjust the transmit power P_s and the relay power P_r under a total sum power constraint aiming at equalizing the average channel variance of the direct channel and the average tap variance of the strongest channel tap of the residual self-interference channel. Since in our model $\mathbb{E}\{|h_{SD}|^2\} = \mathbb{E}\{|h_{SR}|^2\} = \mathbb{E}\{|h_{RD}|^2\} = 1$, the overall average channel variance of the direct channel λ_{SD} and the overall average channel variance of the strongest relay channel tap $\lambda_{Relay,1}$ are represented respectively as

$$\lambda_{SD} = \gamma P \alpha_{SD}^2, \quad (4.25)$$

$$\begin{aligned} \lambda_{Relay,1} &= \gamma P \beta^2 \alpha_{SR}^2 \alpha_{RD}^2 \\ &= \frac{\gamma(1 - \gamma)P^2 \alpha_{SR}^2 \alpha_{RD}^2}{\gamma P \alpha_{SR}^2 + \sigma_{SI}^2 + \sigma_R^2}. \end{aligned} \quad (4.26)$$

Let

$$\lambda_{SD} = \lambda_{Relay,1}, \quad (4.27)$$

we can solve for the power allocation factor γ^* in the proposed method, which is represented by

$$\gamma^* = \frac{P \alpha_{SR}^2 \alpha_{RD}^2 - \alpha_{SD}^2 (\sigma_{SI}^2 + \sigma_R^2)}{P \alpha_{SR}^2 (\alpha_{SD}^2 + \alpha_{RD}^2)}. \quad (4.28)$$

The transmit power P_s and the relay power P_r can be computed by using γ^* in (4.1) and (4.3), respectively. The proposed power allocation balances the power strength of

the direct channel and the strongest relay channel tap and thus it is conjectured that this power allocation method can provide near optimal performance.

4.4 Simulation Results

In this section, computer simulations are conducted to evaluate the error probability performance of the proposed DD OFDM scheme in the full-duplex relay system.

In the simulations, we utilize a simulation setting which resembles closely the 3GPP LTE downlink transmission. OFDM symbols with 1024 subcarriers are used. The subcarrier frequency spacing is 15 kHz. The CP length is $L_{CP} = 16$ if no other CP lengths declared. The rate-1/2 convolutional code with Viterbi decoding is used with information size 8000 bits, generating matrix (133, 171) in octal format, and constraint length 7. This convolutional code has a free distance $d_{\text{free}} = 10$. The Viterbi algorithm traceback length is 64. Coded bits are interleaved with a 32×64 block interleaver and thus interleaving is performed within one OFDM symbol to avoid an extended delay requirement to initialize decoding at the destination node. The path losses are assumed as $\alpha_{SD}^2 = 0.2$, $\alpha_{SR}^2 = 0.8$ and $\alpha_{RD}^2 = 1$. The signal to noise ratio at the relay and at the destination are denoted by SNR_R and SNR_D respectively.

We first have a coded BER comparison of five cases: The first two are our proposed full-duplex DD OFDM scheme with $\sigma_{SI}^2/\sigma_{RD}^2 = -40$ dB and $J = 2$, and with $\sigma_{SI}^2/\sigma_{RD}^2 = -2$ dB and $J = 8$, respectively. For these two cases, the effective residual SI multipath length J is respectively chosen so that over 99.9% of the energy is contained in the first J paths. The third case is full-duplex OFDM without the source-to-destination link, and the fourth one is the direct source to destination coded OFDM transmission via a two-path channel with power delay profile [0.8, 0.2], which is referred to as the “2-path coded OFDM” in Fig. 4.4. The last one is the half-duplex counterpart to our full-duplex DD OFDM. In our simulation, the half-duplex transmission employs two time slots to transmit one time domain sample of the OFDM signal, and hence employs 16-QAM modulation and the same convolutional encoder for a fair comparison. For our proposed full-duplex DD OFDM schemes, the proposed

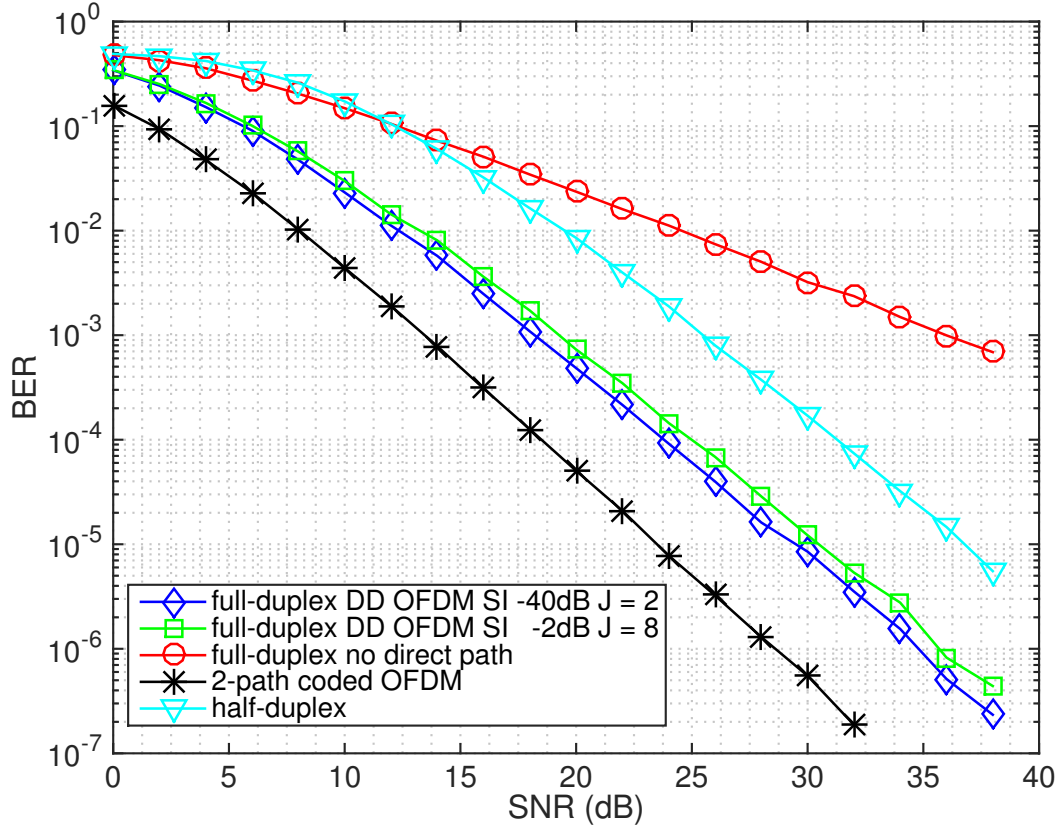


Figure 4.4: Coded BER comparison of full-duplex OFDM without the source-to-destination link, full-duplex DD OFDM, 2-path coded OFDM, and half-duplex OFDM

power allocation is used. For full-duplex OFDM without the source-to-destination link case, equal power allocation is used. QPSK modulated symbols are carried on all subcarriers. In this simulation, SNR_R and SNR_D are assumed to be the same. It can be seen from Fig. 4.4 that in the high SNR region the slopes of the two curves of our proposed DD OFDM scheme are the same as that of the 2-path coded OFDM scheme, which indicates that our proposed scheme for the full-duplex transmission can also achieve a diversity order of two. For the proposed full-duplex DD OFDM scheme, we choose $J = 8$ for the $\sigma_{SI}^2/\sigma_{RD}^2 = -2$ dB SI level and choose $J = 2$ for

the $\sigma_{SI}^2/\sigma_{RD}^2 = -40$ dB SI level, because a longer J is generally required to avoid the detrimental SI effect if the SI power is high. The case of full-duplex DD OFDM with $\sigma_{SI}^2/\sigma_{RD}^2 = -2$ dB has a slightly inferior performance in coded BER contrasted with that of full-duplex DD OFDM with $\sigma_{SI}^2/\sigma_{RD}^2 = -40$ dB, because the former one subjects to higher level of noise at the full-duplex relay. The performance gap between the full-duplex DD OFDM and the 2-path coded OFDM is largely attributed to the composition of the relay link, which is a concatenation of two flat fading links. Lastly, it is observed that the half-duplex BER curve has the same slope as that of the full-duplex DD OFDM but performs 6 dB worse than the case of full-duplex DD OFDM with -2 dB SI due to higher order modulation.

In the next simulation, the coded BER curves our proposed DD OFDM scheme are demonstrated in Fig. 4.5. $\sigma_{SI}^2/\sigma_{RD}^2 = -40$ dB. The SNR_R is fixed at 25 dB. The modulations are QPSK, 16QAM and 64QAM. The proposed power allocation is employed in this simulation. We can see that error floors appear on all three curves in the high SNR range due to the fixed SNR, i.e., SNR_R , at the relay.

In the next, we show the effect of selection of different effective residual SI lengths under a high level of SI. $\sigma_{SI}^2/\sigma_{RD}^2 = -2$ dB. In Fig. 4.6, $J = 1, 2, 4$ are considered, where no SI is also considered as a reference. QPSK is used. It is worthwhile pointing out that the CP length used in this simulation is different from the initial setting. The CP length is $L_{CP} = 2$ for the no SI case. For the rest cases with SI, we let $L_{CP} = J = 1, 2, 4$. We can see that when $J = 1$, the BER curve has an obvious error floor when the SNR is greater than 25dB, because the selected effective residual SI paths length is too short. Too much SI is contributed to the overall noise at the relay and thus eventually enhances the noise level at the destination. When $J = 2$, the BER error floor occurs at a higher SNR and the error floor is approximately a level of magnitude lower than that in the first case. When $J = 4$, the BER error floor is further reduced, because more effective residual SI is utilized rather than being interference. As a result, an adequate effective residual SI multipath length J and accordingly the CP length L_{CP} are obliged to keep the SI at a negligible low level.

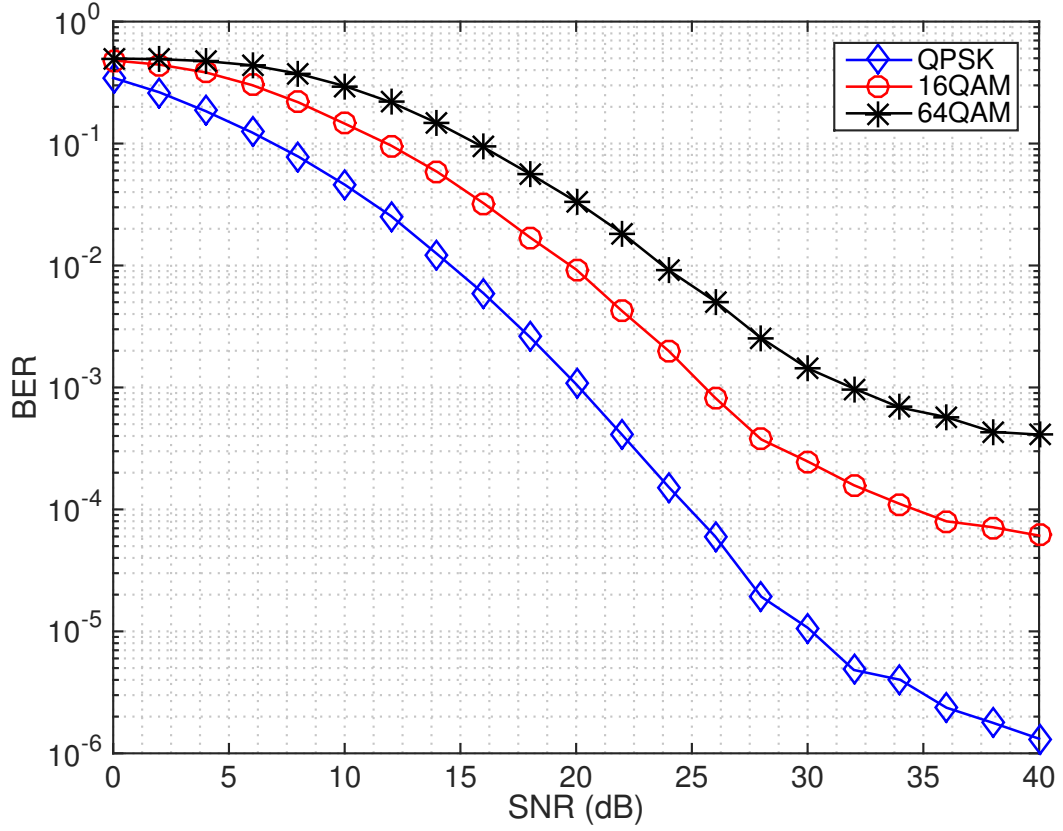


Figure 4.5: Coded BER versus SNR_D with $SNR_R = 25$ dB

Lastly, we evaluate our proposed power allocation method by comparing its performance to the performances of an exhaustive search over power allocation factor γ . In this simulation, the power allocation factor γ is swept from 0.1 to 0.9 with a step size 0.1. The proposed power allocation utilizing a power allocation factor calculated by (4.28). Its BER performance is compared to that of all other power allocations with γ ranging from 0.1 to 0.9. Note that the performance of equal power allocation is illustrated by the BER curve with $\gamma = 0.5$. $\sigma_{SI}^2/\sigma_{RD}^2 = -40$ dB. The modulation is QPSK. The simulation results in Fig. 4.7 indicate that the proposed power allocation method outperforms the equal power allocation. The performance

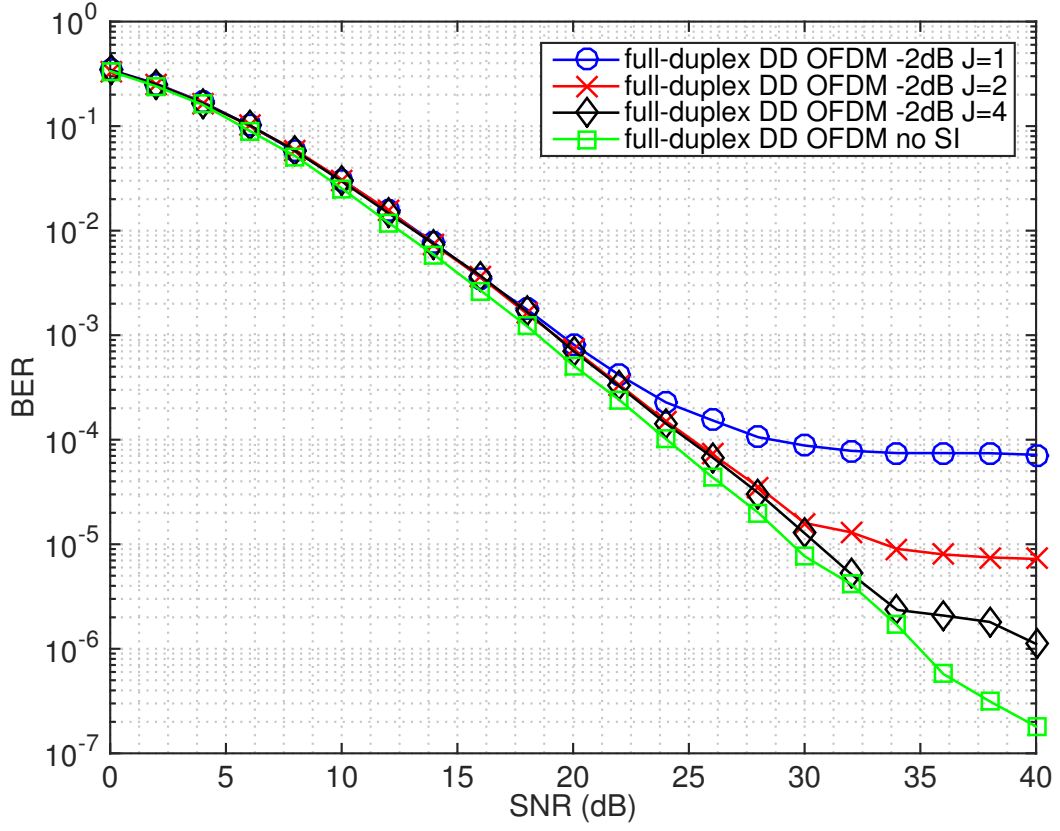


Figure 4.6: BER comparison for different effective residual SI lengths

gain is approximately 0.6 dB when the SNR is in the medium to high region. In this figure, the two curves that perform best correspond to $\gamma = 0.7$ and $\gamma = 0.8$. The curve which represents the proposed power allocation method is also very close to these two curves with best BER performance, which indicates the power allocation method can approach near optimal performance.

4.5 Conclusion

In this paper, one DD OFDM scheme in full-duplex relay communication systems with one source node, one relay node, and one destination node is considered. We

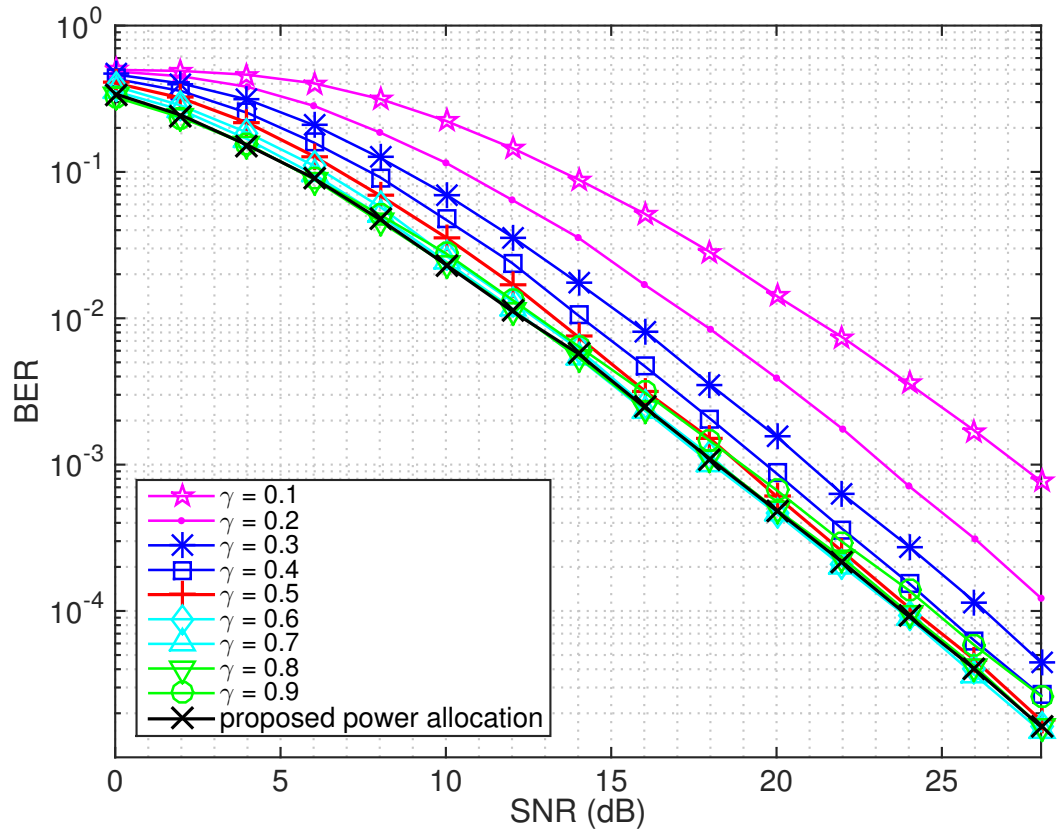


Figure 4.7: BER comparison for different power allocations, including the proposed power allocation and power allocations with γ ranging from 0.1 to 0.9

demonstrate that the full-duplex relay system can be equivalently transformed into a two-antenna DD system by adding CP with an appropriate CP length and using the proposed block based AF relay protocol. The source to destination link and the relay link are two independent transmission links and thus provides spatial diversity. The proposed DD OFDM scheme can transform the system spatial diversity into frequency diversity, which is collected by using bit-interleaved coded OFDM in this paper. Finally, the simulation results validate the performance of the proposed scheme.

Chapter 5

CONCLUSIONS AND FUTURE WORKS

5.1 Conclusions

OFDM has been of great interest for both wireless and wireline communications because of its high data rate communication capability and its robustness to multipath delay spread. However, OFDM systems are much more fragile to a variety of impairments, which mainly cause interference to the OFDM system. Insufficient CP is one of the major sources of impairments which gives rise to severe interference to both point-to-point OFDM systems and cooperative OFDM systems. Self-interference is another source of interference to full-duplex OFDM systems. This dissertation mainly investigates wireless communication techniques which enable reliable communication when either the OFDM systems have insufficient CP or the full-duplex relay OFDM systems are greatly impaired by self-interference. For the OFDM systems with insufficient CP, effective precoding schemes are provided in order to take advantage of the signal structure to eliminate interference and to achieve higher bandwidth efficiency. For the full-duplex OFDM systems with self-interference, a novel signal model is proposed in order to fully utilize the self-interference to increase the system robustness. Moreover, the CP requirement in the full-duplex relay OFDM communication is also discussed. The result is insightful for further studies on the area of full-duplex relay OFDM communication. The detailed contributions of this dissertation are concentrated as follows:

5.1.1 Channel Independent Precoding Design For MIMO OFDM With Insufficient CP

In this paper, we proposed a channel independent precoding for MIMO-OFDM systems with insufficient CP by using the notion of interference nulling that has been also actively used in interference alignment lately. We showed that our proposed precoding is more bandwidth efficient than the conventional zero-padded or CP added MIMO systems, such as, ZP-only, CP-OFDM and SC-FDE systems, when the number of receive antennas is not more than the number of transmit antennas. When the number of receive antennas is more than the number of transmit antennas, it was shown that the IBI in an MIMO-OFDM system can be completely eliminated without any CP or zero-padding or precoding, when the OFDM block size is not too small. The key reason behind these is that instead of making the IBI disappears completely in the conventional sufficient CP or ZP based block transmission systems, the IA based channel independent precoding proposed in this paper aligns the IBI interference subspace disjoint from the signal subspace and then the zero-forcing operator is applied to eliminate the IBI while maintain the signal. Although we only considered CP based block transmission systems in this paper, the theory developed in this paper can be easily generalized to ZP based block transmission systems.

5.1.2 A Robust Precoder Design Based On Channel Statistics For MIMO-OFDM Systems With Insufficient Cyclic Prefix

In this paper, we continue our discussion in the previous chapter on the precoding for MIMO-OFDM systems with insufficient CP. Instead of the channel independent precoding in our previous work in the previous chapter, new precoder based on the channel statistics at the transmitter is proposed. This design retains the property of IBI separation as what we have discussed in the channel independent precoding. Combined with the IBI zero forcing operation at the receiver, more data symbols are transmitted in the MIMO-OFDM system, and thus higher spectral efficiency is

achieved. An interference free equivalent channel can be constructed from the compound of the zero-forcing and channel matrices. Toward this equivalent channel, an optimized precoder design has been carried out aiming at minimizing the maximal MSE of all the data streams. Substantial gains compared to the unoptimized channel independent precoding can be seen from the simulation results.

5.1.3 Full Duplex Delay Diversity Relay Transmission Using Bit-Interleaved Coded OFDM

In this paper, one DD OFDM scheme in full-duplex relay communication systems with one source node, one relay node, and one destination node is considered. We demonstrated that the full-duplex relay system can be equivalently transformed into a two antenna DD system by adding CP with an appropriate CP length and using the proposed block based AF relay protocol. The source to destination link and the relay link are two independent transmission links and thus provides spatial diversity. The proposed DD OFDM scheme can transform the system spatial diversity into frequency diversity, which is collected by using bit-interleaved coded OFDM modulation in this paper. Finally, the simulation results validated the performance of the proposed scheme.

5.2 Future Works

In this section, we briefly discuss some possible interesting works that can be done in the future for the full-duplex relay OFDM communications. We point out possible research topics and discuss viable solutions which may enlighten further studies on these topics.

5.2.1 The Incorporation Of Self-Interference Cancellation In Full-Duplex Relay OFDM Communications

In our current study of the full-duplex relay OFDM communication, the self-interference is assumed to be the residual component which is the inevitable residue

after certain interference cancellation method has been applied. Since the realistic interference cancellation method is not included in our full-duplex relay OFDM communication scheme, the performance evaluation is not very complete in the sense that the actual power level of the residual interference can not be accurately assessed and therefore we must consider both a strong residual interference scenario and a weak residual interference scenario. The system performance will be more convinced if a realistic self-interference cancellation technique is incorporated into the entire system design. We believe that digital interference cancellation/mitigation techniques should be paid sufficient attention since digital interference cancellation/mitigation can be implemented in a very flexible manner. Especially, massive MIMO digital interference cancellation/mitigation could be a very promising technique to handle the self-interference at the full-duplex relay and can suppress the self-interference very efficiently so that the OFDM communication can be very reliable via the full-duplex relay communication link.

5.2.2 More Complicated Full-Duplex Relay Networks

Our work only considers the simplest full-duplex relay system, which comprises of a single source node, a single relay node, and also a single destination node. We provide a very efficient solution for OFDM communication over this full-duplex relay system. The results show that the self-interference can be successfully managed and the full diversity can also be achieved. Our current work can surely serve as a seminal work to inspire more studies on more complicated and more realistic applications. However, this simple system model can not directly provide more direct result for more complicated applications due to the very simple topology of the system model. Researchers can definitely consider more complicated system models which could involve more relay nodes. With more relay nodes in the full-duplex relay OFDM communication systems, a higher level of cooperative diversity may be achieved which renders the system even better robustness. Moreover, several destinations can also be included in

the system model so that diversified novel schemes can be proposed. Different robustness can be applied to different destination nodes based on a system quality of service requirement. Massive MIMO can also be incorporated to provide spatial domain multiplexing so that different spatial streams of data can be directed to different destination nodes. However, when more relay nodes, destination nodes and massive MIMO are incorporated into the system model, there will be new challenges in these more complicated systems, for example, more interference sources inside the system model. Thus, new schemes should propose effective methods to fully suppress the interference or even take advantage of the interference. We believe that numerous meaningful and interesting researches can be conducted toward more complicated full-duplex relay system models. The future research results can be very beneficial options for the current 5G communication applications.

BIBLIOGRAPHY

- [1] Recommendation ITU-R M. 1225, International telecommunication union, guidelines for evaluation of radio transmission technologies for imt-2000, Feb. 1997.
- [2] Enis Akay and Ender Ayanoglu. Achieving full frequency and space diversity in wireless systems via BICM, OFDM, STBC, and Viterbi decoding. *IEEE Trans. Commun.*, 54(12):2164–2172, 2006.
- [3] K. Azarian, H. El Gamal, and P. Schniter. On the achievable diversity-multiplexing tradeoff in half-duplex cooperative channels. *IEEE Trans. Inf. Theory*, 51(12):4152–4172, Dec. 2005.
- [4] G. Bauch and J. S. Malik. Cyclic delay diversity with bit-interleaved coded modulation in orthogonal frequency division multiple access. *IEEE Trans. Wireless Commun.*, 5(8):2092–2100, Aug. 2006.
- [5] V. R. Cadambe and S. A. Jafar. Interference alignment and the degrees of freedom for the k user interference channel. *IEEE Trans. on Information Theory*, 54:3425–3441, Aug. 2008.
- [6] Kok-Wui Cheong and John M Cioffi. Precoder for DMT with insufficient cyclic prefix. In *Proc. IEEE Int. Conf. Commun. (ICC 98)*, pages 339–343, Atlanta, GA, Jun. 7-11, 1998.
- [7] S. Chern, J. Chen, , and C. Wu. Novel frequency-domain DFE equalizer with oblique projection for CP-free space-time block coded MIMO-OFDM systems. In *Proc. International Symp. Intelligent Signal Processing and Communication Systems (ISPACS'09)*, pages 541–545, Kanazawa, Japan, Jan. 19 2010.
- [8] L. J Cimini Jr, Babak Daneshrad, and Nelson R Sollenberger. Clustered OFDM with transmitter diversity and coding. In *Proc. IEEE Global Communications Conference (GLOBECOM) 1996*, pages 703–707, London, UK, Nov. 18-22, 1996.
- [9] M. V. Clark. Adaptive frequency-domain equalization and diversity combining for broadband wireless communications. *IEEE J. Select. Areas Commun.*, 16:1385–1395, Oct. 1998.
- [10] Philip J Davis. *Circulant Matrices*. New York: Wiley, 1979.

- [11] Y. Ding, J.-K. Zhang, and K. M. Wong. The amplify-and-forward half-duplex cooperative system: pairwise error probability and precoder design. *IEEE Trans. Singal Process.*, 55(2):605–617, Feb. 2007.
- [12] M. Duarte, A. Sabharwal, V. Aggarwal, R. Jana, K. Ramakrishnan, C. Rice, and N. K. Shankaranarayanan. Design and characterization of a full-duplex multi-antenna system for WiFi networks. *IEEE Trans. Veh. Technol.*, 63(3):1160–1177, Mar. 2014.
- [13] D. Falconer, S. L. Ariyavisitakul, A. Benyamin-Seeyar, and B. Eidson. Frequency domain equalization for single-carrier broadband wireless systems. *IEEE Commun. Mag.*, 40(4):58–66, Apr. 2002.
- [14] Igor Freire, Chenguang Lu, Per-Erik Eriksson, and Aldebaro Klautau. Low complexity precoder and equalizer for dmt systems with insufficient cyclic prefix. In *Global Communications Conference (GLOBECOM), 2014 IEEE*, pages 3243–3248. IEEE, 2014.
- [15] Y. Fu, C. Tellambura, and W. A. Krzymien. Transmitter precoding for ICI reduction in closed-loop MIMO OFDM systems. *IEEE Trans. Veh. Technol.*, 56(1):115–125, Oct. 2007.
- [16] Andrea Goldsmith, Syed Ali Jafar, Nihar Jindal, and Sriram Vishwanath. Capacity limits of MIMO channels. *IEEE J. Select. Areas Commun.*, 21(5):684–702, 2003.
- [17] Dhananjay Gore, Sumeet Sandhu, and Arogyaswami Paulraj. Delay diversity codes for frequency selective channels. In *IEEE International Conference on Communications (ICC), New York, USA*, volume 3, pages 1949–1953, 2002.
- [18] T. Gou and S. A. Jafar. Degree of freedom of the k user $m \times n$ MIMO interference channel. *IEEE Trans. on Information Theory*, 56:6040–6057, Dec. 2010.
- [19] Marcus Grossmann, Christian Schneider, and Reiner S Thoma. Turbo equalisation for MIMO-OFDM transmission with insufficient guard interval. In *Proc. 2006 IEEE Int. Zurich Seminar Commun.*, pages 114–117, Zurich, Switzerland, Feb. 22-24, 2006.
- [20] J. Guo, S. Ren, and H. Xiang. A non-cyclic prefixed MIMO-OFDM system based on a recursive algorithm of joint channel estimation and data detection. In *Proc. 4th International Conf. Wireless Communications, Networking and Mobile Computing (WiCOM '08)*, pages 1–6, Dalian, China, Oct. 12–14 2008.
- [21] Y. Han, A. Pandharipande, and S. H. Ting. Cooperative decode-and-forward relaying for secondary spectrum access. *IEEE Trans. Wireless Commun.*, 8(10):4945–4950, Oct. 2009.

- [22] Katsuyuki Haneda, Eino Kahra, Shurjeel Wyne, Clemens Icheln, and Pertti Vainikainen. Measurement of loop-back interference channels for outdoor-to-indoor full-duplex radio relays. *Proc. 4th European Conference on Antennas and Propagation (EuCAP)*, pages 1–5, Apr. 2010.
- [23] T. Himsoon, W. Su, and K. Liu. Differential transmission for amplify-and-forward cooperative communications. *IEEE Signal Process. Lett.*, 12(9):597–600, Sep. 2005.
- [24] Chih-Ning Hsu, Hsuan-Jung Su, and Pin-Hsun Lin. Joint subcarrier pairing and power allocation for OFDM transmission with decode-and-forward relaying. *IEEE Trans. Singal Process.*, 59(1):399–414, Jan. 2011.
- [25] S. A. Jafar and S. Shamai. Degree of freedom region for the MIMO x channel. *IEEE Trans. on Information Theory*, 54:151–170, Jan. 2008.
- [26] Leonardo Jimenez Rodriguez, Nghi H Tran, and Tho Le-Ngoc. Performance of full-duplex af relaying in the presence of residual self-interference. *IEEE Journal on Sel. Areas in Commun.*, 32(9):1752–1764, Sep. 2014.
- [27] Yuansheng Jin and X.-G Xia. An interference nulling based channel independent precoding for MIMO-OFDM systems with insufficient cyclic prefix. *IEEE Trans. Commun.*, 61(1):131–143, Jan. 2013.
- [28] Yuansheng Jin and Xiang-Gen Xia. A robust precoder design based on channel statistics for MIMO-OFDM systems with insufficient cyclic prefix. *IEEE Transactions on Commun.*, 62(4):1249–1257, April 2014.
- [29] V. Kotzsch, W. Rave, , and G. Fettweis. ISI analysis in network MIMO OFDM systems with insufficient cyclic prefix length. In *Proc. 7th International Symp. Wireless Commun. Systems (ISWCS)*, pages 189–193, York, UK, Sept. 2010.
- [30] J. N. Laneman, D. N. C. Tse, and G. W. Wornell. Cooperative diversity in wireless networks: efficient protocols and outage behavior. *IEEE Trans. Inf. Theory*, 50(12):3062–3080, Dec. 2004.
- [31] Y. Li, W. Wang, J. Kong, W. Hong, X. Zhang, and M. Peng. Power allocation and subcarrier pairing in OFDM-based relaying networks. In *IEEE International Conference on Communications (ICC), Beijing, China*, pages 2602–2606, May 2008.
- [32] Ye Li, Justin C. Chuang, and Nelson R. Sollenberger. Transmitter diversity for ofdm systems and its impact on high-rate data wireless networks. *IEEE Journal on Sel. Areas in Commun.*, 17(7):1233–1243, Jul. 1999.

- [33] Yuzhou Li, Min Sheng, Chee Wei Tan, Yan Zhang, Yuhua Sun, Xijun Wang, Yan Shi, and Jiandong Li. Energy-efficient subcarrier assignment and power allocation in OFDMA systems with max-min fairness guarantees. *IEEE Trans. Commun.*, 63(9):3183–3195, Sep. 2015.
- [34] Y.-W. Liang and R. Schober. Cooperative amplify-and-forward beam-forming with multiple multi-antenna relays. *IEEE Trans. Commun.*, 59(9):2605–2615, Sep. 2011.
- [35] J.-B. Lim, C.-H. Choi, , and G.-H. Im. MIMO-OFDM with insufficient cyclic prefix. *IEEE Commun. Letters*, 10:356–358, May 2006.
- [36] Yuan-Pei Lin and See-May Phoong. Minimum redundancy for ISI free FIR filter-bank transceivers. *IEEE Trans. Signal Processing*, 50(4):842–853, 2002.
- [37] Jing Liu, Jian-Kang Zhang, and Kon Max Wong. Full-diversity codes for MISO systems equipped with linear or ML detectors. *IEEE Trans. Inform. Theory*, 54(10):4511–4527, 2008.
- [38] Yi Liu, Xiang-Gen Xia, and Hailin Zhang. Distributed space-time coding for full-duplex asynchronous cooperative communications. *IEEE Trans. Wireless Commun.*, 11(7):2680–2688, Jul. 2012.
- [39] Yi Liu, Xiang-Gen Xia, and Hailin Zhang. Distributed linear convolutional space-time coding for two-relay full-duplex asynchronous cooperative networks. *IEEE Trans. Wireless Commun.*, 12(12):6406–6417, Dec. 2013.
- [40] Sili Lu and Naofal Al-Dhahir. A novel CDD-OFDM scheme with pilot-aided channel estimation. *IEEE Trans. Wireless Commun.*, 8(3):1122–1127, Mar. 2009.
- [41] Albert W Marshall, Ingram Olkin, and Barry C Arnold. *Inequalities: Theory of Majorization and Its Applications*. New York: Academic, 1979.
- [42] S. Ohno. Performance of single-carrier block transmissions over multipath fading channels with linear equalization. *IEEE Trans. Signal Processing*, 54:3678–3687, Oct. 2006.
- [43] Ralf Pabst, Bernhard H. Walke, D. C. Schultz, P. Herhold, H. Yanikomeroglu, S. Mukherjee, H. Viswanathan, M. Lott, W. Zirwas, M. Dohler, H. Aghvami, D. D. Falconer, and G. P. Fettweis. Relay-based deployment concepts for wireless and mobile broadband radio. *IEEE Communications Magazine*, 42(9):80–89, Sep. 2004.
- [44] D Perez Palomar, John M Cioffi, and Miguel Angel Lagunas. Joint Tx-Rx beam-forming design for multicarrier MIMO channels: A unified framework for convex optimization. *IEEE Trans. Signal Processing*, 51(9):2381–2401, 2003.

- [45] Daniel Pérez Palomar, Miguel Angel Lagunas, and John M Cioffi. Optimum linear joint transmit-receive processing for MIMO channels with QoS constraints. *IEEE Trans. Signal Processing*, 52(5):1179–1197, May. 2004.
- [46] F. Pancaldi, G. M. Vitetta, R. Kalbasi, N. Al-Dhahir, M. Uysal, and H. Mheidat. Single-carrier frequency domain equalization. *IEEE Signal Process. Mag.*, 25(5):37–56, Sept. 2008.
- [47] Cheol-Jin Park and Gi-Hong Im. Efficient DMT/OFDM transmission with insufficient cyclic prefix. *IEEE Commun. Lett.*, 8(9):576–578, 2004.
- [48] Daiming Qu, Zhiqiang Wang, and Tao Jiang. Extended active interference cancellation for sidelobe suppression in cognitive radio OFDM systems with cyclic prefix. *IEEE Trans. Veh. Technol.*, 59(4):1689–1695, May 2010.
- [49] Vasanthan Raghavan, Akbar M Sayeed, and Venugopal V Veeravalli. Semiunitary precoding for spatially correlated MIMO channels. *IEEE Trans. Inform. Theory*, 57(3):1284–1298, 2011.
- [50] Gregory G Raleigh and John M Cioffi. Spatio-temporal coding for wireless communication. *IEEE Trans. Commun.*, 46(3):357–366, 1998.
- [51] T. Riihonen, S. Werner, and R. Wichman. Hybrid full-duplex/half-duplex relaying with transmit power adaptation. *IEEE Trans. Wireless Commun.*, 8(6):2801–2806, Jun. 2009.
- [52] T. Riihonen, S. Werner, and R. Wichman. Optimized gain control for single-frequency relaying with loop interference. *IEEE Trans. Wireless Commun.*, 8(6):2801–2806, Jun. 2009.
- [53] T. Riihonen, S. Werner, and R. Wichman. Mitigation of loopback self-interference in full-duplex MIMO relays. *IEEE Trans. Signal Process.*, 59(12):5983–5993, Dec. 2011.
- [54] Taneli Riihonen, Stefan Werner, Risto Wichman, and Jyri Hämäläinen. Outage probabilities in infrastructure-based single-frequency relay links. In *Proc. Wireless Communications and Networking Conference (WCNC)*, pages 1–6, 2009.
- [55] A. Sabharwal, P. Schniter, D. Guo, D. W. Bliss, S. Rangarajan, and R. Wichman. In-band full-duplex wireless: Challenges and opportunities. *IEEE Journal on Sel. Areas in Commun.*, 32(9):1637–1652, Sep. 2014.
- [56] H. Sari, G. Karam, and I. Jeanclaude. Transmission techniques for digital terrestrial TV broadcasting. *IEEE Commun. Mag.*, pages 100–109, Feb. 1995.
- [57] Andrew Sendonaris, Elza Erkip, and Behnaam Aazhang. User cooperation diversity—part II: implementation aspects and performance analysis. *IEEE Trans. Commun.*, 51(11):1939–1948, Nov. 2003.

- [58] Andrew Sendonaris, Elza Erkip, and Behnaam Aazhang. User cooperation diversity—part I: System description. *IEEE Trans. Commun.*, 51(11):1927–1938, Nov. 2003.
- [59] Nambi Seshadri and Jack H Winters. Two signaling schemes for improving the error performance of frequency-division-duplex (FDD) transmission systems using transmitter antenna diversity. In *Proc. Vehicular Technology Conference*, pages 49–60, May 1993.
- [60] X. Sun, L. J. Cimini, L. J. Greenstein, and D. S. Chan. ICI/ISI aware beamforming for MIMO-OFDM wireless system. In *Information Sciences and Systems (CISS'09)*, pages 103–107, Baltimore, USA, Mar. 2009.
- [61] Xiantao Sun, Qi Wang, Leonard J Cimini, Larry J Greenstein, and Douglas S Chan. ICI/ISI-aware beamforming for MIMO-OFDM wireless systems. *IEEE Transactions on Wireless Commun.*, 11(1):378–385, 2012.
- [62] Taiwen Tang and Robert W Heath Jr. Space-time interference cancellation in MIMO-OFDM systems. *IEEE Trans. Veh. Technol.*, 54(5):1802–1816, 2005.
- [63] Emre Telatar. Capacity of multi-antenna gaussian channels. *European Transactions on Telecommunications*, 10(6):585–595, 1999.
- [64] Cihan Tepedelenlioglu. Low complexity linear equalizers with maximum multipath diversity for zero-padded transmissions. In *Proc. IEEE Int. Conf. Acoust., Speech, and Signal Process. (ICASSP'03)*, pages IV – 636–639, Hong Kong, Hong Kong, Apr. 6-10, 2003.
- [65] Andre Tkacenko and Palghat P Vaidyanathan. A low-complexity eigenfilter design method for channel shortening equalizers for DMT systems. *IEEE transactions on communications*, 51(7):1069–1072, 2003.
- [66] Steffen Trautmann and Norbert J Fliege. Perfect equalization for DMT systems without guard interval. *IEEE J. Select. Areas Commun.*, 20(5):987–996, 2002.
- [67] Jue Wang, Shi Jin, Xiqi Gao, K Wong, and Edward Au. Statistical eigenmode-based SDMA for two-user downlink. *IEEE Trans. Signal Processing*, 60(10):5371–5383, 2012.
- [68] Z. Wang and G. B. Giannakis. Wireless multicarrier communications: Where Fourier meets Shannon. *IEEE Signal Processing Mag.*, 47:29–48, May 2000.
- [69] X.-G. Xia. Applications of nonmaximally decimated multirate filterbanks in partial response channel ISI cancellation. In *Proc. IEEE Third Time-Frequency Time-Scale Symp. (TFTS)*, Paris, France, June 1996.

- [70] X.-G. Xia. New precoding for intersymbol interference cancellation using nonmaximally decimated multirate filterbanks with ideal FIR equalizers. *IEEE Trans. on Signal Processing*, 45:2431–2441, Oct. 1997.
- [71] Chengwen Xing, Dan Li, Shaodan Ma, Zesong Fei, and Jingming Kuang. Robust transceiver design for MIMO-OFDM systems based on cluster water-filling. *Communications Letters, IEEE*, 17(7):1451–1454, 2013.
- [72] J.-K. Zhang, J. Liu, and K. M. Wong. Linear toeplitz space time block codes. In *Proc. IEEE Int. Symp. Inform. Theory (ISIT'05)*, Adelaide, Australia, Sept. 4-9 2005.
- [73] Xi Zhang, Daniel P Palomar, and Björn Ottersten. Statistically robust design of linear MIMO transceivers. *IEEE Trans. Signal Processing*, 56(8):3678–3689, 2008.

Appendix A

PROOF OF THE IDENTICAL MSE'S FOR FULL CP SISO-OFDM WITH CHANNEL INDEPENDENT PRECODING

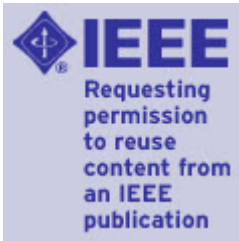
For the SISO-OFDM case, when the CP is full ($v \geq L$), the equivalent channel matrix \mathbf{H}_{eq} is a circulant matrix with the first row $[h(0), 0, \dots, 0, h(L), \dots, h(1)]$ and the first column $[h(0), \dots, h(L), 0, \dots, 0]^T$. The covariance matrix $\mathbf{R}_c = \mathbb{E}\{\mathbf{H}_{eq}^H \mathbf{H}_{eq}\}$ is also circulant.

We are interested in the MSE's of all data streams, i.e., the diagonal values of $\bar{\mathbf{E}}$ in (3.23) with channel independent precoder $\mathbf{Q}_u = \mathbf{I}_N$. To be explicit, write

$$\bar{\mathbf{E}} = \left[\frac{1}{\sigma_s^2} \mathbf{I} + \mathbf{R}_c \right]^{-1} = [\bar{\mathbf{R}}]^{-1}, \quad (\text{A.1})$$

where $\bar{\mathbf{R}} = \frac{1}{\sigma_s^2} \mathbf{I} + \mathbf{R}_c$. Since $\bar{\mathbf{R}}$ is also a circulant matrix, so is its inverse $\bar{\mathbf{E}}$ [10]. As a result, the diagonal elements of $\bar{\mathbf{E}}$ are identical.

Appendix B
REPRINT PERMISSIONS



Title: An Interference Nulling Based Channel Independent Precoding for MIMO-OFDM Systems with Insufficient Cyclic Prefix

Author: Yuansheng Jin

Publication: Communications, IEEE Transactions on

Publisher: IEEE

Date: January 2013

Copyright © 2013, IEEE

LOGIN

If you're a **copyright.com user**, you can login to RightsLink using your copyright.com credentials. Already a **RightsLink user** or want to [learn more?](#)

Thesis / Dissertation Reuse

The IEEE does not require individuals working on a thesis to obtain a formal reuse license, however, you may print out this statement to be used as a permission grant:

Requirements to be followed when using any portion (e.g., figure, graph, table, or textual material) of an IEEE copyrighted paper in a thesis:

- 1) In the case of textual material (e.g., using short quotes or referring to the work within these papers) users must give full credit to the original source (author, paper, publication) followed by the IEEE copyright line ◆ 2011 IEEE.
- 2) In the case of illustrations or tabular material, we require that the copyright line ◆ [Year of original publication] IEEE appear prominently with each reprinted figure and/or table.
- 3) If a substantial portion of the original paper is to be used, and if you are not the senior author, also obtain the senior author's approval.

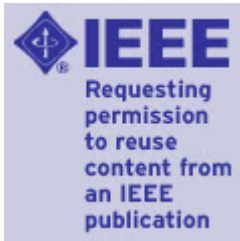
Requirements to be followed when using an entire IEEE copyrighted paper in a thesis:

- 1) The following IEEE copyright/ credit notice should be placed prominently in the references: ◆ [year of original publication] IEEE. Reprinted, with permission, from [author names, paper title, IEEE publication title, and month/year of publication]
- 2) Only the accepted version of an IEEE copyrighted paper can be used when posting the paper or your thesis on-line.
- 3) In placing the thesis on the author's university website, please display the following message in a prominent place on the website: In reference to IEEE copyrighted material which is used with permission in this thesis, the IEEE does not endorse any of [university/educational entity's name goes here]'s products or services. Internal or personal use of this material is permitted. If interested in reprinting/republishing IEEE copyrighted material for advertising or promotional purposes or for creating new collective works for resale or redistribution, please go to http://www.ieee.org/publications_standards/publications/rights/rights_link.html to learn how to obtain a License from RightsLink.

If applicable, University Microfilms and/or ProQuest Library, or the Archives of Canada may supply single copies of the dissertation.

BACK ◆◆◆

CLOSE WINDOW



Title: A Robust Precoder Design Based on Channel Statistics for MIMO-OFDM Systems with Insufficient Cyclic Prefix

Author: Yuansheng Jin

Publication: Communications, IEEE Transactions on

Publisher: IEEE

Date: April 2014

Copyright © 2014, IEEE

LOGIN

If you're a **copyright.com user**, you can login to RightsLink using your copyright.com credentials. Already a **RightsLink user** or want to [learn more?](#)

Thesis / Dissertation Reuse

The IEEE does not require individuals working on a thesis to obtain a formal reuse license, however, you may print out this statement to be used as a permission grant:

Requirements to be followed when using any portion (e.g., figure, graph, table, or textual material) of an IEEE copyrighted paper in a thesis:

- 1) In the case of textual material (e.g., using short quotes or referring to the work within these papers) users must give full credit to the original source (author, paper, publication) followed by the IEEE copyright line ◆ 2011 IEEE.
- 2) In the case of illustrations or tabular material, we require that the copyright line ◆ [Year of original publication] IEEE appear prominently with each reprinted figure and/or table.
- 3) If a substantial portion of the original paper is to be used, and if you are not the senior author, also obtain the senior author's approval.

Requirements to be followed when using an entire IEEE copyrighted paper in a thesis:

- 1) The following IEEE copyright/ credit notice should be placed prominently in the references: ◆ [year of original publication] IEEE. Reprinted, with permission, from [author names, paper title, IEEE publication title, and month/year of publication]
- 2) Only the accepted version of an IEEE copyrighted paper can be used when posting the paper or your thesis on-line.
- 3) In placing the thesis on the author's university website, please display the following message in a prominent place on the website: In reference to IEEE copyrighted material which is used with permission in this thesis, the IEEE does not endorse any of [university/educational entity's name goes here]'s products or services. Internal or personal use of this material is permitted. If interested in reprinting/republishing IEEE copyrighted material for advertising or promotional purposes or for creating new collective works for resale or redistribution, please go to http://www.ieee.org/publications_standards/publications/rights/rights_link.html to learn how to obtain a License from RightsLink.

If applicable, University Microfilms and/or ProQuest Library, or the Archives of Canada may supply single copies of the dissertation.

BACK ◆◆◆

CLOSE WINDOW